DOE/PC/93207--T6

Development and Evaluation of Mn Oxide-Coated Composite Adsorbent for the Removal and Recovery of Heavy Metals from Coal Processing Wastewater

FINAL REPORT, DECEMBER 1995

Huan-Jung Fan and Paul R. Anderson

Work Performed Under Grant No. DE-FG22-93PC93207
of the University Coal Research Program

For:
United States Department of Energy
Pittsburgh Energy Technology Center
Pittsburgh, PA 15236

By:
Department of Chemical and Environmental Engineering
Illinois Institute of technology
Chicago, IL 60616

TABLE OF CONTENTS

CHAPTER Page

LIST OF TABLES

LIST OF FIGURES

Figure Page

Figure Page

LIST OF SYMBOLS

Symbol	Definition
b	Langmuir isotherm constant related to the enthalpy of adsorption
C	solution concentration (M/ L^3)
C_a	concentration of acid added (mol/ L^3)
C_b	concentration of base added (mol/L^3)
C_o	initial concentration (M/ L^3)
C_p	concentration in the pore space (M/L^3)
C_s	solution concentration at external surface of particle (M/ L^3)
D_h	dispersion coefficient (L^2/T)
D_l	liquid phase diffusivity (L^2/T)
D_p	pore diffusivity (L^2/T)
D_s	surface diffusivity (L^2/T)
F	Faraday constant (96500 coulomb/mol)
H^+	hydrogen ions
$[H^+]$	concentration of H^+
$[H^+]_S$	concentration of hydrogen ion at solid surface (mole/ L^3)
K	Freundlich isotherm constant ((L^3/M)^n)
$K_{a1}{}^S$	first apparent equilibrium coefficient
$K_{a2}{}^S$	second apparent equilibrium coefficient
$K_{a1}{}^S$(int)	first intrinsic acidity coefficients of surface hydroxides
$K_{a2}{}^S$(int)	second intrinsic acidity coefficients of surface hydroxides

K_f	film transfer coefficient (L/T)
L_b	bed length (L)
m	weight of the adsorbent (M)
M^{z+}	cations ions
n	Freundlich isotherm exponent (dimensionless)
q	surface concentration (M/M)
Q	mean surface charge on the adsorbent (mol/M)
Q_0	Langmuir isotherm constant related to a maximum surface coverage corresponding to complete monolayer coverage (M/M)
r	radial distance (L)
R	particle radius (L)
Re	Reynolds number (dimensionless)
$[OH^-]$	concentration of OH^-
Sc	Schmidt number (dimensionless)
S	oxide surface
t	time (T)
μ	viscosity of the fluid (centipose)
v	average linear velocity (L/T)
V	solution volume (L^3)
V_s	superficial loading velocity (L/t)
X	mass of adsorbent (M)
z	axial distance (L)

δ	the thickness of the boundary layer (L)
ρ	*a*pparent density of particle (M/ L^3)
ρ_1	fluid density (M/L^3)
ρ_p	particle density (M/L^3)
ε	porosity of batch reactor
ε_p	intraparticle porosity
ε_B	porosity of fixed-bed
σ_0	surface charge (coulomb/ L^2)
Γ_{H^+}	adsorption density of H^+ (mol/ L^2)
Γ_{OH^-}	adsorption density of OH^- (mol/L^2)

ABSTRACT

The overall objective of this research was to evaluate a Mn oxide-coated granular activated carbon (MnGAC) for the removal and recovery of metals from wastewaters. The composite adsorbent was prepared by coating Mn-oxide onto granular activated carbon.

Three coating methods (adsorption, precipitation, and dry oxidation) were developed and studied in this research.

In the adsorption method, factors affecting the amount of coating on GAC were type of GAC, GAC pore volume, GAC particle size, coating time, Mn dosage, and the duration of prewash time. In batch tests with Cu(II), relative to GAC by itself, adsorption capacities were increased more than three times after coating and Mn oxides dominated the adsorption process. Complete breakthrough for a fixed-bed column occurred after 3000 empty bed volumes (BV) were processed. In multiple adsorption/regeneration cycles, although total Cu(II) removal decreased from the first to the third cycle, Cu(II) removal stayed about the same in the third and subsequent cycles.

In the precipitation method, the Mn oxide was precipitated on the GAC surfaces by evaporation. Nine composite adsorbents were prepared by using three GAC (WVB, APC, TOG) and three manganese salts (manganese nitrate (N), manganese sulfate (S), and manganese chloride (C)). The manganese chloride resulted in the highest amount of coating. MnAPC had a higher amount of Mn coating than did MnWVB or MnTOG. However, in adsorption edge tests, MnWVB had the highest amount of Cu(II) adsorption capacity.

The adsorbent (MnTOG) prepared by a dry oxidation method had the highest Cu(II) adsorption capacity of the three synthesis methods. In multiple adsorption/regeneration cycle tests, MnTOG had better Cu(II) removal relative to those adsorbents prepared by other methods. MnTOG had the ability to remove Cu(II) and Cd(II) to trace level (< 4 ug/L) in a column process at least through 3000 and 1400 BV, respectively. Cd(II) removal was hindered by the presence of Cu(II). However, Cu(II) removal was only slightly reduced by the presence of Cd(II). Cu(II) adsorption in batch and fixed-bed processes onto MnTOG was successfully modeled with a homogeneous surface diffusion model (HSDM). However, the HSDM could only successfully describe the adsorption of Cd(II) onto MnTOG in the batch process, but not the fixed-bed process.

Mn oxide can be deposited on GAC to create a composite adsorbent with an increased Cu(II) or Cd(II) adsorption capacity. Composite adsorbent (MnGAC) has the potential to become an efficient way to remove metals from metal contaminated wastewater.

CHAPTER I

INTRODUCTION

With 29 percent of the world reserves, coal is the most abundant fossil energy resource in the United States. This amount of coal is equivalent to 2 trillion barrels of crude oil; more than twice the world's known oil reserves. According to DOE's National Energy Strategy, the 770 million tons of coal per year used in 1990 will increase 50 percent by 2010. This number will nearly double by 2030. In 1990, 55 percent of US electricity was produced by coal (US DOE, 1994).

Although metals are found in coal in relatively low concentrations, total emissions of metals can be significant because of the extremely large quantities of coal consumed. Due to the increase use of coal, mobilization of heavy metals contained in the coal is a growing concern.

Traditional techniques to treat metal contaminated wastewater involve some form of a precipitation process. However, these processes have potential disadvantages. For example, complexing agents may inhibit the precipitation process, the optimal pH for precipitation varies from one metal to another, and there are problems associated with sludge management.

An alternative treatment process is the removal of metals by adsorption onto oxide adsorbents, such as aluminum oxides, iron oxides, and manganese oxides. However, one of the major limitations of the adsorption process is solid separation. Because a typical oxide adsorbent is in a colloidal form, it is difficult to separate from

aqueous solution. One approach to this problem is to prepare a granular composite adsorbent that can be used in a column process. Based on this concept, a composite adsorbent prepared from manganese and granular activated carbon (MnGAC) may address some of these problems. The reason for choosing Mn oxides is that relative to Fe or Al oxides, Mn oxides have a higher affinity for many heavy metals (McLaren and Crawford, 1973; Oakley *et al.*, 1981; Faust and Aly, 1983). Furthermore, several investigators have suggested applications for Mn oxides in water and wastewater treatment (Kinniburgh and Jackson, 1981; Gray, 1981; Faust and Aly, 1983). Results form these studies suggest that Mn oxides can be used to synthesize an effective adsorbent for metal removal. GAC, which has a high surface area, should provide an efficient surface for the Mn oxide. At the same time, the Mn oxides can improve the metal adsorption capacity of GAC. The resulting composite adsorbent (MnGAC) has good potential to become a very efficient way to remove metals from metal contaminated wastewater.

This report starts with background and literature review that includes a discussion of potential problems of ingorganics in coal and problems associated with precipitation and adsorption treatment processes for metals removal. Adsorption models and adsorption kinetics are also reviewed. Materials and experimental methods are discussed in Chapter III. Three coating methods (adsorption, precipitation, and dry oxidation) were studied to prepare MnGAC and adsorption properties of these MnGAC and these are discussed in chapters IV to VI, respectively. The adsorbent (MnTOG) prepared by the dry oxidation method had the highest Cu(II) adsorption capacity of the three coating methods. Multiple adsorption/regeneration and column tests are presented in Chapter VII. In multiple

adsorption/regeneration process, MnTOG could be regenerated and reused through at least six adsorption/desorption cycles and more than 70 % of the adsorbed Cu(II) can be recovered. MnGAC also had the ability to remove Cu(II) and Cd(II) to trace level (< 4 ug/L) in a column process. Adsorption kinetics of Cu(II) and Cd(II) onto MnGAC is presented in Chapter VIII. A homogeneous surface diffusion model (HSDM) was used to model both batch and fixed-bed tests and results of these modeling are listed in the following table.

System	K_f (cm/s)*	D_s (cm^2/s)**
Batch reactor		
Cu(II)	0.005	$9*10^{-11}$
Cd(II)	0.005	$1*10^{-9}$
Fixed-bed reactor		
Cu(II)	0.0006	$9*10^{-11}$
Cd(II)	0.0006	$1*10^{-9}$

* K_f = Film transfer coefficient (cm/s)
** D_s = Surface diffusivity (cm^2/s)

Finally, summary conclusions and suggestions for future study are presented in chapter IV.

CHAPTER II

BACKGROUND AND LITERATURE REVIEW

Coal is an alternative important future energy resource. Potential problems associated with coal process wastewaters are becoming more important due to the large amount of coal consumption. There are many ways to treat coal process wastewater, such as precipitation or adsorption onto oxides. However, there are potential problems associated with these methods including high effluent concentration, separation problems, and sludge management problems. Potential problems of heavy metals in coal and treatment processes for treating metal contaminated wastewater are discussed in this chapter.

2.1 Potential Problems of Inorganics in Coal

Three groups of trace elements in coal-fired power plants have been identified (Chadwick and Lindman, 1982). Group I elements include Al, Ba, Ca, Ce, Cs, Fe, K, Mg, Mn, and Th. Group II elements include the more volatile elements As, Cd, Cu, Pb, Sb, Se, and Zn. Group III elements included Br, Hg, and I. Group I elements do not volatlize during the combustion process and are equally distributed between bottom ash and fly ash. Group II elements are initially volatile and then condense on small fly ash particles. As a result, they tend to be more concentrated in the outlet fly ash relative to the inlet fly ash or

the bottom ash. Group III elements are the most volatile and appear mostly in the gas phase.

Elements found in the ash are important because the majority of the solid waste produced by the electric utility industry is fly ash or bottom ash (Fruchter et al., 1990). Production of ash is approaching 100 million tons per year. Most of this material is currently disposed of in ponds or landfills, which ultimately may contaminate ground and surface waters.

Theis and coworkers have investigated the potential for contaminants to leach from ash fills into soils and groundwater (Theis et al., 1978; Theis and Richter, 1979). They concluded that Fe and Mn oxides in the surrounding soils probably controlled the migration of contaminants. However, they also noted that the contaminants might continue to travel further after these adsorbents became exhausted.

Chadwick and Lindman (1982) reported that the projected increases in coal use would lead to a greater quantity of fly ash for disposal and Clarke and Sloss (1992) believe that trace element emissions from coal will be regulated in the near future. When these regulations take effect, treatment processes that can effectively deal with low levels of contaminants will be required.

A typical treatment process for metal contaminated wastewater is a precipitation process. This technique has several potential disadvantages. For example, complexing agents may need to be removed before a precipitation step because these agents may inhibit precipitation (Bhattacharyya and Cheng, 1987). The minimum solubility of different metals in a wastewater generally occurs at different pH values. As a result,

maximum removal of one metal may occur at a pH value where the solubility of another is very high. Furthermore, the resulting sludge needs to be further treated. An alternative recovery and recycle technology, adsorption may be able to overcome these problems.

2.2 Adsorption Treatment Processes

One potential treatment process is the removal of metals by adsorption onto activated carbon or oxide adsorbents, such as Fe oxide or Mn oxide. Numerous researchers have investigated the use of activated carbon to remove heavy metals form aqueous solutions (Sigworth and Smith, 1972; Corpapcioglu and Huang, 1987; Ku and Peters, 1987; Gajghate et. al., 1992; Reed and Matsumoto, 1992; Reed and Arunachalam, 1994). Potential applications of oxides for industrial treatment have also been suggested and discussed (Kinniburgh and Jackson, 1981; Benjamin et. al., 1982; Dzombak and Morel, 1990). Composite adsorbents, such as Fe-coated sand, Fe-coated GAC, and Mn-coated sand, have also been proposed for metals removal. These studies are discussed in this section.

2.2.1 Activated Carbon. Activated carbon has been commercially produced from a wide range of raw materials, such as coconut shell, sawdust, wood char, coal, petroleum coke, bone char, molasses, peat, and paper-mill waste (lignin) (Mattson and Mark, 1971; McGuire and Suffet, 1983). Activated carbon can be classified as either powdered activated carbon (PAC) or granular activated carbon (GAC). Powdered activated carbon

(PAC) consists of particles at and below US Sieve Series No. 50, and granular activated carbon (GAC) consists of larger particles (Clark and Lykins, 1989). Most applications and research on activated carbon emphasize organics removal. However, a number of investigators have suggested using activated carbon to remove heavy metals form aqueous solutions (Sigworth and Smith, 1972; Huang and Wu, 1977; Huang and Bowers, 1979; Bowers and Huang, 1980; Hayes and Leckie, 1982; Netzer and Hughes, 1984; Bhattacharyya and Cheng, 1987; Corapcioglu and Huang, 1987; Ku and Peters, 1987; Gajghate et. al., 1992; Kuennen *et al.* 1992; Reed and Matsumoto, 1992; Reed and Arunachalam, 1994).

Adsorption properties of activated carbon primarily depend on the total surface area, the pore structure, and the chemical reactivity of the material. Surface areas of activated carbon are in the range of 500 to 2000 m^2/g. Activated carbons can be classified as L or H type. The L-type carbon assumes a negative charge in water and adsorbs primarily strong bases. Usually, the L-type carbon is activated at low temperatures (below 500-600 C°). Surface functional groups on the L-type carbon for adsorbing alkali from aqueous solution are probably phenol, n-lactone, f-lactone, carboxyl groups, quinone-type carbonyl groups, carboxylic acid anhydrides, and the cyclic peroxide. In contrast with the L-type carbon, H-type carbon assumes a positive charge in water and adsorbs strong acids. It can be prepared at high temperatures (above 500-600 C°). The functional group on H-type carbon is the chomene group which contains activated $>CH_2$ or >CHR groups. These functional groups can react with a strong acid or oxygen (Mattson and Mark, 1971;

Huang, 1978). An L-type carbon can be converted to an H-type carbon by either chemical oxidation or aging in the atmosphere (Corapcioglu and Huang 1987a).

Theoretically, adsorption capacity is independent from particle size of activated carbon. However, measured adsorption capacities typically increase as particle size decrease (Voice, 1988). This observation probably reflects a kinetic effect. For example, it is known that GAC has a slower adsorption rate compared to PAC (Reed and Arunachalam, 1994).

Huang (1978) stated that L-type carbons had a better Cd(II) adsorption capacity than did H-type carbons. Strong chelating agents, such as nitriloriacetate (NTA) and ethylenediamine tertaacetate (EDTA) could also improve Cd(II) adsorption. The author also believes that increased Cd(II) adsorption was caused by Cd(II) attachment to an adsorbed anion. Cu(II) adsorption capacity depended on solution pH, Cu(II) concentration, and whether or not organic chelates were present. However, the Cu(II) adsorption capacity was very small in these H-type carbons.

Huang and Smith (1981) used activated carbons to remove Cd(II) form plating waste water. The important factors for removal of Cd(II) were carbon type, carbon dose/Cd(II) concentration, pH, wastewater composition, and ionic strength. An activated carbon (Nuchar S-A or Nuchar S-N) with a lower pH_{ZPC} had a better Cd(II) adsorption capacity than did an activated carbon (HD 3000 or F400) with a higher pH_{ZPC}. They found that the maximum Cd(II) removal was in the neutral pH range when fluoroborate or cyanide was present. In the lower pH range, there was competition for adsorption sites between Cd(II) and hydrogen ions. A higher ionic strength inhibited Cd(II) adsorption,

probably because it would compress the electrical double layer (EDL), decrease the electrostatic potential, and reduce the coulombic free energy.

Ten commercial activated carbons and three adsorbates (copper, lead, cobalt) were tested by Netzer and Hughes (1984). They reported that carbon type and pH were the most important variables for metal removal. The contact time required for equilibrium of the metal species between the carbon and solution depended on the ratio of the number of adsorption sites to the number of metal species that can be adsorbed. For complete metals removal, 2 h contact time was required. They also concluded that there was competition between different metals for adsorption sites.

A similar test was conducted by Huang and Corpapcioglu (1987). They tested 14 different activated carbons for Cu(II), Pb(II), Ni(II), and Zn(II) removal from aqueous solutions. They concluded that carbon type, pH, and surface loading were the most important factors affecting the amount of metal removal, and the adsorption reaction could be described with a surface complex formation model.

Bhattacharyya and Cheng (1987) also reported that in the presence of complexing agents the amount of metal adsorption onto activated carbon was based on metal and ligand types, ligand-to-metal ratio, pH, and metal chelate species distribution.

Activated carbon also has been suggested as a polishing step for trace metal removal following precipitation process (Ku and Peters, 1987) and added into precipitation reactors to enhance metal removal (Peters and Ku, 1987).

Wiczar and Keinath (1993) studied kinetics of sorption and desorption of Cu(II) and Pb(II) on activated carbons (Nuchar SA, and F 400). The authors observed a two

step adsorption process. There was initial rapid sorption followed by a slow and prolonged sorption that could last several weeks. The authors believe that this behavior was due to the nonhomogeneity of the activated carbon surface, which contains a variety of functional groups. The groups that serve as sorption sites may have different metal adsorption strength and adsorption rate. Both adsorbed Cu(II) and Pb(II) on Nuchar SA could be desorbed rapidly. The desorption rate of Pb(II) was slower, which may due to a stronger affinity. However, Cu(II) and Pb(II) were not completely desorbed from F400 after 20 days.

Reed and coworkers (Reed and Arunachualam, 1994; Reed, Arunachualam, and Thomas, 1994) used GAC columns for lead and cadmium removal form aqueous waste streams. The authors stated that the critical parameters influencing GAC column adsorption were column pH and influent characteristics. Both acetic acid and EDTA had adverse effects on lead removal. The authors believed that acetic acid reacted with the carbon associated OH^-, which decreased the solution pH then reduced the removal of lead. However, acetic acid did not have a significant effect on cadmium removal. The authors believed that the difference might be due to the solution chemistry. When EDTA complexed with lead, the resulting complex was not adsorbed. The GAC column was regenerated by using a 0.1 N HNO_3 rinse followed by a 0.1 N NaOH rinse without losing any significant adsorption capacity. Although, a significant amount of lead was retained in the GAC column after the desorption process, it did not interfere with subsequent adsorption cycles. The authors believed that the lead removal mechanism was dominated

by precipitation in the column process, because NaOH was used in the regeneration process.

In summary, activated carbon can be used for metals removal form aqueous solution. Factors affecting adsorption onto activated carbon include type and amount of carbon, solution pH, adsorbate, ionic strength, complexing agents, and contact time. GAC can be used in a column process, which can eliminate separation problem and minimize the sludge production.

2.2.2. Oxides. An alternative treatment technique for metal removal involves adsorption of metal ions onto oxides surfaces. Adsorption processes may overcome many limitations associated with precipitation process. These processes do not depend on metal solubility and therefore have greater process flexibility. Furthermore, the adsorption process is pH dependent; adsorbed metals can be desorbed by lowering the pH of the solution. In theory, adsorbed metals can be recovered and reused. Iron and manganese oxides, which have been suggested as appropriate adsorbents for metals removal, are discussed in this section.

Iron Oxides. Many researchers have evaluated and demonstrated the feasibility of an Fe oxide-based adsorption treatment process for metal removal (Leckie et al., 1980; Schultz et al., 1987; Edwards and Benjamin, 1989). An excellent review and modeling of hydrous ferric oxide can be found in works by Dzombak and Morel (1987,

1990). Adsorption of cations by hydrous metal oxides usually is very rapid, reflecting the fact that adsorption occurs on oxide surfaces (Kinniburgh and Jackson, 1981)

Dzombak and Morel (1987) reported that cation adsorption onto oxide surfaces is similar to metal hydrolysis. Cation sorption increases with increasing pH. Cation sorption involves formation of bonds with surface oxygen atoms. They concluded that the surface binding sites are heterogeneous because the sorption density is not proportional to the dissolved concentration. There is little competition between adsorbing cations at relatively low adsorption densities.

Schultz *et al.* (1987) examined Cr(III), Pb, Ni, Cu(II), Zn, and Cd adsorption onto an Fe oxide. An accumulation of slowly reversible Zn was observed during adsorbent cycling. They concluded that the accumulation resulted from extended contact between the adsorbate and the adsorbent. They also reported that the presence of this slowly reversible Zn did not interfere with subsequent adsorption of additional Zn. Several mechanisms for slowly reversible sorption were suggested and discussed. These mechanisms included diffusion limitation, restructuring of the solid in the presence of the adsorbate, surface precipitation, and formation of a dilute, mixed hydrous oxide.

Edwards and Benjamin (1989a) used an Fe oxide to treat wastewater from a metal plating shop. They compared adsorption to traditional hydroxide precipitation. Adsorption onto the Fe oxide was able to remove soluble Cu, Cd, Zn, Cr(III), Ni, and Pb from solution over the pH range from 8 to 12.5. Precipitation, in contrast, was not as successful at any pH value. The Fe oxide was regenerated and reused through 50 adsorption and desorption cycles with no loss in metal removal efficiency. They also

reported that the fraction of metal recovered during regeneration depended on the pH of regeneration and the metal. Only relatively small amounts of Cd, Ni, and Zn remained attached to the solid. For Cu, about 20% of the total metal stayed attached to the adsorbent after 50 treatment cycles. At a lower pH for regeneration it was possible to recover all of the Cu. The attached metal did not interfere in subsequent adsorption steps, which was in agreement with the results of Schultz *et al.* (1987).

Mn Oxide. McKenzie (1977) reported that Mn oxides found in soils contain very high heavy metal concentrations. Relative to organic matter, clays, or Fe oxides, Mn oxides in soils (McLaren and Crawford, 1973) and sediments (Oakley *et al.*, 1981; Lion *et al.*, 1982) have a higher affinity for heavy metals. Faust and Aly (1983) also pointed out that manganese dioxide was more effective relative to iron oxide and aluminum oxides for removal of Cd from water and wastewater. Furthermore, several investigators have suggested applications in water and wastewater treatment (Kinniburgh and Jackson, 1981; Gray, 1981; Faust and Aly, 1983). Results form these studies indicate that Mn oxides could be used as an effective adsorbent for metal removal.

Although manganese has nine oxidation states, most manganese exists in oxidation states +2 and +4 (Schiele, 1991; Kemmitt, 1973). At least thirty mineral species of Mn oxides have been identified by X-ray diffraction (Bricker, 1965). Healy *et al.* (1966) studied zero point of charge (ZPC) of five typical manganese dioxides using microelectrophoresis and coagulation-sedimentation techniques. ZPC values of δ-MnO_2, Mn^{II}-manganite, α MnO_2, β MnO_2 and γ MnO_2 were about 1.5,1.8, 4.5, 5.5, and 7.3,

respectively. More detailed results of their tests are summarized in Table 2.1. Murray (1974) also reported that δ-MnO_2 had a pH of zero charge (ZPC) about 2.25, so that most of these minerals have a negative surface charge in aqueous solution. Mn oxides have a high sorption capacity for heavy metals because of their negative surface charge, surface functional groups, and high surface area (up to 300 m^2/g). A typical manganese oxide (MnO_2) can be prepared from the oxidation of manganese ion by permanganate. This Mn oxide had a surface area of 263 m^2/g, and a ZPC of 2.25 (Murray, 1974). Murray also reported that the solubility of MnO_2 was negligible for pH > 3.5.

Loganathan *et al.* (1977) studied the sorption behavior of Co^{2+}, Zn^{2+}, and Ca^{2+} onto δ-MnO_2 at different pH values. Surface charge of δ-MnO_2 was negative in the pH values tested (pH 3-9) in the absence of Co(II), Zn(II), or Ca(II). At pH values < 5, there was not much change in the sorption of these cations with increase in pH and Mn^{2+} and H^+ were released into solution in the process of Co(II) or Zn(II) adsorption. However, only H^+ was released in the process of Ca(II) sorption. The authors believed that the sorption of Co(II) or Zn(II) onto Mn oxides was due to the interchange of structural Mn of the δ-MnO_2 or by exchange with the bound H on δ-MnO_2 surface. Co(II) with the highest amount of Mn release exchanged with both Mn^{2+} and Mn^{3+} in the δ-MnO_2 structure but Zn(II) only exchanged with Mn^{2+} in the δ-MnO_2 structure. However, Ca(II) could only adsorb on the surface by exchange with bound H. At pH values > 6, the uptake of Co(II) or Zn(II) by δ-MnO_2 increased sharply with increasing pH. The authors believed that the additional Co(II) or Zn(II) adsorption was due to either the adsorption of hydroxylated species ($CoOH^+$ or $ZnOH^+$) or surface precipitation of $Co(OH)_2$ or $Zn(OH)_2$.

Table 2.1. ZPC of Manganese Dioxides Tested by Healy et al. (1966)

Name	ZPC by electrophoresis	ZPC by coagulation	Properties
δ-MnO_2 (birnessite)	NA	1.5 ± 0.5	Oxygen to manganese ratio grater than 1.9. BET surface area about 300 m^2/g.
Mn^{II}-manganite (manganous manganite or 10 A manganite)	~2.5 (Extrapolated)	1.8 ± 0.5	Oxygen to manganese ratio 1,7 to 1.9. Formula $3MnO_2Mn(OH)_2\ nH_2O$ BET surface area about 30-50 m^2/g.
α MnO_2 (cryptomelane)	4.6 ± 0.2	4.6 ± 0.2	Formula KMn_8O_{16} or $NaMn_8O_{16}$
γ MnO_2 (electrolytic MnO_2)	5.6 ± 0.2	5.5 ± 0.2	Typical formula $MnO_{1.93}$
β MnO_2 (pyrolusite)	7.3 ± 0.2	7.3 ± 0.2	Formula MnO_2

The authors also believed that the OH concentration at the oxide-solution interface was higher than the concentration in the bulk phase, therefore, surface precipitation occurred at pH values lower than the pH values that would be expected in the solution. Finally, the authors demonstrated that the electrophoretic mobility of δ-MnO_2 in the presence of high Zn(II) concentration was similar to a $Zn(OH)_2$ precipitate.

Results form these studies indicate that Fe or Mn oxides could be used as an effective adsorbent for metal removal and adsorbed metals can be recovered and reused.

In all of the adsorption processes noted, the soluble metal concentration depends on the adsorbate:adsorbent ratio. Increasing the adsorbent concentration will increase uptake, so it is possible to remove metals to trace levels. This behavior is in contrast with a precipitation process where soluble metal concentration is fixed by the solubility of the metal. Furthermore, because metal removal is pH dependent in an adsorption process, adsorption should be reversible. Therefore, adsorption processes could be used to not only remove but also recover and recycle metals. On the other hand, in a precipitation process, it is difficult to recover and recycle metals from sludge. These observations suggest that adsorption processes have the potential to overcome many of the limitations associated with precipitation treatment methods.

However, a limitation of adsorption processes is solid separation and sludge management. A typical oxide adsorbent is a colloidal particle that is difficult to remove from water. Separation processes such as flotation or sedimentation are available, but these process usually require additional chemical treatment to destabilize the particles. These added chemicals would increase the cost of the overall treatment process and also

may interfere with subsequent metal recovery and recycle. Even if the separation step is successful, the resulting sludge requires an additional treatment. One possible solution for this problem is using a composite adsorbent.

2.2.3 Coatings/Composites. Although Edwards and Benjamin (1989a) reported that an adsorption treatment process was feasible, one of the major limitations of this process was the step of solids separation. One solution to this problem is to prepare a granular adsorbent that can be used in a column process. Based on this concept, several composite adsorbents have been synthesized and evaluated for this purpose, such as Fe^{2+} treated activated carbon (Huang and Vane 1989), Fe-coated sand (Edwards and Benjamin 1989b, Stahl and James 1991a), Mn oxide-coated sand (Stahl and James, 1991b), granular iron oxide (Theis *et al.* 1992), and Fe-coated GAC (Wang *et al.* 1994). These studies will be briefly reviewed in the following paragraphs.

Fe(II) Treated GAC. Huang and Vane (1989) used Fe^{2+} treated activated carbon to remove As^{5+}. Fe^{2+} treated activated carbon was prepared by soaking activated carbon in an aqueous ferrous perchlorate solution for 4 h, followed by rising with distilled water. After the rinse, the treated activated carbon was dried in an oven at 80 ° C overnight then cooled to room temperature until further usage. The authors showed that a ten-fold increased in removal could be achieved under the optimal pretreatment conditions when compared to the untreated activated carbon. The improved removal was attributed to the formation of ferrous arsenate surface complexes and not to the formation

of precipitates in the bulk solution. They also showed that ferrous salts could be used to regenerate the spent activated carbon after it was stripped with acid.

Fe Coated Sand. Edwards and Benjamin (1989b) studied adsorption of Cu, Ni, Cr(III), Cd, and Pb onto an Fe oxide-coated sand in a column process. They prepared the composite adsorbent by precipitating Fe oxide in a suspension of sand through alkaline or evaporative precipitation methods. Evaporative precipitation resulted in a higher Fe oxide coating and the resulting coating was more durable in a mild acid solution. The coated sand could remove a significant amount of metal at lower pH, and almost completely remove all metals above pH 8.0. Following an adsorption step the adsorbent was regenerated at pH 3. The authors reported that desorption efficiencies were 63, 83, 91, 100, and 100 % for Cr(III), Pb, Ni, Cd, and Cu, respectively. They also believed that any retained metals would not affect subsequent adsorption steps.

Stahl and James (1991a) studied zinc sorption by iron-oxide-coated sand. They prepared goethite-coated sand (GS) and hematite-coated sand (HS). GS was prepared by the following method: Goethite was precipitated on 500 g acid-washed sand by adding 87.5 mL of 0.17 M $Fe(NO)_3$ and 90 mL of 0.52 M NaOH in an evaporating dish, then the mixture was placed in a drying oven for 72 h at 105 °C. HS was transformed from GS by heating at 500 °C in a muffle furnace for 120 h. Surface areas for uncoated sand, GS and HS were about 4.5, 5.4, and 6.1 m^2/g, respectively. The net surface charges (PZNC) of GS and HS were also calculated by determining the difference between the means of the cation exchange capacity (CEC) and anion exchange capacity (AEC) at a given pH, and

regressing these values against pH. The *x* intercepts of the linear equations were interpreted as the effective PZNCs for the surfaces. The PZNCs calculated for GS and HS were 7.8 and 9.6, respectively. CECs of GS and HS increased with pH (4-7.6), however, the authors concluded that the net surface charge was a poor indicator of the amount and form of zinc retained. GS retained the zinc principally in a nonexchangeable form. In contrast, HS retained the zinc in both exchangeable and nonexchangeable forms. The authors showed that the distribution between the exchangeable and nonexchangeable zinc fractions changed from predominately exchangeable to predominately nonexchangeable zinc retention as pH increased in both GS and HS. Their results showed that relative to HS, GS sorbed more zinc due to surface-induced hydrolysis of zinc by surface OH groups. Finally, the authors concluded that the form of sorbed zinc was a function of pH and a function of Fe-oxide mineralogy.

Granular Iron Oxide. Theis *et al.* (1992) used granular iron oxide (0.5-1.0 mm) as an adsorbent to remove lead form drinking water. Granular iron oxide was generated by cementation of iron oxide particles using a binding material. Optimum pH values for lead removal were between 5 and 7. Granular iron oxide, with a 20 m^2 of surface area/g, has an adsorption capacity about 4.3 mg Pb/g adsorbent. The authors also showed that the adsorbent can be regenerated by flushing with an acidic solution (pH 3). During regeneration, for short-duration continuous tests (one to two days), most of the lead was removed rapidly, however, for longer times, some of the lead would gradually buildup within the oxide pores.

Fe Coated GAC. Wang *et al.* (1994) used an Fe oxide-coated granular activated carbon (GAC) to remove Cu(II) from aqueous solution. In this study the Fe oxide coating was formed through evaporative precipitation of $Fe(NO_3)_3$ in a suspension of GAC. Relative to a discrete Fe oxide, adsorption capacity per gram of Fe present in the composite adsorbent had a significantly higher capacity. The authors suggested that this enhanced capacity may be because spreading the Fe oxide on the GAC surface created an adsorbent with a higher site density, or because the coated and discrete Fe oxides were not the same. In a column process, the adsorbent was able to decrease Cu(II) concentration form 100 ppb to less than 3 ppb. The authors also demonstrated that the adsorbent could be reused through at least 15 adsorption and desorption cycles without significant adsorption capacity loss. Furthermore, although a fraction of adsorbed Cu(II) was retained in the adsorbent after regeneration, there was no apparent adsorption capacity loss in subsequent adsorption cycles.

Mn Coated GAC. Knocke *et al.* (Knocke et al., 1988; Knocke et al., 1991) studied Mn^{2+} adsorption onto Mn oxide-coated filter media in water treatment systems. They produced Mn oxide-coated media by adding HOCl or $KMnO_4$ to a suspension of sand or anthracite coal in a manganese sulfate solution. They reported that higher oxidized media ($MnO_{1.8-2.0}$) were more effective relative to less oxidized media ($MnO_{1.4-1.6}$), and concluded that more Mn oxide coating generally yielded greater

Mn(II) removal. The authors also believed that there was a redox reaction between Mn(II) and the surface $MnO_{2(s)}$ if the pH was higher than 9.

Mn Coated Sand. Stahl and James (1991b) studied zinc sorption by Mn oxide-coated sand which paralleled a previous study that examined iron-oxide coated sand (Stahl and James, 1991a). They prepared two Mn-oxide sands, birnessite-hausmanite-coated sand (BHS) and pyrolusite-coated sand (PS). BHS was prepared by a wet oxidation procedure. The oxide was precipitated by adding 78 mL of 0.5 M $MnCl_2$ and 97 mL of 5.5 M NaOH to 500 g acid-washed quartz sand in a crystallization dish. The mixture was placed in a drying oven at 44 °C for 120 h. PS was prepared by using a dry oxidation procedure. The oxide was formed by adding 90 mL of 2.8 M $Mn(NO_3)_2$ in 15.9 M HNO_3 to 500 g acid-washed quartz sand. The mixture was placed in a drying oven at 105 °C for 24 h then transferred to a muffle furnace at 160 °C for 24 h. Surface areas for uncoated sand, BHS and PS were about 4.5, 5.4, and 6.3 m^2/g, respectively. The net surface charges (PZNC) of BHS and PS were 3.6 and 8.3. They concluded that birnessite-hausmanite and pyrolusite coatings increased Zn sorption on quartz, principally in nonexchangeable form. Relative to PS, both total Zn retention and nonexchangeable Zn sorption were greater on BHS. The CEC of BHS and PS increased with pH (4-7.6), however, the authors also concluded that the net surface charge was a poor indicator of the amount and form of zinc retained.

In summary, an ideal adsorbent for metal removal should have the following properties: Ability to remove metals to trace levels, strong affinity for metals, large metal

adsorption capacity, rapid adsorption kinetics, readily separable form aqueous solution, large enough to be used in a column process, the ability to be reused, and the adsorbed metals can be recovered. Traditional techniques, such as precipitation, do not meet these requirements. Adsorption using oxides can resolve some of these requirements, such as strong affinity for metals and the ability to treat metal to trace levels, but there may be separation problems.

Results from the above studies suggest that a composite adsorbent may resolve these potential problems. Composite adsorbents can be synthesized by forming an oxide surface coating on another solid. The composite adsorbents can be easily separated form aqueous solution after an adsorption process. Concerns about sludge management could be resolved by using the composite adsorbent in a column process. The adsorbent could be reused after regeneration and the metals could be concentrated for recovery. Furthermore, the composite adsorbent could be used to remove heavy metals to trace levels by increasing the adsorbent-adsorbate ratio.

Base on these observations, a composite adsorbent, Mn oxide-coated GAC (MnGAC), was studied in this research. Mn oxides have a strong metal affinity and a large metal adsorption capacity. Unfortunately, Mn oxides typically occur as colloidal particles that can not be used in a column process. GAC which has a very large surface area can be use in a column process, but GAC metal adsorption capacity is relatively small. The composite adsorbent (MnGAC) has advantages of both Mn oxide and GAC. It has a strong metal affinity, and a large metal adsorption capacity, and it can be used in a column process.

2.3 Adsorption Phenomena

Cations can be removed by adsorption onto solid adsorbents such as activated carbons and oxides. Adsorption is the accumulation of species at the interface of two phases, such as liquid-solid, gas-solid, liquid-liquid, or gas-liquid; only the liquid-solid interface will be discussed in here. The adsorbate is the ion or molecule that is removed onto the solid-liquid interface, and the adsorbing phase (solid) is the adsorbent. Physical, chemical, and hydrophobic forces are three major forces that attract adsorbate onto adsorbent (Roth, 1991). Forces of physical adsorption include dipole-dipole, London-vander Waals force, and hydrogen bonding. The forces of physical adsorption are about 10 to 20 Kcal/mol, which is lower than those found in chemical adsorption (about 40-60 Kcal/mol). It is possible for an adsorbate to migrate from one adsorption site to an adjacent site when the adsorbate is adsorbed by physical forces. However, it may not be true in the case of chemical adsorption which is usually site specific and generally can't adsorb more than one layer (Roth, 1991). Many adsorption models have been proposed to described the adsorption processes. Some commonly used equilibrium models and adsorption kinetics will be discussed in the following sections.

2.3.1 Equilibrium Models. Several adsorption models have been developed to describe equilibrium conditions between adsorbates and adsorbents. Adsorption isotherms, such as Freundlich and Langmuir isotherms, can be used to describe the

adsorption capacity of the adsorbent. A surface complex model, which is one commonly used mechanistic model, will also be discussed.

Adsorption Isotherms. The capacity of an adsorbent can usually be described using an adsorption isotherm, which is an expression of distribution of an adsorbate between the adsorbed phase and the solute phase under equilibrium conditions and constant temperature. The most commonly used adsorption isotherms are the Freundlich and Langmuir isotherms (Rubin and Mercer, 1981; Kline 1990, Weber *et al.* 1991, Noll *et al.*, 1992).

The Freundlich isotherm assumes that adsorption is a physical process and has the form:

$$q = KC^n \tag{2.1}$$

Where, K = Freundlich isotherm constant ($(cm^3/mg)^n$)

n = Freundlich isotherm exponent (dimensionless)

q = surface concentration (mg adsorbate/g adsorbent)

This equation can be transformed into a linear form by converting into the following equation.

$$\log q = \log K + n \log C \tag{2.2}$$

In this form, both K and n can be estimated form a log-log plot.

The Langmuir isotherm was derived assuming a monolayer adsorption with a constant adsorption energy and adsorbate that will not migrate on adsorbent surfaces.

$$q = \frac{Q_0 bC}{1 + bC} \tag{2.3}$$

Where, q = surface concentration (mg adsorbate/g adsorbent)

Q_0 = Langmuir isotherm constant related to a maximum surface coverage corresponding to complete monolayer coverage (mg adsorbate/g adsorbent)

b = Langmuir isotherm constant related to the enthalpy of adsorption

Langmuir isotherm constants, Q_0 and b, can be estimated by fitting a set of experimental data to a linearized form of the Langmuir model (equation 2.4), which is the inverse of equation 2.3.

$$\frac{1}{q} = \frac{1}{Q_0} + \frac{1}{bQ_0}\frac{1}{C} \tag{2.4}$$

Complex Model. Surface charges on oxides can result from solid surfaces donating or accepting hydrogen ions (Stumn and Morgan, 1981; Batchelor and Dennis, 1987; Corapcioglu and Huang, 1987).

$$\equiv S\text{-}OH_2^+ \Leftrightarrow \equiv S\text{-}OH + H^+ \quad (2.5)$$

$$K_{a1}^{\,s} = \{\equiv S\text{-}OH\}\,[\,H^+\,] \,/\, \{\equiv S\text{-}OH_2^+\,\} \quad (2.6)$$

$$\equiv S\text{-}OH \Leftrightarrow \equiv S\text{-}O^- + H^+ \quad (2.7)$$

$$K_{a2}^{\,s} = \{\equiv S\text{-}O^-\,\}\,[\,H^+\,] \,/\, \{\equiv S\text{-}OH\,\} \quad (2.8)$$

Where, $\equiv S\text{-}OH_2^+$ = pronated surface hydroxide species

$\equiv S\text{-}OH$ = neutral surface hydroxide species

$\equiv S\text{-}OH^-$ = depronated surface hydroxide species

H^+ = hydrogen ions

$K_{a1}^{\,s}$ = first apparent equilibrium coefficient

$K_{a2}^{\,s}$ = second apparent equilibrium coefficient

{ } = concentration of surface species (mole/kg)

[ ] = concentration of species in aqueous solution (mole/L)

These reactions are analogous to proton exchange reactions in solution. However, acid reactions in solution are not exactly the same as these reactions, because these apparent equilibrium coefficients are not constant. These constants will vary with surface charge, because the rate of surface reactions should depend on the concentrations of reactants at the surfaces not concentrations in solution. Equations (2.6) and (2.8) can be modified as shown by the following equations.

$$\equiv S\text{-}OH_2^+ \Leftrightarrow \equiv S\text{-}OH + H^+_S \tag{2.9}$$

$$K_{a1}{}^S(int) = \{\equiv S\text{-}OH\}\,[H^+]_S \,/\, \{\equiv S\text{-}OH_2^+\} \tag{2.10}$$

$$\equiv S\text{-}OH \Leftrightarrow \equiv S\text{-}O^- + H^+_S \tag{2.11}$$

$$K_{a2}{}^S(int) = \{\equiv S\text{-}O^-\}\,[H^+]_S \,/\, \{\equiv S\text{-}OH\} \tag{2.12}$$

Where, $K_{a1}{}^S(int)$ = first intrinsic acidity coefficients of surface hydroxides

$K_{a2}{}^S(int)$ = second intrinsic acidity coefficients of surface hydroxides

$[H^+]_S$ = concentration of hydrogen ion at solid surface (mole/L)

In contrast with apparent equilibrium coefficients, the intrinsic acidity coefficients are constants and they will not vary with the surface charge. These surface

charges are strongly pH-dependent. At low pH, the surface has a positive charge; at high pH, the surface has a negative charge.

If the H^+ and OH^- are the only adsorbing ions in the system, the surface charge can be expressed as the following.

$$\sigma_0 = F\,(\Gamma_{H}{}^{+} - \Gamma_{OH}{}^{-}) \qquad (2.13)$$

Where, σ_0 = surface charge (coulomb/m^2)

F = Faraday constant (96500 coulomb/mol)

$\Gamma_{H}{}^{+}$ = adsorption density of H^+ (mol/ m^2)

$\Gamma_{OH}{}^{-}$ = adsorption density of OH^- (mol/m^2)

The pH where surface charge (σ_0) or ($(\Gamma_{H}{}^{+} - \Gamma_{OH}{}^{-})$ equals zero is called the zero point of charge (pH_{zpc}). When the pH of the solution is less than the pH_{zpc}, the surface charge will be positive and the surface is more likely to adsorb anions. If the pH higher than the pH_{zpc}, the surface has a negative charge and favors the adsorption of cations.

Cations ions (M^{z+}) can be adsorbed onto solid surfaces by formation of surface complexes. Cations compete with hydrogen ions for available adsorption sites.

$$\equiv S\text{-}OH + M^{z+} \Leftrightarrow \equiv S\text{-}OM^{(z-1)+} + H^{+} \quad (2.14)$$

$$^{*}K_{ml}{}^{S} = \{ S\text{-}OM^{(z-1)+}\}[H^{+}] / \{\equiv S\text{-}OH\}\{ M^{z+}\} \quad (2.15)$$

or

$$2 \equiv S\text{-}OH + M^{z+} \Leftrightarrow (\equiv S\text{-}O)_2M^{(z-2)+} + 2H^{+} \quad (2.16)$$

$$^{*}K_{ml}{}^{S} = \{(\equiv S\text{-}O)_2M^{(z-2)+}\}[H^{+}]^2 / \{\equiv S\text{-}OH\}^2 \{ M^{z+}\} \quad (2.17)$$

Furthermore, metal ions can also be adsorbed as metal-ligand complexes form solution.

2.3.2 Adsorption Kinetics. Adsorption onto porous particle (e.g. oxides or activated carbons) can be generally divided into three steps: external diffusion, internal diffusion, and physical or chemical adsorption process (Thacker *et al.*, 1981; Froment and Bischoff, 1990; Noll *et al.*, 1992).

1. External diffusion (or film diffusion): Transfer the adsorbate from the bulk solution to the external surface of the particle through a stagnant boundary layer (liquid film).

2. Internal diffusion (pore or/and surface diffuison): Transfer the adsorbate within the particle by diffusion of the adsorbate through fluid in the pores (pore diffusion) and/or by migration of adsorbates along the pore surface (surface diffusion).

3. Physical or chemical adsorption: The adsorbate on the internal surface site of the particle. This step is usually believed to be fast compared to steps 1 and 2.

In film theory, the external film mass transfer coefficient (K_f) is related to the free liquid diffusivity of the adsorbate (D_l) and the thickness of the boundary layer (δ).

$$K_f = D_l/\delta \tag{2.18}$$

The difficulty with this theory is that there is no simple way to predict the thickness of the boundary layer. However, there are several ways to estimate the external film mass transfer coefficient; one of them is using mass transfer correlations (McKay *et al.*, 1986; Crittenden *et al.*, 1987). For example, the following correlation can be used to estimated K_f in a fixed bed system (Crittenden *et al.*, 1987).

$$K_f = 2.4\ V_s / (Sc^{0.58}\ Re^{0.66}) \tag{2.19}$$

$$Re = 2\ R\ \rho_l\ V_s/(\varepsilon\mu) \tag{2.20}$$

$$Sc = \mu/(\rho_l D_l) \tag{2.21}$$

(Valid for $0.08 < Re < 150$ and $150 < Sc < 1300$)

Where, V_s= superficial loading velocity (L/t)

Sc = Schmidt number (dimensionless)

Re = Reynolds number (dimensionless)

ρ_1 = fluid density (M/L^3)

ε = porosity of fixed bed (dimensionless)

μ = viscosity of the fluid (centipose)

D_l = liquid phase diffusivity (L^2/t)

Internal diffusion can be classified as pore diffusion, surface diffusion, or combined diffusion (Thacker *et al.*, 1981; Noll *et al.*, 1992).

Pore Diffusion Model. This model assumes that the adsorbate diffuses into the pores of the particle then it adsorbs onto the pore surface of the particle. For a spherical particle with a constant diffusivity, the pore diffusion equation can be derived from a mass balance.

$$\rho_p \frac{\partial q}{\partial t} + \varepsilon_p \frac{\partial C_p}{\partial t} = \frac{\varepsilon_p D_p}{r^2} \frac{\partial}{\partial r}\left(r^2 \frac{\partial C_p}{\partial r}\right) \tag{2.22}$$

Where, q = surface concentration (M/M)

C_p = concentration in the pore space (M/L^3)

D_p = pore diffusivity (L^2/T)

ρ_p = particle density (M/L^3)

ε_p = intraparticle porosity (dimensionless)

r = radial distance (L)

t = time (T)

Surface Diffusion Model. This model assumes that the adsorbate on the surface of the particle migrates from site to site. Assuming a spherical particle and a constant surface diffusivity, the mass balance yields:

$$\rho_p \frac{\partial q}{\partial t} + \varepsilon_p \frac{\partial C_p}{\partial t} = \frac{\rho_p D_s}{r^2} \frac{\partial}{\partial r}\left(r^2 \frac{\partial q}{\partial r}\right) \tag{2.23}$$

where, D_s = surface diffusivity (L^2/T)

Assuming that the surface concentration is higher than the concentration in the pore fluid, this model can be further simplified as the following equation.

$$\frac{\partial q}{\partial t} = \frac{D_s}{r^2} \frac{\partial}{\partial r}\left(r^2 \frac{\partial q}{\partial r}\right) \tag{2.24}$$

This equation is often referred to as the homogeneous solid diffusion model (HSDM) (Thacker *et al.*, 1981).

Combined Diffusion Model. If both pore and surface diffusions are important, the internal diffusion can be expressed by a combined diffusion model with constant diffusivities.

$$\rho_p \frac{\partial q}{\partial t} + \varepsilon_p \frac{\partial C_p}{\partial t} = \frac{\varepsilon_p D_p}{r^2} \frac{\partial}{\partial r}\left(r^2 \frac{\partial C_p}{\partial r}\right) + \frac{\rho_p D_s}{r^2} \frac{\partial}{\partial r}\left(r^2 \frac{\partial q}{\partial r}\right) \tag{2.25}$$

Among these diffusion model, the homogeneous solid surface diffusion model (HSDM) is one of the most widely used models for activated carbons (Thacker *et al.*, 1981; Traegner and Suidan 1989; Wang and Roy, 1993; Roy *et al.*, 1993).

2.3.3 Adsorption Modeling for Batch and Column Process. Adsorption processes both in batch and column systems have been successfully modeled by the HSDM (Traegner and Suidan 1989; Thacker *et al.*, 1981). The HSDM is based on the following assumptions: The adsorbent is a homogenous spherical particle, intraparticle transport can be described by surface or solid diffusion, liquid-diffusion resistance (liquid film) exists at the external surface of the adsorbent, and local equilibrium occurs at the external surface of an adsorbent particle and can be described by a Freundlich isotherm.

Equations describing a batch system are (Thacker *et al.*, 1981):

$$\frac{\partial q}{\partial t} = \frac{D_s}{r^2} \frac{\partial}{\partial r}\left(r^2 \frac{\partial q}{\partial r}\right) \tag{2.26}$$

$$@\ t = 0,\ q = 0 \tag{2.27}$$

$$@\ t \geq 0,\ r = 0,\ \frac{\partial q}{\partial r} = 0 \tag{2.28}$$

$$@\ t \geq = 0,\ R = 0,\ \frac{R^2 K_f (C - C_s)}{\rho} = \frac{\partial}{\partial t}\int_0^R qr^2 dr \tag{2.29}$$

$$\text{or } \rho D_s \left.\frac{\partial q}{\partial r}\right|_{r=R} = K_f (C - C_s) \tag{2.30}$$

$$@\ r = R,\ q = K\ C^n \tag{2.31}$$

$$\frac{dC}{dt} = -\frac{3XK_f}{V\varepsilon R\rho}(C - C_s) \tag{2.32}$$

$$@\ t = 0,\ C = C_o \tag{2.33}$$

Where, C = Solution concentration (mg Cu(II)/L)

C_o = Initial concentration (mg Cu(II)/L)

C_s = Solution concentration at external surface of particle (mg Cu(II)/L)

D_s = Surface diffusivity (cm^2/s)

K = Freundlich isotherm constant

K_f = Film transfer coefficient (cm/s)

n = Freundlich isotherm exponent

q = Surface concentration (mg Cu(II)/g adsorbent)

r = Radial distance (cm)

R = Particle radius (cm)

t = Time (s)

V = Solution volume (L)

X = Mass of adsorbent (g)

ρ = Apparent density of particle (g/L)

ε = Porosity of batch reactor

Equations (2.26-31) are the homogeneous solid diffusion equations and equations (2.32-33) are a mass balance for the batch reactor. Two physical parameters (K_f and D_s) can be determined by minimizing the difference between the experimental values and the model calculated values.

A mass balance equation for a column process can be described by the following equations (Weber *et al.*, 1991; Thacker *et al.*, 1981).

$$\frac{dC}{dt} = -D_h \frac{\partial^2 C}{\partial z^2} - v\frac{\partial C}{\partial z} - \frac{3(1-\varepsilon_B)}{\varepsilon_B R} K_f (C - C_s) \tag{2.34}$$

This equation can be further simplified by assuming that dispersion in the column is negligible.

$$\frac{dC}{dt} = -v\frac{\partial C}{\partial z} - \frac{3(1-\varepsilon_B)}{\varepsilon_B R} K_f (C - C_s) \tag{2.35}$$

$$@\ t = 0,\ 0 \le z \le L_b,\ C = 0 \tag{2.36}$$

$$@\ t = 0,\ z = 0,\ C = C_o \tag{2.37}$$

Where, D_h = Dispersion coefficient (cm^2/s)

L_b = Bed length (cm)

v = Average linear velocity (cm/s)

z = Axial distance (cm)

ε_B = Porosity of fixed-bed

A column process can be modeled by solving equations (2.26-31) and (2.35-37). Equations (2.26-31) are HSDM and equations (2.35-37) are the mass balance equation around the column.

In summary, metals can be removed by adsorption onto solid adsorbents such as activated carbon or oxides. The adsorption method might overcome some of the problems encountered by the traditional precipitation method. However, activated carbon has a relatively small amount of metal adsorption capacity and a small metal affinity compared to oxides. On the other hand, oxides are typically in the form of colloidal particles that can not be used in a column process. Results from the above studies suggest that a composite adsorbent may resolve these potential problems. A composite adsorbent, Mn oxide-coated GAC (MnGAC), was studied in this research. The composite adsorbent (MnGAC) has advantages of both Mn oxide and GAC. It has a strong metal affinity, and a large metal adsorption capacity, and it can be used in a column process. Some commonly used adsorption equilibrium models such as Freundlich isotherm, Langmuir isotherms and surface complex were discussed. Adsorption onto porous particle can be described by the homogeneous surface diffusion model (HSDM). Both batch and fixed batch adsorption systems will be studied and modeled by the HSDM in this research.

CHAPTER III

MATERIALS AND METHODS

This chapter includes two sections, adsorbent preparation and adsorbent characterization. Composite adsorbents (MnGAC) were prepared by coating Mn-oxide onto GAC. The adsorbents were characterized by adsorption isotherms, adsorption edge tests, multiple adsorption/regeneration tests, and batch and column tests. Reagent grade chemicals were used throughout this study unless specified, and all labware was acid washed and thoroughly rinsed with double distilled water (DDW).

3.1 Adsorbent Preparation

Composite adsorbents (MnGAC) were prepared by coating Mn oxide onto granular activated carbon (GAC). Three coating methods (adsorption, precipitation, and dry oxidation) were developed in this research. These composite adsorbents were prepared following techniques similar to those described by Knocke *et al.* (1988) or Stahl and James (1991b).

3.1.1 Coating Method I : Adsorption Method. Several composite adsorbents were prepared following techniques similar to those described by Knocke *et al.* (1988). GAC was first mixed with a known amount of $MnSO_4$ and NaOH solutions for 0.5-4 h, then the resulting mixture was mixed with HOCl and NaOH solutions for additional 0.5-4

h. During the coating process, Mn ions first adsorbed onto GAC surfaces and then were oxidized to Mn oxide by addition of HOCl. The mixture was placed in an oven at 60 °C for 3 days than washed with DDW until the run off was clear. The resulting composite was placed in an oven at 105 °C for 3 days then stored at room temperature.

Five different activated carbons (HD3000, SGL, F400, APC, and WVB) were studied. A more detailed description of these activated carbons is listed in Table 3.1.

3.1.2 Coating Method II: Precipitation Method. Nine composite adsorbents were prepared following techniques similar to those described by Stahl and James (1991b). Mn oxide was precipitated on the GAC surfaces by evaporation. Fifty g of GAC was submerged in DDW for 24 h. The solid was removed and mixed with 50 mL of 1 M manganese salt solution (see below) and 100 mL of 5 M NaOH solution. The mixture was placed in an oven at 90 °C for 3 days than washed with DDW until the run off was clear. The resulting composite was placed in an oven at 105 °C for 3 days then stored at room temperature.

Three GACs (WVB, APC, TOG) and three manganese salts (manganese nitrate (N), manganese sulfate (S), and manganese chloride (C)) were evaluated in this coating process. GAC was sieved into 20*40 ranges (average particle size = 0.5 mm) before coating. Characteristics of these GAC are shown in Table 3.2.

Table 3.1. Characteristics of Activated Carbons Used in the Adsorption Method. Data are from the GAC supplier's bulletins.

Carbon*	HD3000	SGL	F400	APC	WVB
Raw material	Lignite coal	Bituminous coal	Bituminous coal	Bituminous coal	Wood
Particle size (mm)	0.59-2.38	0.59-2.38	0.42-1.68	0.42-1.68	0.71-2.00
Surface area (m^2/g)	625	900-1100	900-1100	1525	1400-1600
Pore Volume (m^3/g)	0.93	0.85	0.85-0.95	1.00	1.1

*SGL, F400 and APC were manufactured by Calgon Carbon Corporation. HD3000 was provided by American Norit Company, Inc. and WVB was supplied by Westvaco.

Table 3.2. Characteristics of Activated Carbons Used in the Precipitation and Dry Oxidation Methods. Data are from the GAC supplier's bulletins except as noted.

Carbon*	TOG	APC	WVB
Raw material	Bituminous coal	Bituminous coal	Wood
Average particle size** (mm)	0.5	0.5	0.5
Surface area (m^2/g)	800-900	1525	1400-1600
Pore Volume (m^3/g)	0.82	1.00	1.1

*TOG and APC were manufactured by Calgon Carbon Corporation and WVB was supplied by Westvaco.

**Activated carbons were sized into mesh sizes 24*40.

3.1.3 Coating Method III: Dry Oxidation Method. One composite adsorbent was prepared following techniques similar to those described by Stahl and James (1991b). MnTOG was prepared by mixing 50 g of TOG, 50 mL of 1 M $Mn(NO_3)_2$, and 100 mL of 70 % HNO_3. This mixture was dried in an oven for 3 days at 105 °C to remove excess solution then dried at 160°C for 3 more days. The resulting composite adsorbent was washed with DDW adjusted to pH 3 with HNO_3, then dried again at 105 °C before further tests. TOG was sized (20*40 mesh size), washed, and dried (200 °C) before coating.

The amount of Mn oxide coating on GAC was determined by extraction tests (Knocke et al., 1988). Samples of coated activated carbon (MnGAC) were agitated for 24 h in a 10% hydroxyl amine sulfate solution (adjusted pH<2). The resulting solution was analyzed by atomic absorption spectrophotometry (AAS). The average amount of coating was based on triplicate tests.

3.2 Adsorbent Characteristics

All tests were conducted in 0.01 N $NaNO_3$ (background electrolyte) with a known amount of Cu(II) or Cd(II). Some tests were conducted with a 1 or $4*10^{-4}$ M $NaHCO_3$ buffer present.

Adsorption capacities were determined from adsorption isotherm and adsorption edge tests. For adsorption isotherm tests, a known amount of adsorbent was added into a series of 250 mL bottles that contained a known amount of Cu(II)or Cd(II), 1 or

$4*10^{-4}$ M $NaHCO_3$, and 0.01 N $NaNO_3$ adjusted to pH 6. These bottles were rotated for 3, 7, 14 or 28 days in a shaker and pH was repeatedly adjusted to 6 throughout the experimental period. Cu(II) or Cd(II) was analyzed by AAS at the end of the test. Adsorption capacity (amount of Cu(II) or Cd(II) adsorbed on the MnGAC divided by the amount of MnGAC) was determined form a mass balance. For adsorption edge tests, experimental procedures were similar to adsorption isotherm tests except that the bottle solutions were adjusted to various specific pH values.

The zero point of charge (ZPC) of an adsorbent was also estimated. A known amount of adsorbent was added into a series of 100 mL bottles that contained 0.01 N $NaNO_3$ and various amounts of acid or base. These bottles were rotated for 2 days in a shaker and pH was measured and recorded at the end of the test, then the ionic strength was adjusted to 0.1 N $NaNO_3$ by adding 2 mL of 5 N $NaNO_3$ into each bottle. These bottles were rotated for 2 more days in the shaker and final pH was measured. pH_{zpc} was obtained by calculating the mean surface charge.

Multiple adsorption/regeneration tests were used to test the reusability of the adsorbent and the recovery of adsorbed Cu(II). A known amount of adsorbent (0.1 g) was added into a 250 mL bottle that contained 4 mg Cu(II)/L, 0.01 N $NaNO_3$, and $4*10^{-4}$ N $NaHCO_3$ adjusted to pH 6. The bottle was rotated for 3 days in a shaker and pH was repeatedly adjusted to 6 throughout this period. At the end of the test, the solution was adjusted to pH 3 by adding HNO_3 and the sample was rotated for 1 day after taking a 10 mL sample. The purpose of this step was to recover adsorbed Cu(II)

and regenerate the adsorbent. After regeneration, the solution was decanted and fresh Cu(II) solution was added to start another adsorption/desorption cycle.

Batch tests were designed to study the kinetics for adsorption of Cu(II) or Cd(II) onto MnGAC. These tests were conducted in a 2 L beaker that contained a known amount of Cu(II) or Cd(II), 0.01 N $NaNO_3$, and 1 or $4*10^{-4}$ N $NaHCO_3$ adjusted to pH 6. MnGAC was pre-equilibrated with a buffer solution (0.01 N $NaNO_3$, and 1 or $4*10^{-4}$ N $NaHCO_3$ adjusted to pH 6) before the test. This solution was completely mixed by a fixed propeller during the experiment. Samples were collected periodically and analyzed for Cu(II) or Cd(II).

Another kinetic study was conducted in a fixed-bed column test. A 2.54 cm diameter polymethylmethacrylate column was filled with a known amount of MnGAC and Cu(II) or Cd(II) solution was fed from the bottom of the column. The adsorption bed was pre-equilibrated with the buffer solution (0.01 N $NaNO_3$, and $4*10^{-4}$ N $NaHCO_3$ adjusted to pH 6) then switched to a 2 ppm Cu(II) or 1 ppm Cd(II) solution with 5 mL/min flow rate. Samples were collected periodically and analyzed for Cu(II) or Cd(II).

A quality assurance program was performed to ensure the quality of the experimental data. At least 10 % of the samples were analyzed in duplicate. At least 10 % of samples were analyzed for recovery of known additions. A quality control sheet for AAS analysis is shown on the following page.

Quality Control Sheet

Sample ID.: _____

Date: _____

Reference Standards and Calibration:

1. No. of reference standards: _____
2. r^2 = _____
3. Analyzed before and after sample measurements: _____

Samples and Reagent Blanks:

1. No. of samples :_____
2. No. of reagent blanks :_____
3. Was the reagent blanks analyzed periodically during the analysis process? _____

Recovery of Known Addition:

1. No. of known additions: _____(>10% of samples).
2. Results:

No.	Original	Added	Composite	% recovered
___	_____	_____	_____	_____
___	_____	_____	_____	_____
___	_____	_____	_____	_____
___	_____	_____	_____	_____

Analysis of Duplicates:

1. No. of duplicates: _____(>10% of samples)
2. Results:

No.	Original	Added	Composite	% recovered
___	_____	_____	_____	_____
___	_____	_____	_____	_____
___	_____	_____	_____	_____
___	_____	_____	_____	_____

CHAPTER IV

MnGAC PREPARED BY ADSORPTION METHOD

Composite adsorbents (MnGAC) were prepared by coating Mn oxide onto granular activated carbon (GAC). Three coating methods (adsorption, precipitation, and dry oxidation) were developed to prepare MnGAC. This research was divided into two stages. In the first stage, adsorbents were prepared by the adsorption method and the purpose of this stage was to study the properties of the Mn oxide composite adsorbents (MnGAC) and the feasibility of using these adsorbents for metal removal and recovery. Results of this stage will be presented in this chapter. After demonstrating that MnGAC had the potential to become an efficient way to remove metals from metal contaminated wastewater, the next step was to prepare a better MnGAC with a higher adsorption capacity and to further understand the adsorption behaviors of this composite adsorbent. Two more coating methods were developed and studied for this purpose and results of these coatings will be discussed in the following chapters. Adsorption properties of these coated GACs such as adsorption capacity and adsorption kinetics were examined in multiple adsorption/regeneration cycle test, batch and column processes were also examined.

Adsorbents prepared by the adsorption method were subjected to a series of tests such as coating efficiency, adsorption capacity, batch and column tests to evaluate the characteristics of the Mn oxide composite adsorbents (MnGAC).

4.1. Coating Efficiency

Factors affecting Mn oxide coating efficiency are discussed in this section. These factors include type of GAC, pre wash time, Mn applied dosage, and coating time.

Because different characteristics of GAC may have different effects on the coating efficiency, five different activated carbons (HD3000, SGL, F400, APC, and WVB) with a range of different characteristics were selected for this study. These GACs were made from three different raw materials, which included lignite coal, bituminous coal, and wood. Surface areas of these GAC ranged form 625 m^2/g to 1600 m^2/g and pore volume ranged from 0.85 to 1.1 mL/g (Table 3.1). To explore relationships between activated carbon characteristics and coating efficiency, five characteristics of GAC that might affect the results of Mn oxide coatings were evaluated. These characteristics included raw material, particle size, surface area, pore volume, and pH value of activated carbons.

These activated carbons were coated under the following conditions: Applied 14.57 mg Mn/g GAC, prewash time = 0 h, and coating time = 45 min. Results of these coating procedures are listed in Table 4.1. Among these five GACs, WVB had the highest amount of Mn coating (4.84 mg Mn/ g carbon). A statistics test (F test) was performed to examine the relationships between the amount of coating and the factors listed above (Table 4.2). GAC pore volume had a significant relationship with the amount of coating. The higher the total pore volume the higher the coating efficiency (Figure 4. 1).

Coating amount (mg Mn/g GAC) = -6.314 + 9.920 * Pore Volume (mL/g GAC)

Table 4.1. Activated Carbon Characteristics and the Amount of Mn Coating. Data are from the GAC supplier's bulletins except as noted.

Carbon*	HD3000	SGL	F400	APC	WVB
Raw material	Lignite coal	Bituminous coal	Bituminous coal	Bituminous coal	Wood
Particle size (mm)	0.59-2.38	0.59-2.38	0.42-1.68	0.42-1.68	0.71-2.00
Surface area (m^2/g)	625	900-1100	900-1100	1525	1400-1600
Pore Volume (m^3/g)	0.93	0.85	0.85-0.95	1.00	1.1
pH**	4.44	8.09	8.86	6.42	4.9
Coating** (mg Mn/g)	2.91	2.05	2.96	3.09	4.84

*SGL, F400 and APC were manufactured by Calgon Carbon Corporation. HD3000 was provided by American Norit Company, Inc. and WVB was supplied by Westvaco.

**Measured in this study.

Table 4.2. Statistics F Tests for Factors Affecting Coating Efficiencies

(1) Model: Amount of coating = Constant + $\beta 1$ * Surface area of GAC
Hypothesis(Ho): $\beta 1 = 0$ $F(1,3,0.95) = 10.1 > F=1.461$, Accept Ho.

(2) Model: Amount of coating = Constant + $\beta 2$ * pH of GAC
Hypothesis(Ho): $\beta 2 = 0$ $F(1,3,0.95) = 10.1 > F=1.368$, Accept Ho.

(3) Model: Amount of coating = Constant + $\beta 3$ * Pore volume of GAC
Hypothesis(Ho): $\beta 3 = 0$ $F(1,3,0.95) = 10.1 < F=24.794$, Rejected Ho.

(4) Model: Amount of coating = Constant + $\beta 4$ * Particle size of GAC
Hypothesis(Ho): $\beta 4 = 0$ $F(1,3,0.95) = 10.1 > F=0.029$, Accept Ho.

Conclusion: The only significant correlation is

Amount of coating (mg/g) = -6.314 + 9.920 * pore volume (mL/g)

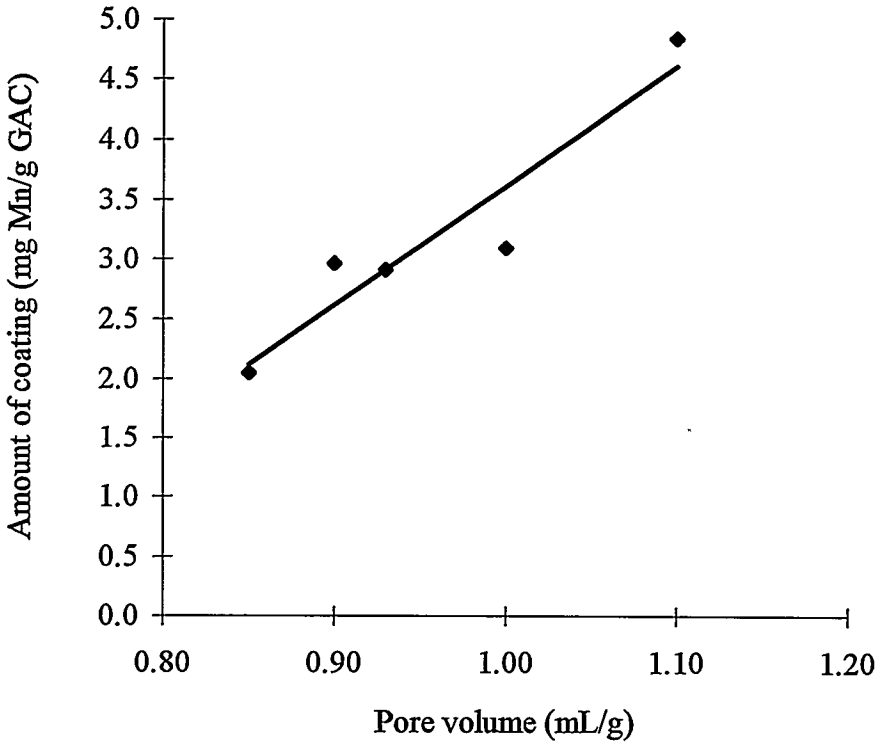

Figure 4.1. Coating Efficiency Versus GAC Total Pore Volume

Total surface area is one of the most commonly cited characteristics for GAC because the total surface area is related to the adsorption capacity. Surprisingly, the total surface area of activated carbons did not have a significant correlation with the amount of coating. For example, F400 and SGL had similar surface areas and pore volumes (Table 4.1) but they had different coating efficiencies. The difference might be caused by different particle sizes. F400 had a smaller particle size with a higher coating efficiency. If the adsorption process is a diffusion controlled process, particle size should have an effect on the coating process. The reason that particle size did not appear to have a significant effect in the previous statistics tests may be because the particle sizes of GAC in these tests were not uniform. For example, HD3000 and SGL had particle size ranging from 0.59 to 2.38 mm, F400 and APC ranged form 0.42 to 1.68 mm, and WVB ranged form 0.71 to 2.00 mm. However, the previous statistics test was based on the average sizes of these particles. Because of this possible discrepancy, an experiment was designed to examine the effect of particle size on coating efficiency.

Three different particle sizes of WVB were coated by the adsorption method under the same conditions. Surface coatings for particle sizes 0.5, 1.0, and 1.4 mm were 24.81, 19.86, and 12.42 mg Mn /g WVB, respectively (Figure 4.2). Smaller size particles had a higher coating efficiency. These results suggest that most of the Mn oxide was spread near the external portion of the activated carbon. Compared to the larger particles, smaller particles of GAC have a larger total external surface area per gram and apparently

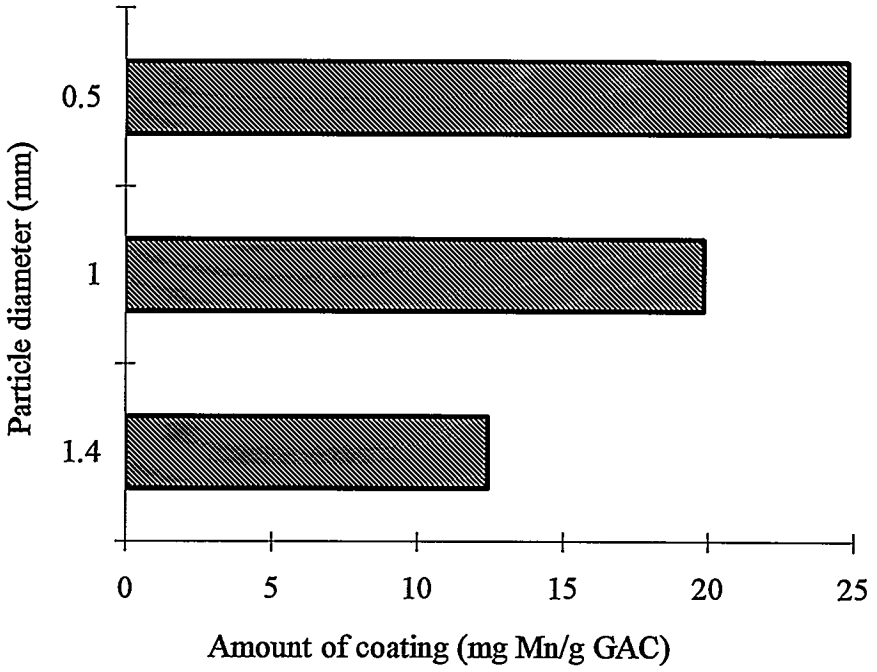

Figure 4.2. Coating Efficiency for Different WVB Particle Sizes. Adsorption method, applied 97 mg Mn/g WVB, prewash time = 24 h, and coating time = 4 h.

a higher coating efficiency. The amount of Mn coatings can be normalized to the external surface area of GAC by assuming that the GAC particles are spheres and the particle density is equal to 1 cm^3/g. The results of these normalizations are shown in Table 4.3.

Table 4.3. Coating Efficiency for Different WVB Particle Sizes. Adsorption method, applied 97 mg Mn/g WVB, prewash time = 24 h, and coating time = 4 h.

Particle size (mm)	Coating (mg Mn/g)	Coating (mg Mn/cm^2 external surface area)
0.50	24.81	41.35
1.00	19.86	66.20
1.40	12.42	57.96

Differences in the amount of coating among different particles are reduced when these values are normalized, suggesting that external surfaces are an important factor for coating efficiency.

The duration of prewash also had an effect on the coating. Coating efficiencies for APC were 8.4, 9.0, and 12.5 % for prewash times of 0, 3, and 24 h, respectively (Figure 4.3). A longer prewash time resulted in a larger amount of coating. One likely reason is that adsorption of Mn(II) onto GAC could be inhibited if the micropores are not saturated with DDW. Another reason might be that the prewash process extracts some impurities contained in the GAC, thus enhancing the coating efficiency. In either case, the prewash with DDW seems to improve the coating process. A longer coating time resulted in a larger amount of coating (Figure 4.4). Five different coating times (0.5, 2, 4, 8, and 24 h) were applied for coating 1.0 mm WVB. A longer coating time resulted a higher amount of coating up to a coating time of 8 h. This result indicates that diffusion into the

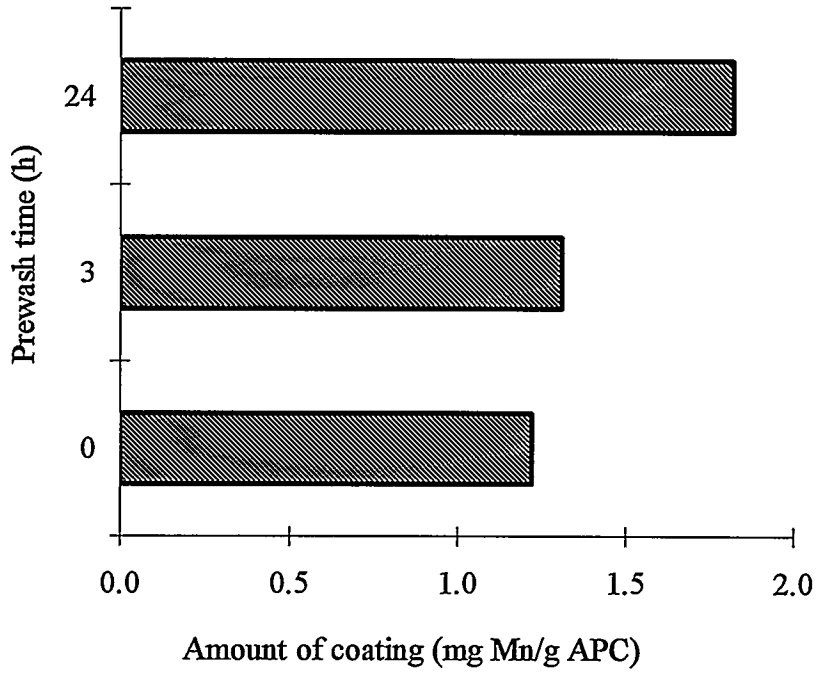

Figure 4.3. Comparison of Coating Efficiency by Various Prewash Time. Applied 14.57 mg Mn/g APC and coating time 45 min.

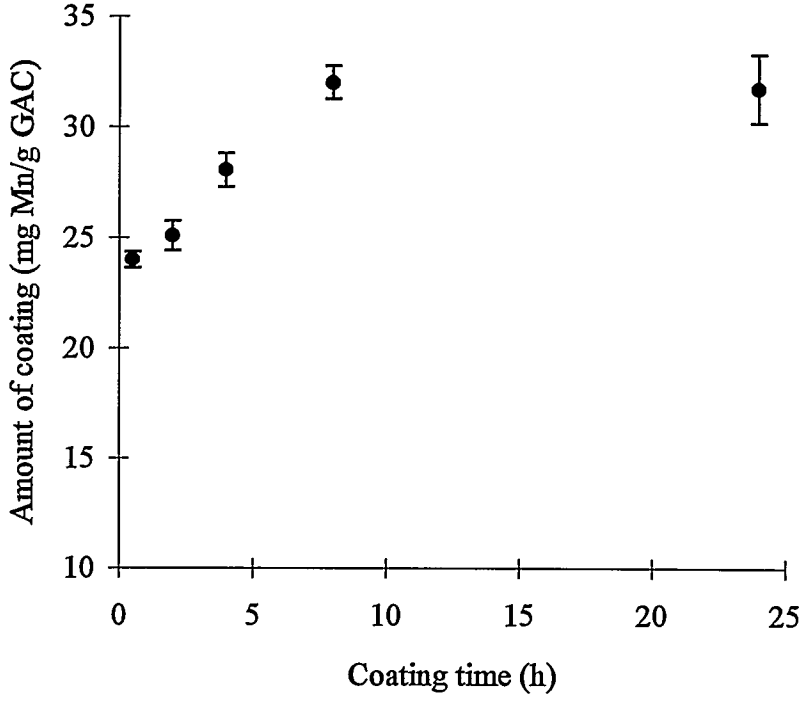

Figure 4.4. Mn Oxide Coating Efficiency onto 1.0 mm WVB at Various Coating Times. Data points are means ± standard deviation for 3 replicates.

particle played an important role in the coating process when the coating time was less than 8 h. However, there was no significant difference between 8 and 24 h, perhaps because the maximum amount of coating was reached at 8 h.

Applied Mn dosage also had an influence on the amount of coating. A range of Mn dosages (from 9 to 273 mg Mn/g WVB) was applied to WVB. A higher Mn applied dosage had a higher amount of coating. However, a higher Mn applied dosage also had a smaller coating efficiency (Figure 4.5). For example, 9 mg Mn/g WVB applied had coating efficiency about 58 % (5.3 mg Mn/g WVB coating) but with 273 mg Mn/g WVB applied only had about 20 % coating efficiency (57.5 mg Mn/g WVB coating).

Factors affecting the amount of coating on GAC were type of GAC, GAC pore volume, GAC particle size, coating time, Mn dosage, and the duration of prewash time. The coating process was a diffusion controlled process. Among five different GACs, WVB had the highest coating efficiency, so WVB was selected for further investigations.

4.2. Adsorption Capacity of MnGAC

Adsorption capacity is one of the most important properties for adsorbents. Factors affecting MnGAC adsorption capacity included type of carbon, solution pH and amount of Mn coating.

Adsorption capacities for the five different MnGACs were evaluated from adsorption isotherms (Figure 4.6). MnWVB had the highest adsorption capacities among

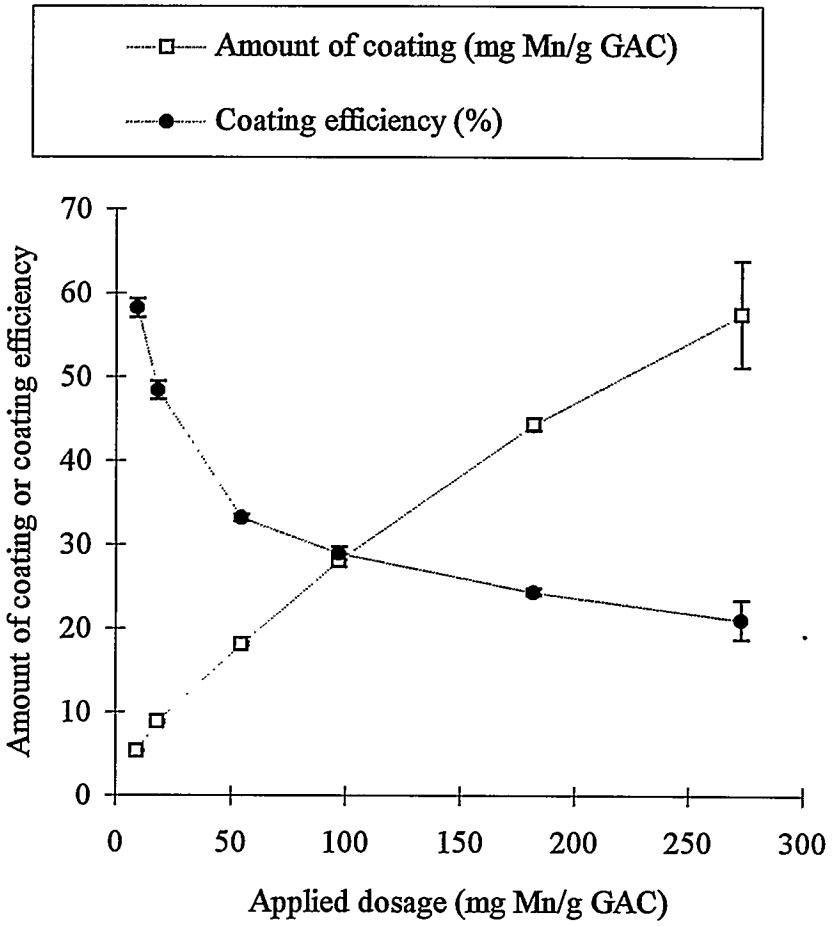

Figure 4.5. Mn Oxide Coating Efficiency onto 1.0 mm WVB at Various Applied Mn Dosages. Data points are means ± standard deviation for 3 replicates.

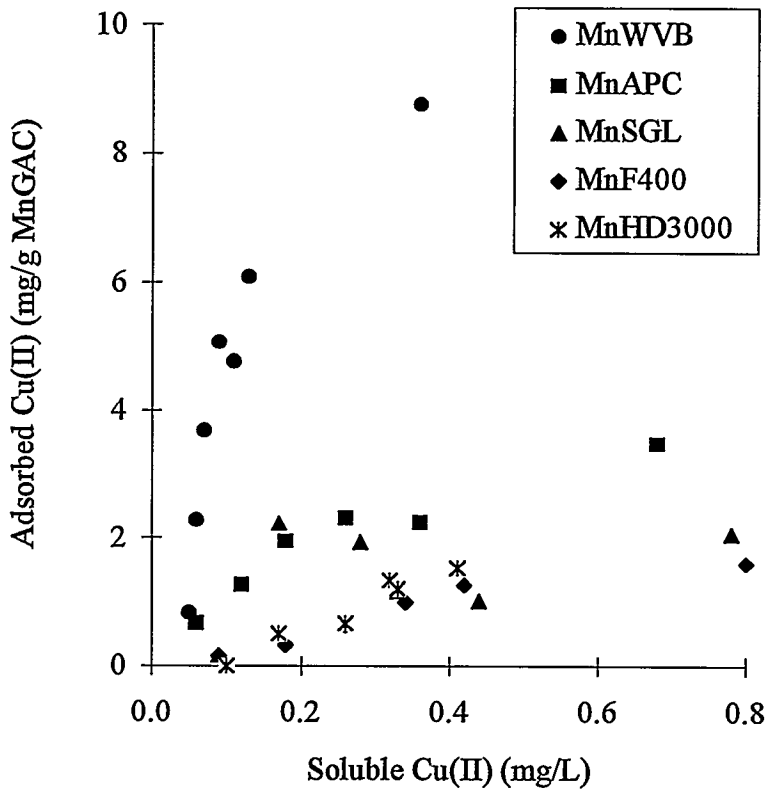

Figure 4.6. Adsorption Isotherms for Five Different MnGAC's. Applied 14.57 mg Mn/g GAC, prewash time = 0 h, and coating time = 45 min.

these MnGACs. It is also true that MnWVB had the highest Mn oxide content. However, if the adsorption isotherms are normalized to Mn content, the relationship between these isotherms still holds, except distances between isotherms becomes smaller (Figure 4.7). The reason that the data do not converge into one line is probably due to some of the Cu(II) being adsorbed by GAC surfaces, because different GACs have different Cu(II) adsorption capacity. Based on the results of these initial tests, MnWVB was the GAC selected for more detailed studies.

A Mn oxide coating of about 20 mg Mn/g solid increased the adsorption capacity of WVB for Cu(II) by at least a factor of three (Figure 4.8). Interestingly, the untreated WVB appeared to be saturated with adsorbed Cu(II), with a capacity of about 2.5 mg Cu(II)/g solid. In contrast, Cu(II) uptake by MnWVB increased with increased solution concentration.

Adsorption isotherms for two different particle sizes of MnWVB (1.0 mm and 1.4 mm) are presented in Figure 4.9. The smaller diameter particle had a greater Mn oxide coating, and a greater Cu(II) adsorption capacity. When these adsorption data were expressed in terms of mg Cu(II) adsorbed per mg of Mn coating (mg Cu/ mg Mn), the isotherms converged into one line (Figure 4.10). Apparently, Mn oxide dominated the adsorption process. This result is in contrast with the previous results for five different MnGACs. In the previous tests, five different carbons were used and each carbon had its own Cu(II) adsorption capacity. When a relatively low amount of Mn oxide was applied, a significant part of the GAC surface was still available for adsorption so that composite

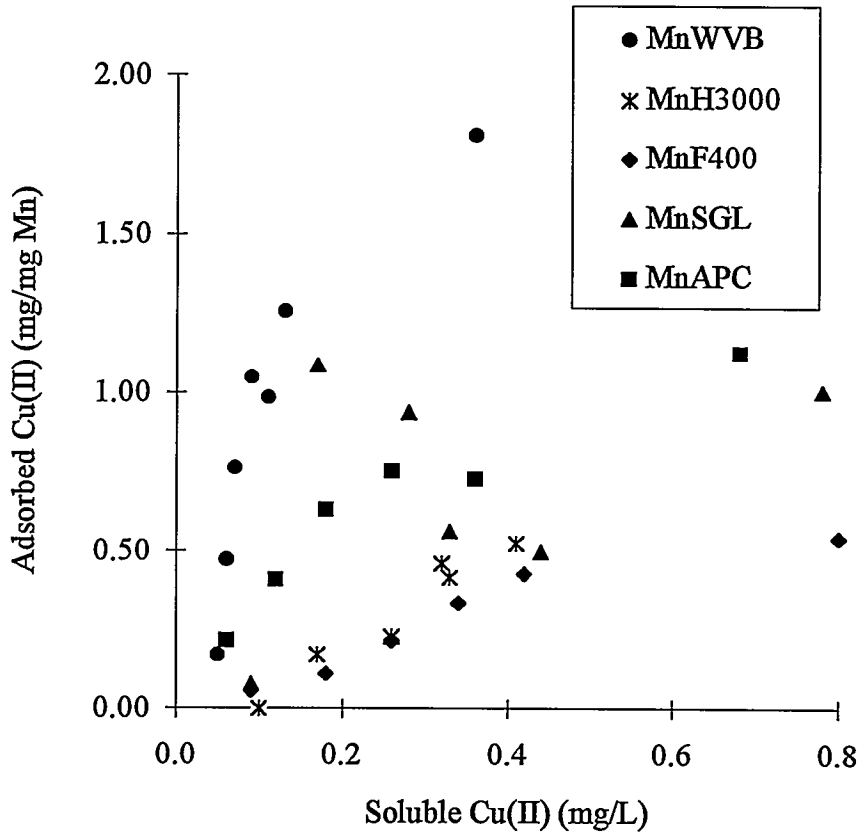

Figure 4.7. Adsorption isotherms (normalized to Mn content) mg Cu(II)/mg Mn) for five different MnGAC's. Applied 14.57 mg Mn/g GAC, prewash time = 0 h, and coating time = 45 min.

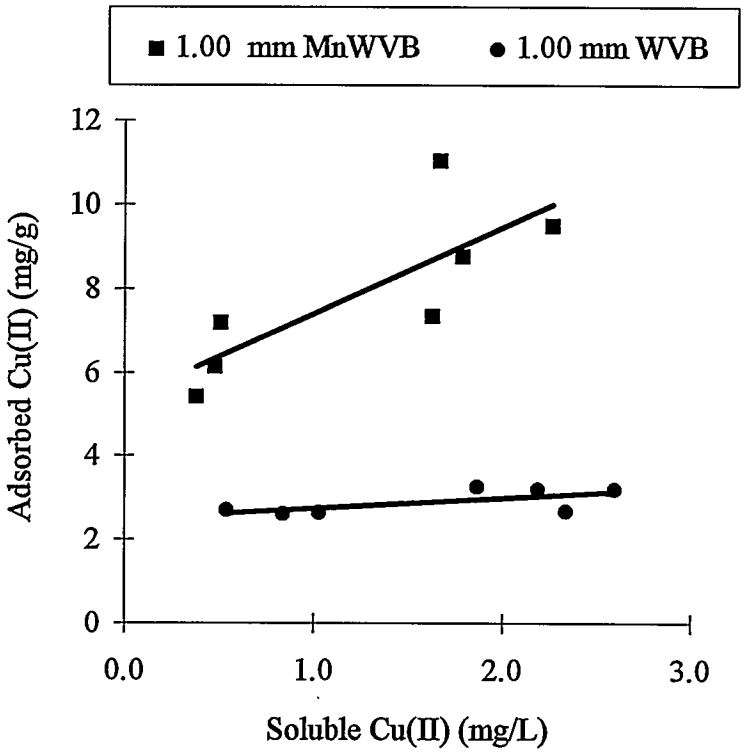

Figure 4.8. Cu(II) Adsorption Isotherms for 1.0 mm MnWVB (19.86 mg Mn/g) and WVB. Solutions were in contact with solids for 7 days at pH = 6, 0.01 N $NaNO_3$, and 10^{-4} N $NaHCO_3$.

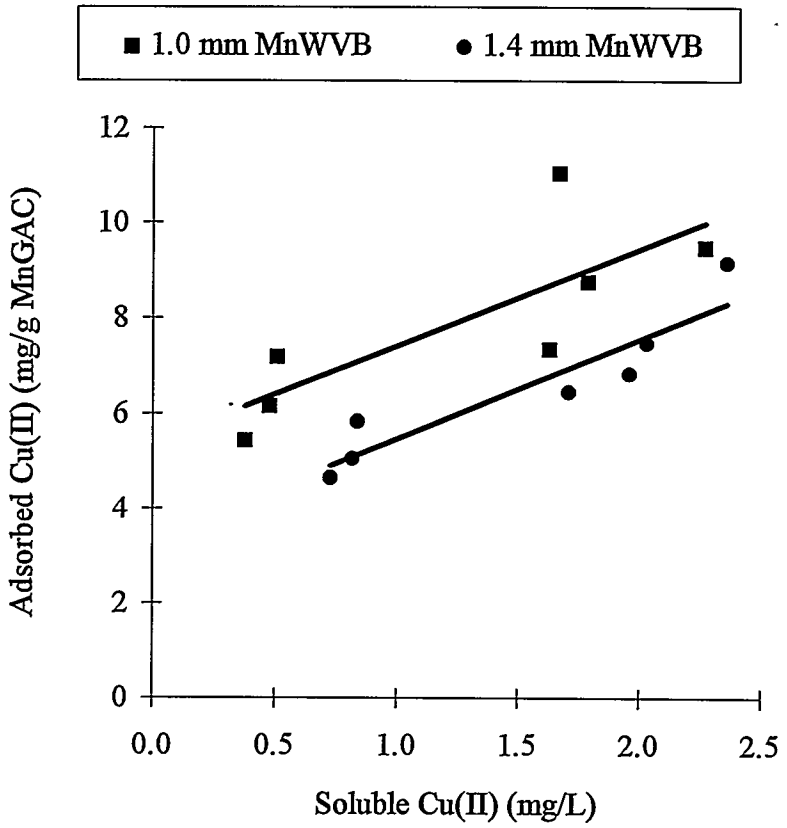

Figure 4.9. Cu(II) Adsorption Isotherms for 1.0 mm MnWVB (19.86 mg Mn/g) and 1.4 mm MnWVB (12.42 mg Mn/g). Solutions were in contact with solids for 7 days at pH = 6, 0.01 N $NaNO_3$, and 10^{-4} N $NaHCO_3$.

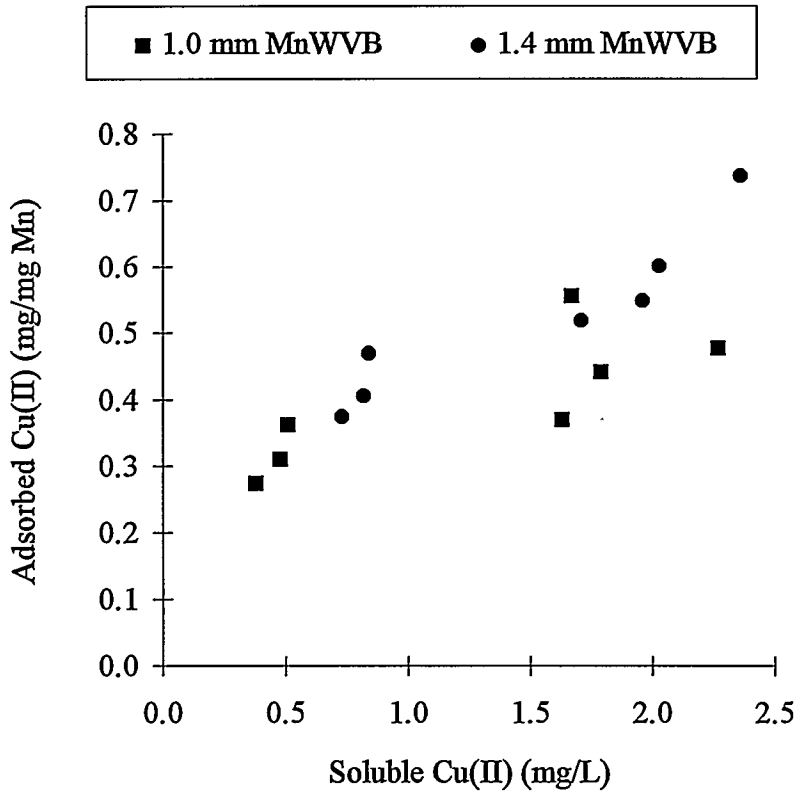

Figure 4.10. Cu(II) Adsorption Isotherms Normalized to Mn Content for 1.0 mm MnWVB (19.86 mg Mn/g) and 1.4 mm MnWVB (12.42 mg Mn/g). Solutions were in contact with solid for 7 days at pH = 6, 0.01 N $NaNO_3$, and 10^{-4} N $NaHCO_3$.

adsorbent reflected part of the GAC character.

The relationship between adsorption capacity and pH was examined in an adsorption edge test (Figure 4.11). A series of 250 mL bottles was filled with 0.1 g MnWVB (19.86 mg Mn/g), 4 mg Cu(II)/ L, 0.01 N $NaNO_3$ solution, then adjusted to a range of pH values (from 3 to 7). These bottles were rotated in a shaker for 24 h, after which there was almost 100 % Cu(II) removal at pH 7 and only a small amount of adsorption below pH 4. This result is typical for an adsorption edge curve for oxides (Stumm and Morgan, 1981; Batchelor and Dennis, 1987). The extent of adsorption of Cu(II) is strongly pH-dependent. A higher pH value has a better Cu(II) removal. This curve also suggests that it is possible to recover the adsorbed metal by changing pH values.

The relationship between Cu(II) adsorption capacity and the amount of coating was also studied. A higher amount of Mn coating has a higher Cu(II) adsorption capacity (Figure 4.12). However, when the adsorption capacity was normalized to the amount of Mn coating, it decreased with increasing amount of coating (Figure 4.13). With low Mn oxide coating, total Cu(II) adsorption capacity was due to both active sites on GAC surfaces and Mn oxides; only a small amount of active sites on GAC was covered or replaced by Mn oxides. When the amount of Mn oxide coating increased, more active sites on GAC surfaces were replaced by Mn oxides and these active sites on GAC were no longer available for further adsorption. As a result, the adsorption capacity contributed by GAC decreased with increasing amounts of Mn coating. Adsorption capacity remained about the same when the amount of Mn coating was larger than 50 mg Mn/g GAC

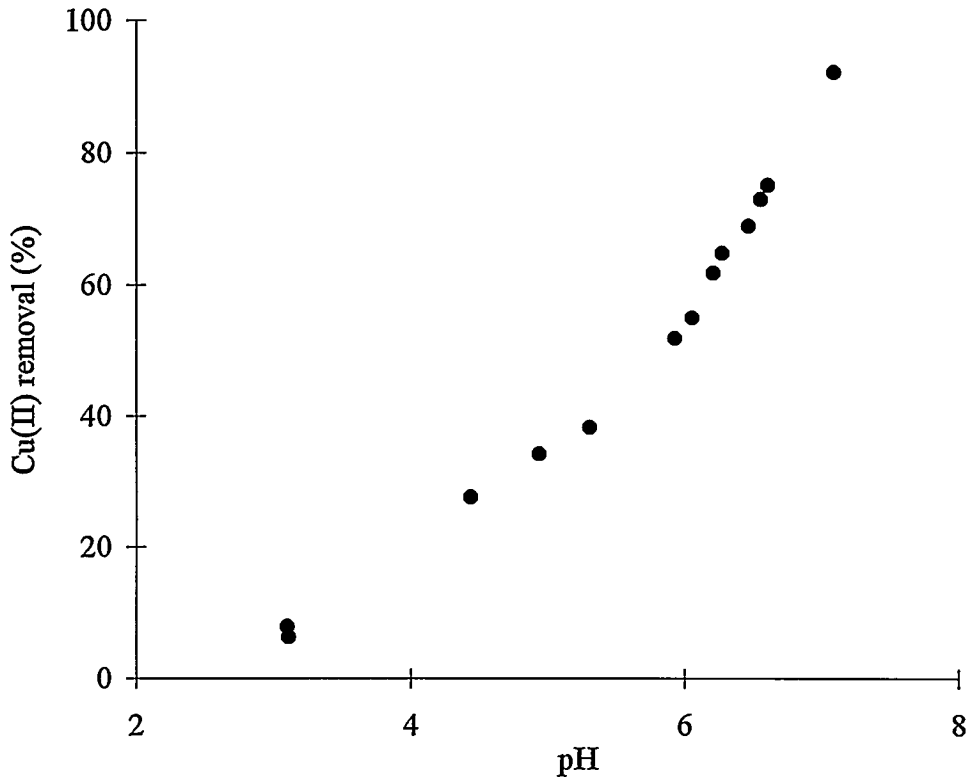

Figure 4.11. The Adsorption of Cu(II) by 1.0 mm MnWVB (19.86 mg Mn/g) as a Function of pH. Adsorbent concentration 0.1 g/ 250 mL, contact time 3 days, 4 mg Cu(II)/L, and 0.01 N $NaNO_3$.

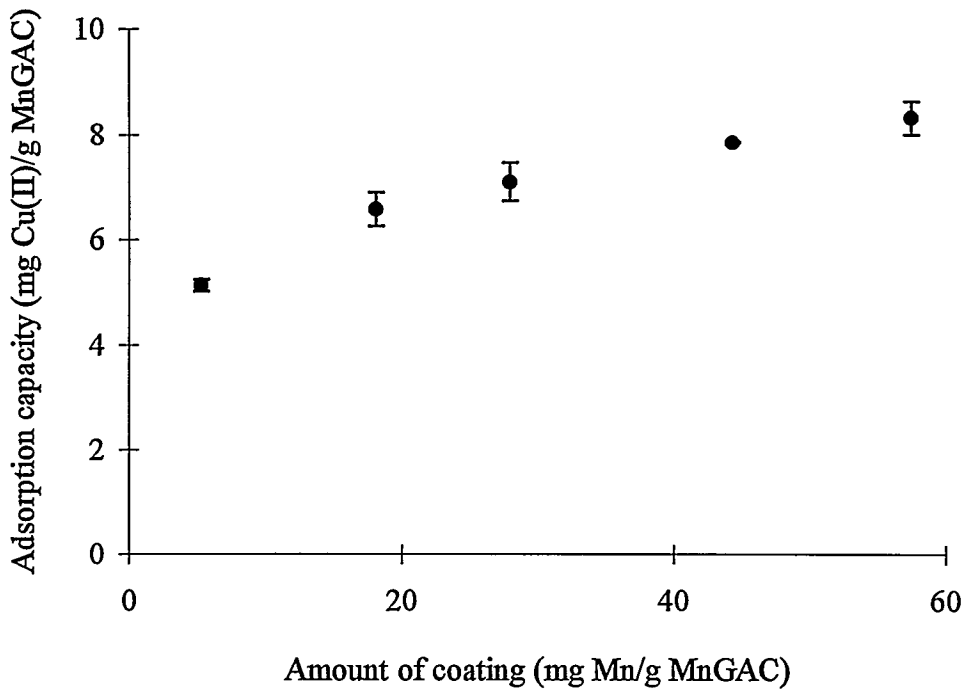

Figure 4.12. Cu(II) Adsorption Capacity onto MnWVB at Various Amounts of Mn Coating. Adsorbent concentration 0.05 g/ 250 mL and solutions were in contact with solid for 7 days at pH = 6, C_o = 3 mg Cu(II)/L, 0.01 N $NaNO_3$, and 10^{-4} N $NaHCO_3$. Data points are means ± standard deviation for 3 replicates.

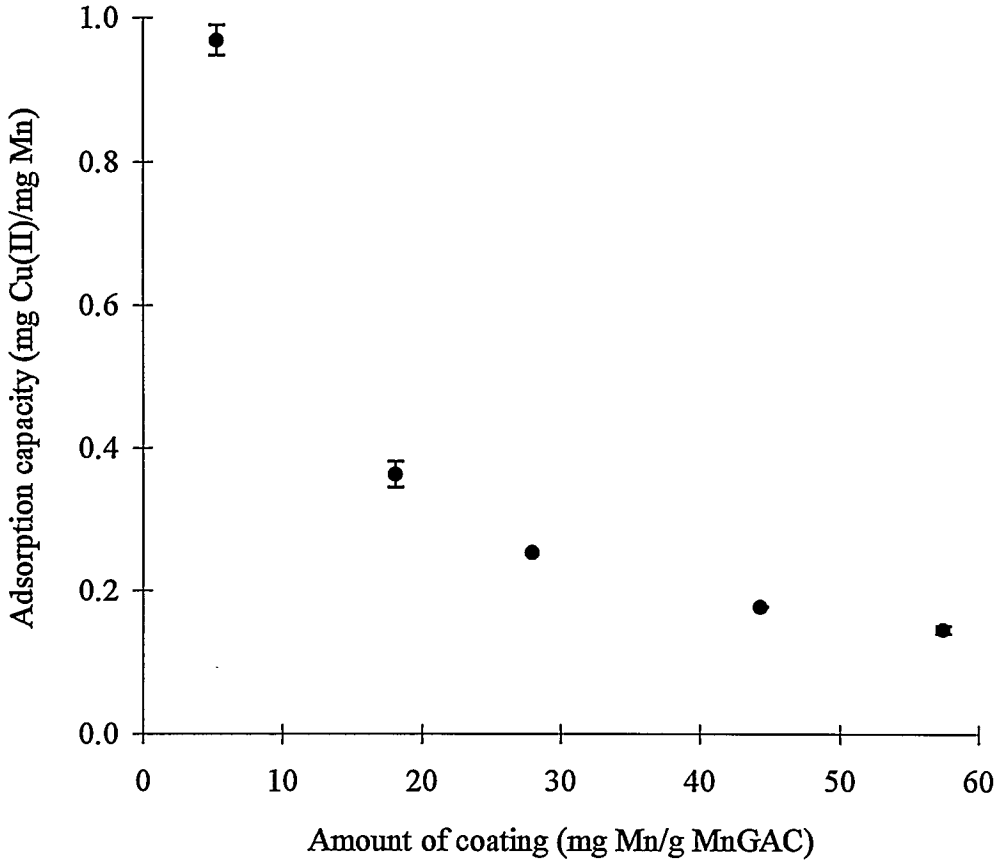

Figure 4.13. Cu(II) Adsorption Capacity (Normalized to Mn Content) onto MnWVB at Various Amounts of Mn coating. Adsorbent concentration 0.05 g/ 250 mL and solutions were in contact with solid for 7 days at pH = 6, 3 mg Cu(II)/L, 0.01 N $NaNO_3$, and 10^{-4} N $NaHCO_3$. Data points are means ± standard deviation for 3 replicates.

(Figure 4.13) and the adsorption capacity for Mn oxide was about 0.15 mg Cu(II) per mg of Mn. Mn oxides dominated Cu(II) adsorption at high coating levels.

4.3. Column Studies

One type of kinetic study was conducted in columns tests. A 2.54 cm diameter column was filled with MnWVB (19.98 mg Mn/g). This adsorption bed contained 7 g of MnWVB, and total adsorption bed volume (BV) was about 25 cm^3. About 3000 bed volumes (BV) were required to reach complete breakthrough for a final adsorption capacity 15.55 mg Cu(II)/g MnWVB (Figure 4.14). The effluent concentration was less than 10 μg/L in the initial 200 BV (Figure 4.15).

4.4. Multiple Adsorption/Regeneration Cycles Tests

This batch test was used to simulate multiple adsorption/regeneration column tests in a shorter time; column tests need much longer time (about 1 month for one cycle) than do the tests used here (about 4 days for one cycle). This test had two main goals: To evaluate the reusability of the adsorbent after regeneration and to determine the feasibility of metal recovery after adsorption. A known amount of adsorbent (0.1 g) was added into a 250 mL bottle that contained 4 mg Cu(II)/L, 0.01 N $NaNO_3$, and $4*10^{-4}$ N $NaHCO_3$ adjusted to pH 6. The bottle was rotated for 3 days in a shaker and pH was adjusted to 6

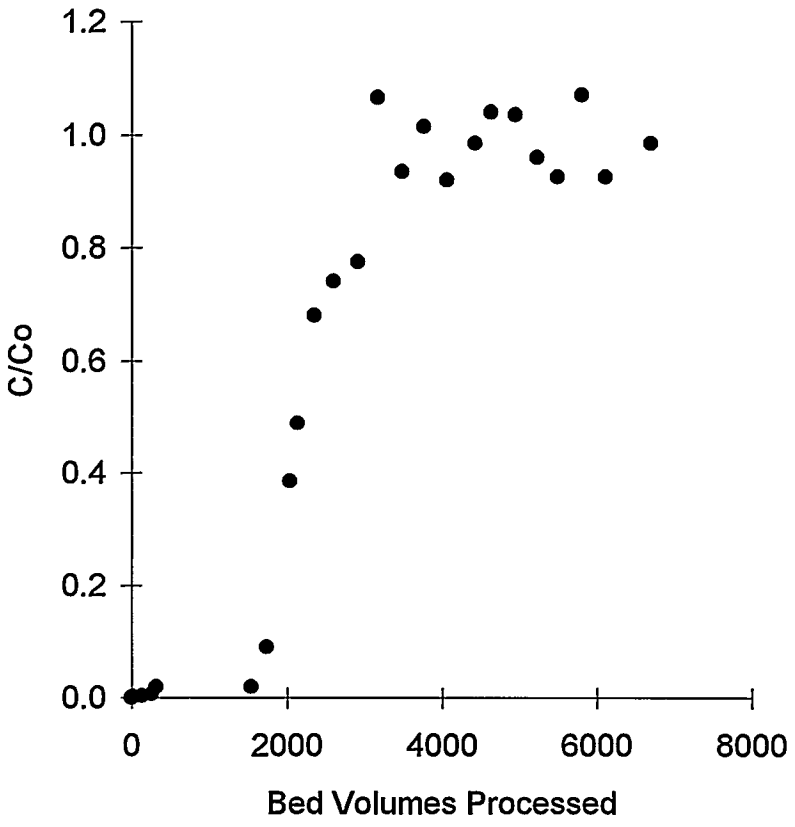

Figure 4.14. Breakthrough Curve for Cu(II) Removal by MnWVB (19.98 mg Mn/g). Loading 5 mL/min, adsorbent 7 g, bed volume = 25 mL, influent Cu(II) = 2 mg/L, and pH = 6.

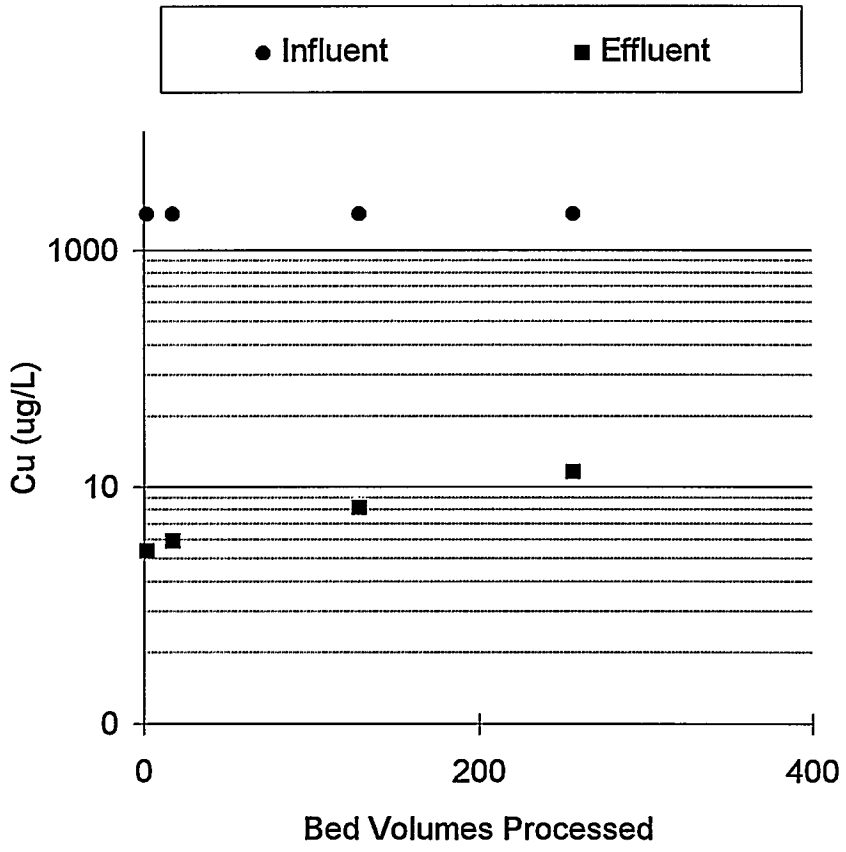

Figure 4.15. Cu(II) Removal by MnWVB (19.98 mg Mn/g) in a Column Process. Loading 5 mL/min, adsorbent 7 g, bed volume = 25 mL, influent Cu(II) = 2 mg/L, and pH = 6.

throughout this period. At the end of the test, the solution was adjusted to pH 3 by adding nitric acid and rotated for 1 day after taking a 10 mL sample. The purpose of this step was to recover adsorbed Cu(II) and regenerate the adsorbent. After regeneration, the solution was decanted and fresh Cu(II) solution was added to start another adsorption/desorption cycle. Results of this test are shown in Figure 4.16. For the first three cycles Cu(II) removal decreased from 65 % to 45 %. It seems that the adsorption capacities remained constant after the third cycle. The amount of adsorbed Cu(II) recovered is shown in Figure 4.17. Most of the adsorbed Cu(II) can be recovered during these cycles. These results suggest that the adsorbent can be regenerated and reused through several cycles and most of the adsorbed Cu(II) can be recovered. The amount of the retained Cu(II) was estimated by using a mass balance calculation (Figure 4.18). The retained Cu(II) reached a maximum amount at about 1.5 mg Cu(II)/g after the third cycle.

4.5. Kinetics Study

Batch tests were used to study the kinetics of Cu(II) adsorption onto MnWVB. These tests were conducted in a 2 L beaker that contained 4 mg Cu(II)/L, 0.01 N $NaNO_3$, and 10^{-4} N $NaHCO_3$ adjusted to pH 6. MnGAC (0.2g/L) was pre-equilibrated with a buffer solution (0.01 N $NaNO_3$ and 10^{-4} N $NaHCO_3$ adjusted to pH 6) before the test. This solution was completely mixed by a fixed propeller during the experiment.

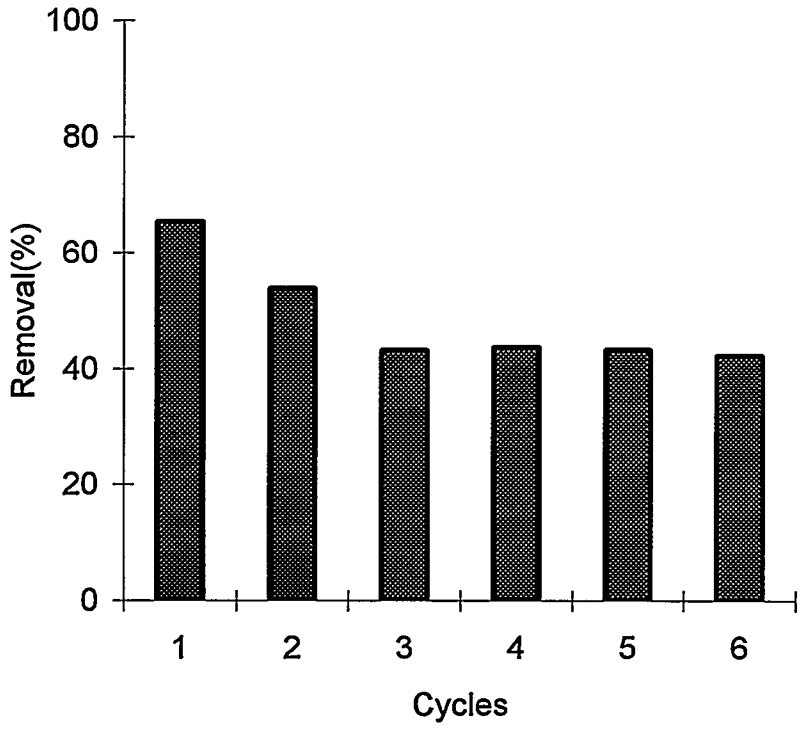

Figure 4.16. Cu(II) Removal from MnWVB/ads in Multiple Adsorption Cycles. C_o = 4 mg Cu(II)/L, pH 6 and solid concentration 0.1g/250 mL.

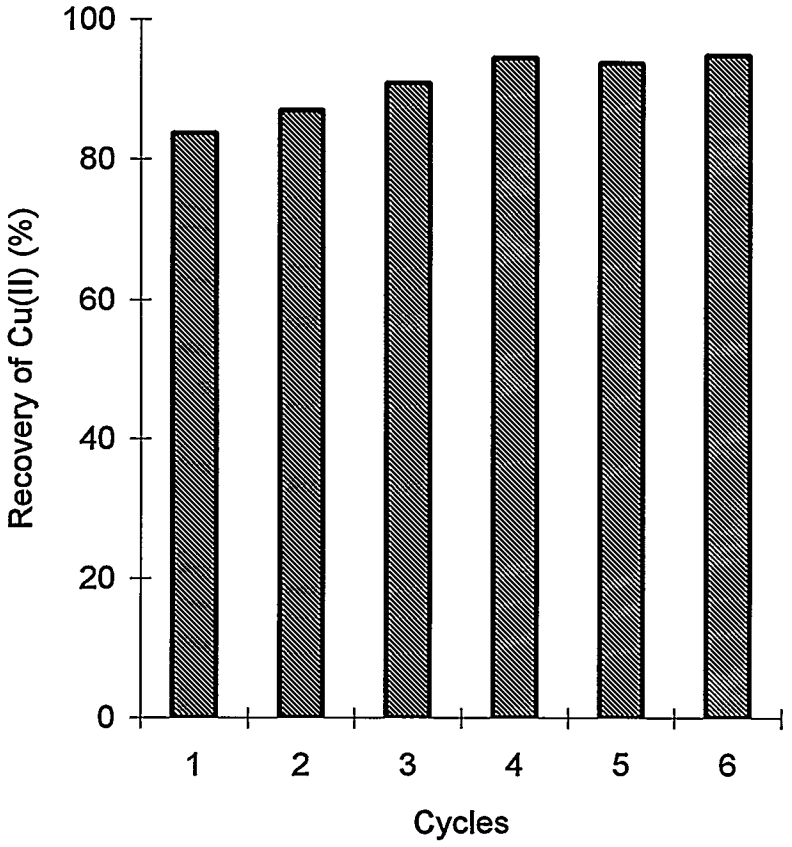

Figure 4.17. Cu(II) Recovery from MnWVB/ads in Multiple Adsorption Cycles. C_o = 4 mg Cu(II)/L, pH 6, and solid concentration 0.1g/250 mL.

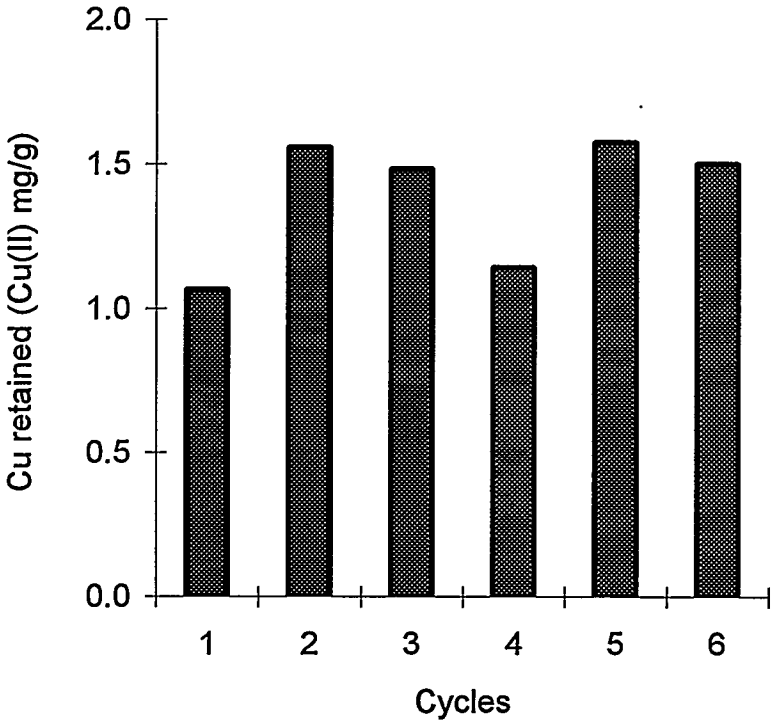

Figure 4.18. Total Cu(II) Retained in MnWVB/ads in Multiple Adsorption Cycles. C_o = 4 mg Cu(II)/L, solid concentration 0.1g/250 mL, and pH 3.

Samples were collected periodically and analyzed for Cu(II). A typical Cu(II) adsorption curve is shown in Figure 4.19.

Reversibility of adsorption Cu(II) was studied. A desorption test (pH 3) was conducted after a 24 h adsorption step (pH 6). This test was conducted in a 2 L beaker with 1 g MnWVB, and 0.01 N $NaNO_3$, 10^{-4} N $NaHCO_3$, and pH 6 solution for the adsorption process. At the end of the adsorption process, solution pH was adjusted to 3 for desorption. Most of the adsorbed Cu(II) at pH 6 was desorbed at pH 3 (Figure 4.20). The desorption process was much faster than the adsorption process. In the adsorption process, 90 % adsorption occurred at about 9 h, but 90 % of desorption occurred in less than 2 h. It is probably due to a higher driven force (concentration gradient) in the lower pH solution, which has a higher Cu(II) solubility.

4.6. Summary

Mn oxide can improve the metal adsorption capacity of GAC. Factors affecting the amount of coating on GAC were type of GAC, GAC pore volume, GAC particle size, coating time, Mn dosage, and the duration of prewash time. In batch tests with Cu(II), relative to GAC by itself, adsorption capacities were increased more than three times after coating and Mn oxides dominated the adsorption process. Complete breakthrough for a column occurred after 3000 bed volumes (BV) were processed. In multiple adsorption/regeneration cycles, although total Cu(II) removal decreased from the first to the third cycle, Cu(II) removal stayed about the same in the third and subsequent cycles.

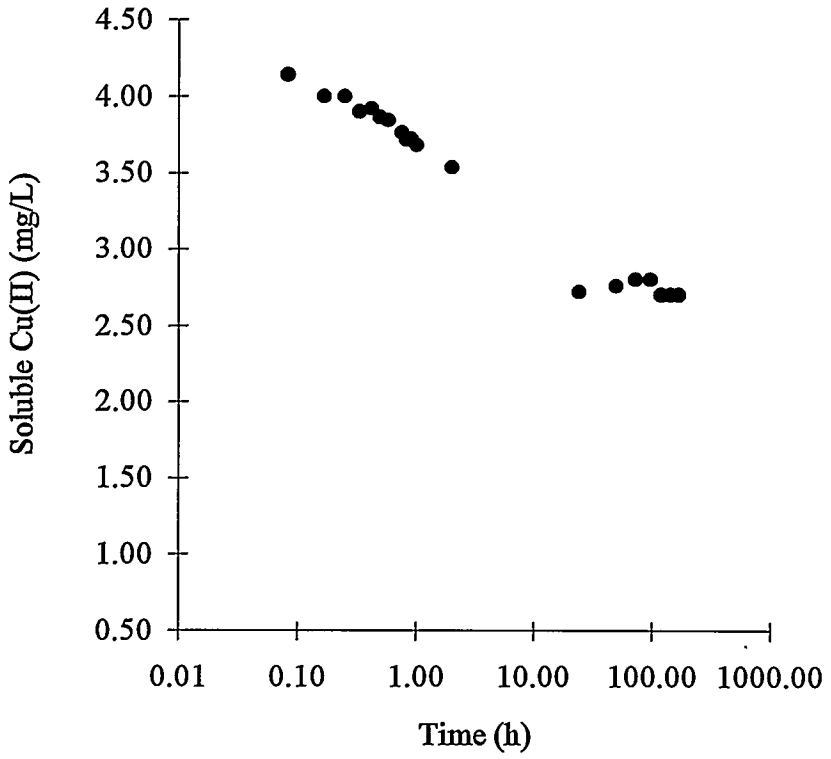

Figure 4.19. Uptake of Cu(II) by 1.0 mm MnWVB (19 mg Mn/g) as a Function of Time. MnWVB (0.2g/L) in contact with solutions at pH = 6, and 0.01 N $NaNO_3$, and 10^{-4} N $NaHCO_3$.

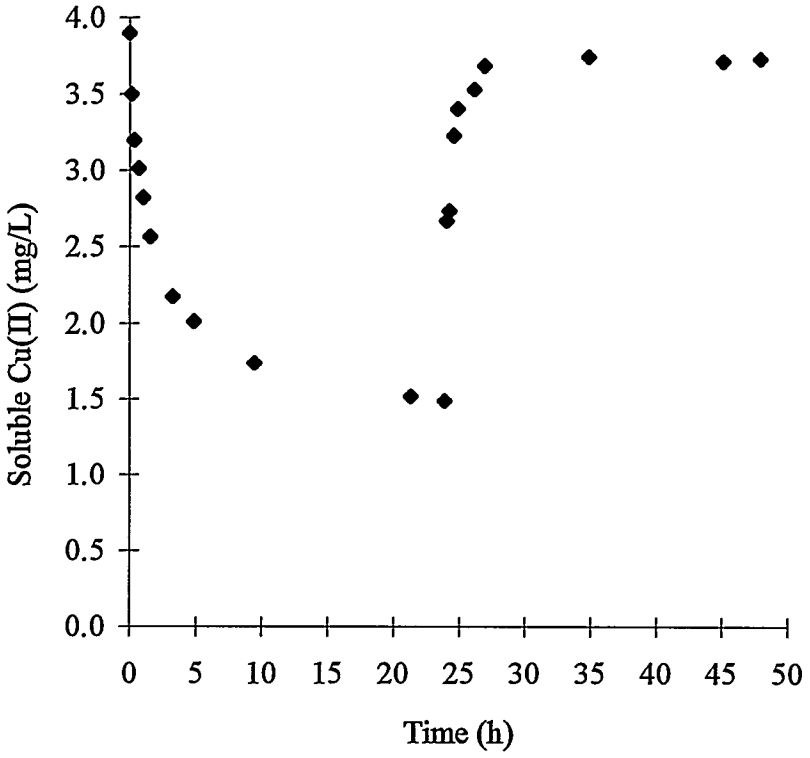

Figure 4.20. Kinetics of Cu(II) Adsorption (pH 6) and Desorption (pH 3) on MnWVB. Adsorbent concentration 0.5g/L, initial concentration 4 mg Cu(II)/L, 0.01 N $NaNO_3$, and 10^{-4} N $NaHCO_3$.

Mn oxide-coated GAC has the potential to become an efficient material for metal removal and recovery from wastewater. However, with the hope of bringing the effluent concentration to less than 5 ug/L and increasing the Cu(II) removal efficiency in the multiple adsorption/regeneration cycles, alternative coating methods were explored.

Two coating methods, precipitation and dry oxidation, were developed for this purpose and results of these results are presented in Chapters V and VI.

CHAPTER V

MnGAC PREPARED BY PRECIPITATION METHOD

Nine composite adsorbents were prepared following techniques similar to those described by Stahl and James (1991). Mn oxide was precipitated on GAC surfaces by evaporation. Nine composite adsorbents were prepared by using three GAC (WVB, APC, TOG) and three manganese salts (manganese nitrate (N), manganese sulfate (S), and manganese chloride (C)). Properties of these coated adsorbents were characterized by measuring coating efficiency and adsorption capacity, performance in multiple adsorption/regeneration tests.

5.1. Amount of Coating

Nine different adsorbents were prepared by using the precipitation method and results of these coatings are shown in Figure 5.1. Both the type of salt and the type of GAC influenced the amount of Mn oxide coatings. MnAPC/C had the highest amount of Mn oxide coating and the MnTOG/S was the lowest among these coated GAC. In general, the sequences of the amount of coatings were manganese chloride > manganese nitrate > manganese sulfate and APC > WVB > TOG.

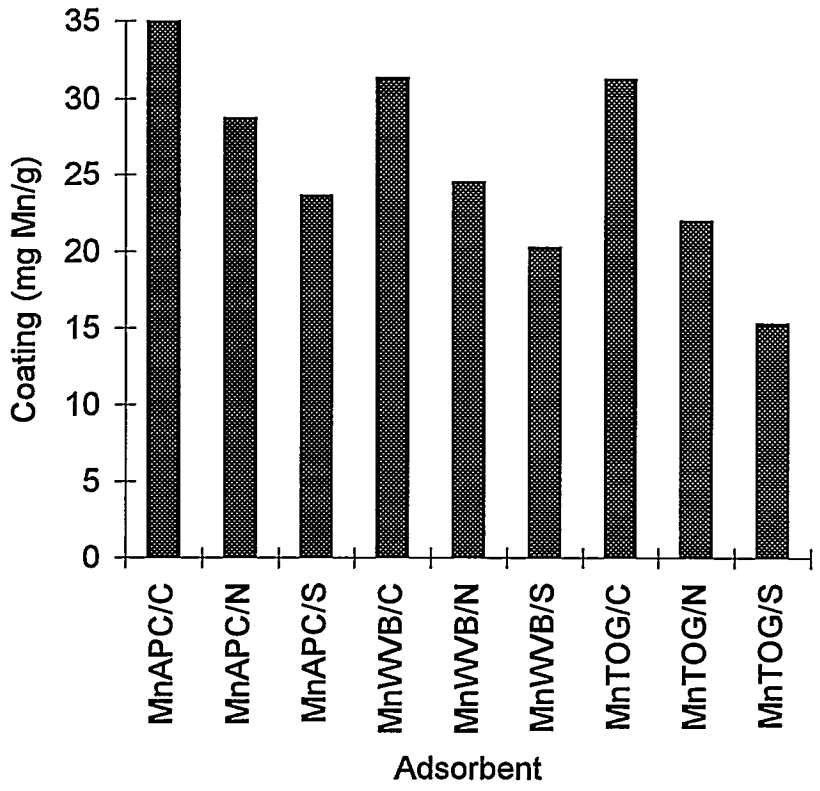

Figure 5.1. Mn Coatings for Nine Different Adsorbents Prepared by Precipitation Method. Applied 55 mg Mn/g. C = manganese chloride, N = manganese nitrate, and S = manganese sulfate.

5.2. Adsorption Edge Tests

The adsorption capacities of these coated adsorbents along with uncoated GAC were characterized by adsorption edge tests. These tests were conducted in a series of 250 mL bottles that contained 0.1 g of adsorbent, 4 mg Cu(II)/L, 0.01 N $NaNO_3$ and $4*10^{-4}$ N $NaHCO_3$ adjusted to desired pH values (3, 4, or 6) with 3 days contact time. Adsorption edge curves for APC, WVB, and TOG are shown in Figure 5.2. Despite the fact that APC had a much higher surface area (1525 m^2/g) relative to TOG (800-900 m^2/g), both GACs had similar adsorption capacities that ranged from 10 to 40 % Cu(II) removal in the range of pH tested. WVB had the highest Cu(II) adsorption capacity among these carbons and % Cu(II) removal onto WVB ranged form 20 to 90 %. Cu(II) removal was significantly improved by applying Mn oxide onto WVB (Figure 5.3). MnWVB prepared by different manganese salts seemed to have similar amounts of Cu(II) adsorption capacities (ranged from 85 to 99 % Cu(II) removal). Similar results were obtained for MnTOG (Figure 5.4), but the effects of the Mn oxide coating were much less than for WVB. The MnTOG had similar % Cu(II) removal (form 10 to 60 %). MnAPC/N had better Cu(II) adsorption than did MnAPC/C or Mn APC/S (Figure 5.5). For example, at pH 6, MnAPC/N could remove almost 100 % of Cu(II) but MnAPC/C and MnAPC/S could only remove 70 % of Cu(II). In general, MnWVB had better Cu(II) adsorption capacities than did MnAPC or MnTOG. Interestingly, these results are not in agreement with the amount of Mn coatings on these GAC. For example, MnAPC had a higher amount of coating than did MnWVB, but the Cu(II) adsorption capacity for

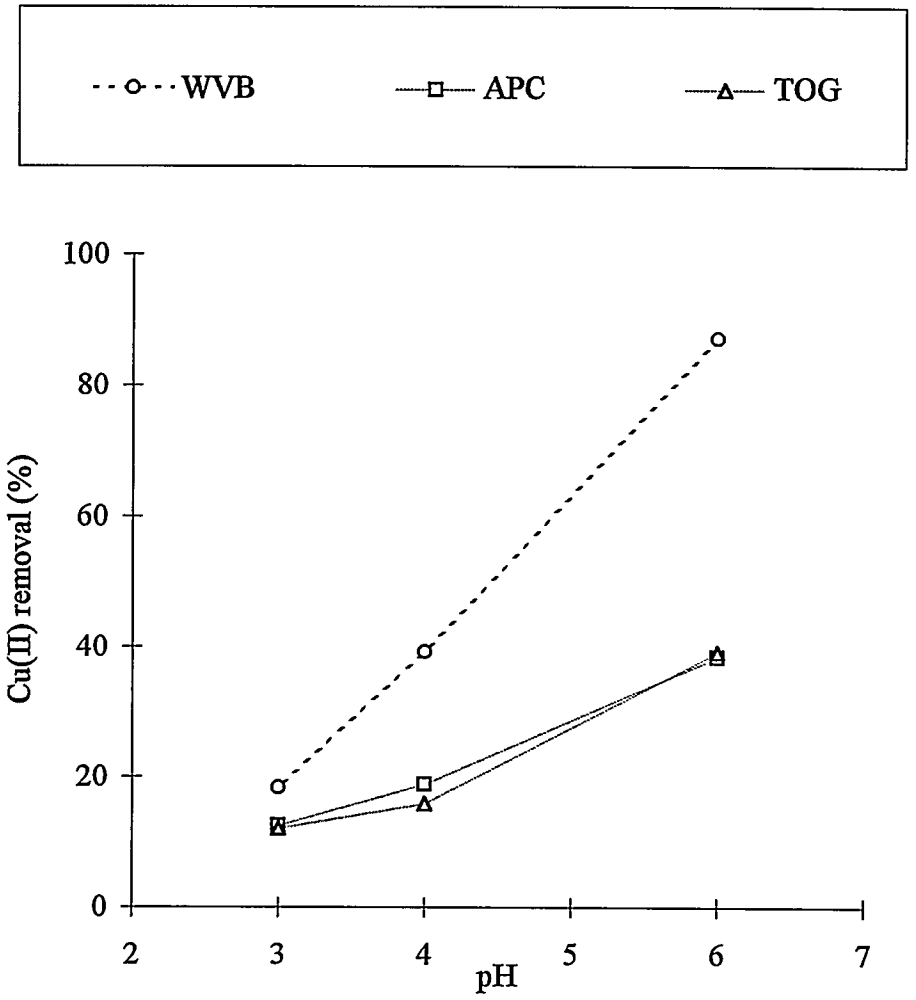

Figure 5.2. Adsorption of Cu(II) by WVB, APC and TOG as a Function of pH. Adsorbent concentration 0.1 g/ 250 mL, contact time 3 days, 4 mg Cu(II)/L, 0.01 N $NaNO_3$, and $4*10^{-4}$ N $NaHCO_3$.

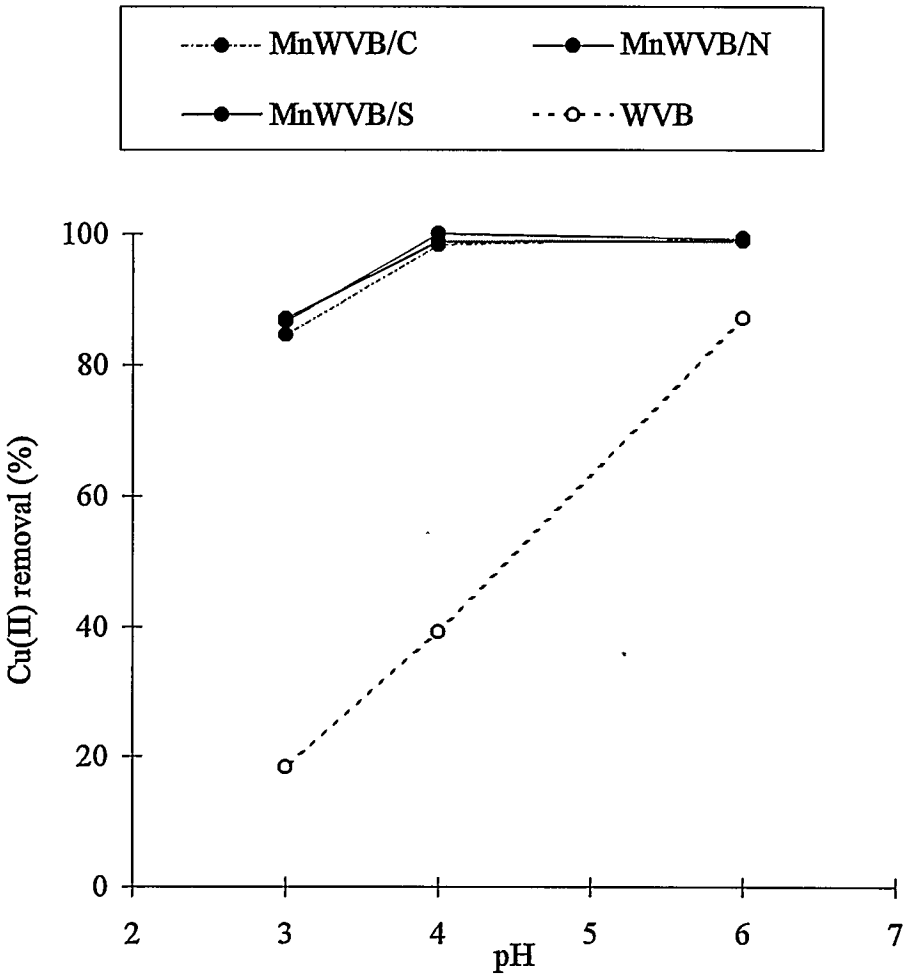

Figure 5.3. Adsorption of Cu(II) by MnWVB and WVB as a Function of pH. Adsorbent concentration 0.1 g/ 250 mL, contact time 3 days, 4 mg Cu(II)/L, 0.01 N $NaNO_3$, and $4*10^{-4}$ N $NaHCO_3$. C = manganese chloride, N = manganese nitrate, and S = manganese sulfate.

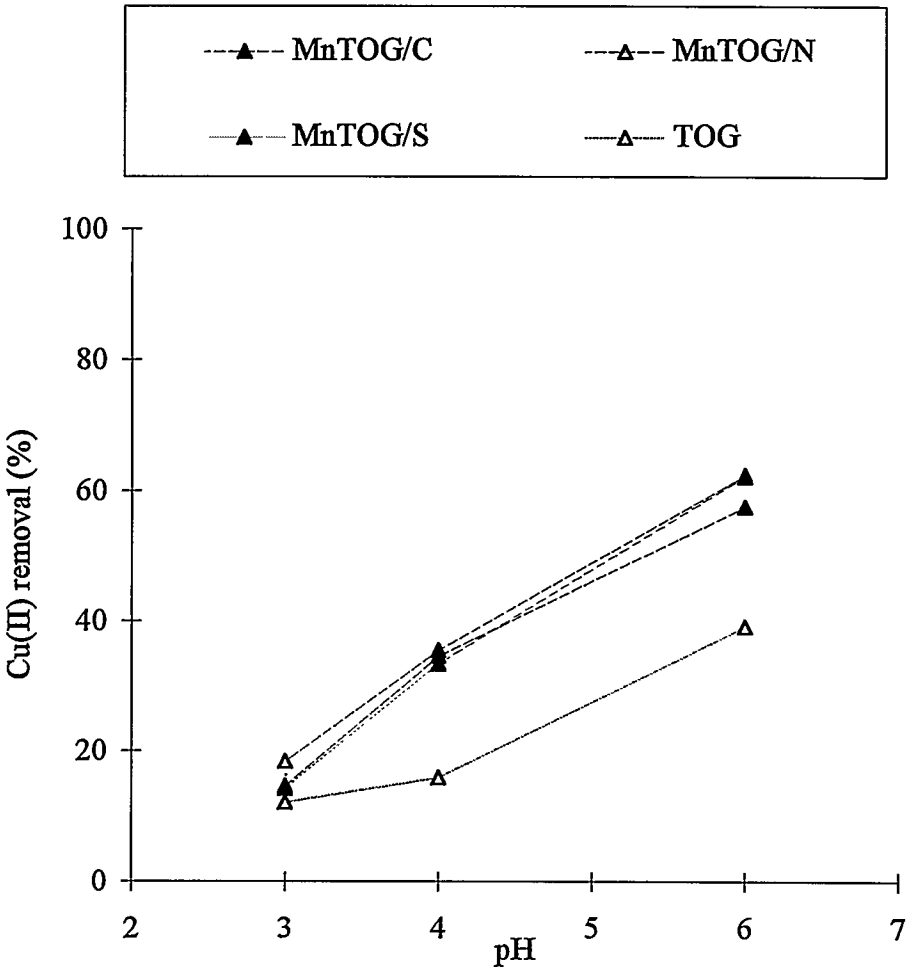

Figure 5.4. Adsorption of Cu(II) by MnTOG and TOG as a Function of pH. Adsorbent concentration 0.1 g/ 250 mL, contact time 3 days, 4 mg Cu(II)/L, 0.01 N $NaNO_3$, and $4*10^{-4}$ N $NaHCO_3$. C = manganese chloride, N = manganese nitrate, and S = manganese sulfate.

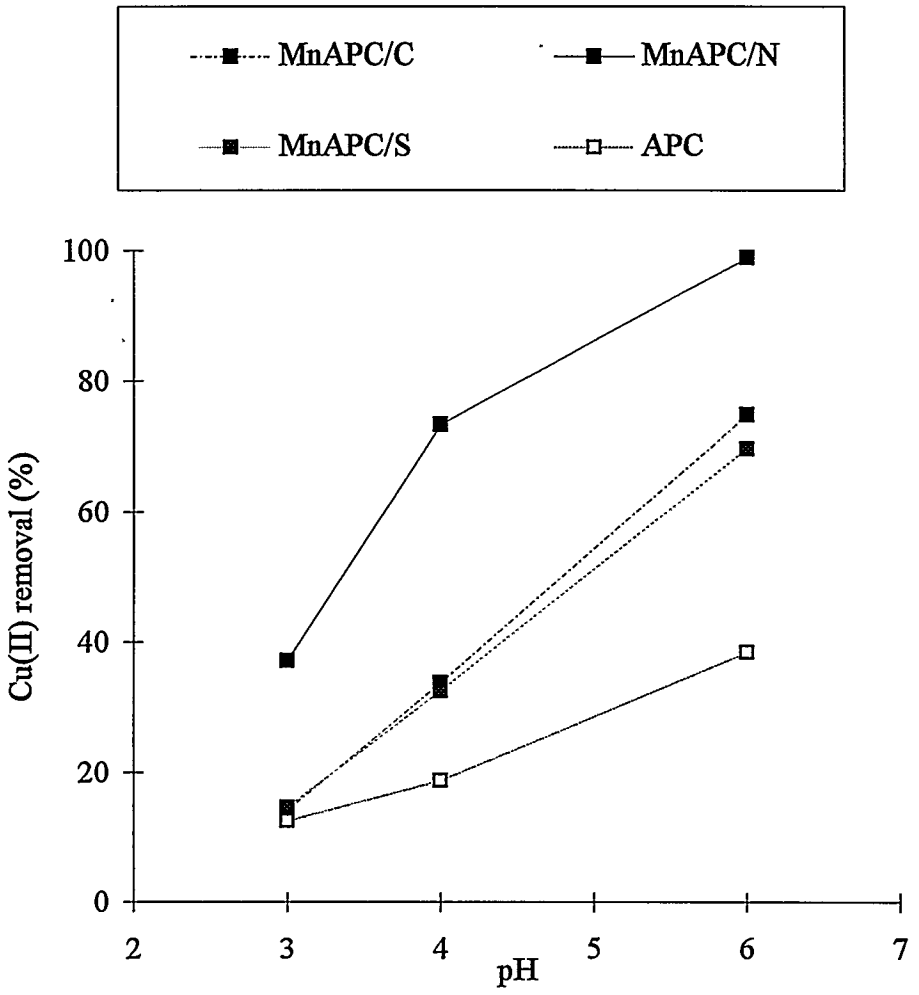

Figure 5.5. Adsorption of Cu(II) by MnAPC and APC as a Function of pH. Adsorbent concentration 0.1 g/ 250 mL, contact time 3 days, 4 mg Cu(II)/L, 0.01 N $NaNO_3$, and $4*10^{-4}$ N $NaHCO_3$. C = manganese chloride, N = manganese nitrate, and S = manganese sulfate.

MnWVB was higher, probably because that WVB itself had a better Cu(II) adsorption capacity. In general, Cu(II) adsorption capacities of these coated carbons were improved by applied Mn oxide coatings and the % removal of Cu(II) was a function of pH.

5.3. Multiple Adsorption/Regeneration Tests

These tests were used to simulate the multiple adsorption/regeneration column tests in a shorter time; equivalent column tests would require months to generate the same information. This test had two main objectives, to test the reusability of the adsorbent after regeneration, and to evaluate the feasibility of metal recovery after adsorption.

Three GACs (APC, TOG, and WVB) and three coated GACs (MnAPC/N, MnTOG/N and MnWVB/N) were prepared by using manganese nitrate; results are shown in Figure 5.6. Cu(II) removal decreased to a certain value and then was maintained at that level. MnWVB/N appeared to have the best Cu(II) removal. However, WVB also had the highest Cu(II) removal. The amount of Cu(II) retained in the adsorbent after regeneration was obtained by using mass balances and results are shown in Figure 5.7. Surprisingly, even though WVB had much higher Cu(II) removal, WVB, TOG, and APC had similar amounts of Cu(II) retained (about 5 mg/g). There were no significance difference between MnTOG/N and TOG in terms of amount of retained Cu(II) despite the fact that MnTOG/N had a higher amount of Cu(II) removal. Cu(II) retained on MnAPC was about 3 mg Cu(II)/g more than APC. MnWVB/N had the highest amount of retained

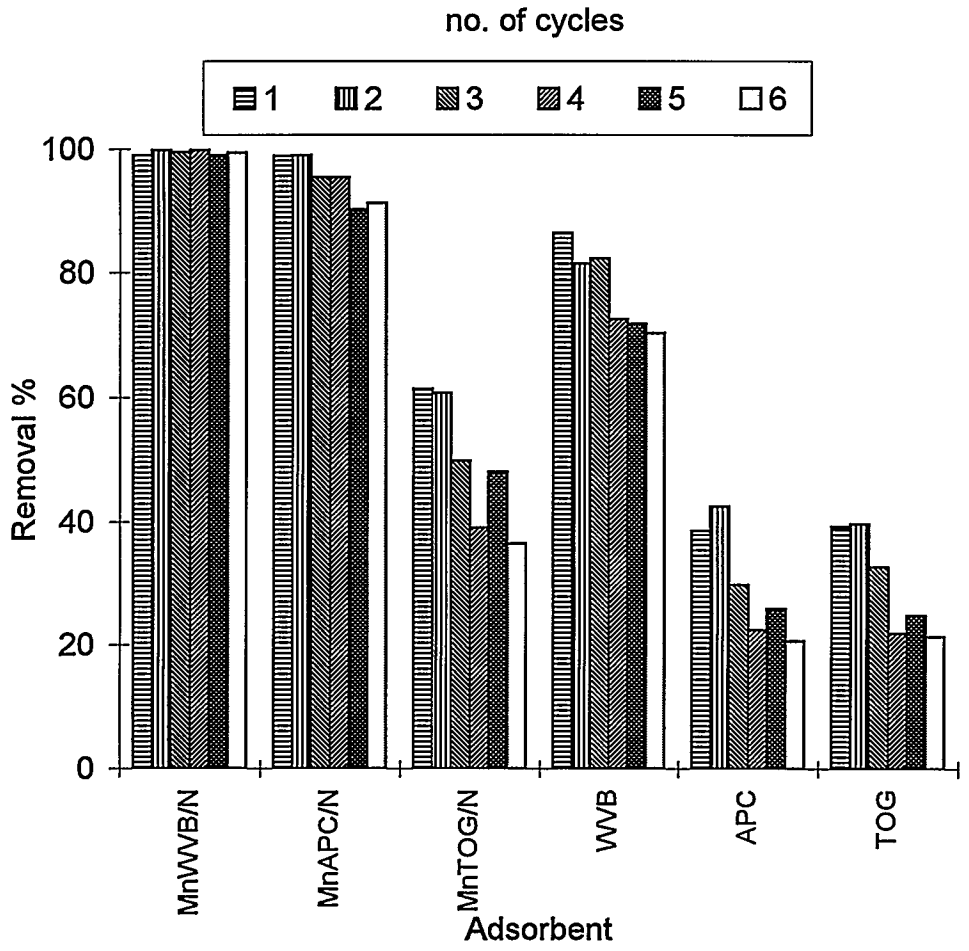

Figure 5.6. Cu(II) Removal from MnGAC and GAC in Multiple Adsorption Cycles. Adsorbent concentration 0.1 g/ 250 mL, contact time 3 days, 4 mg Cu(II)/L, 0.01 N $NaNO_3$, and $4*10^{-4}$ N $NaHCO_3$.

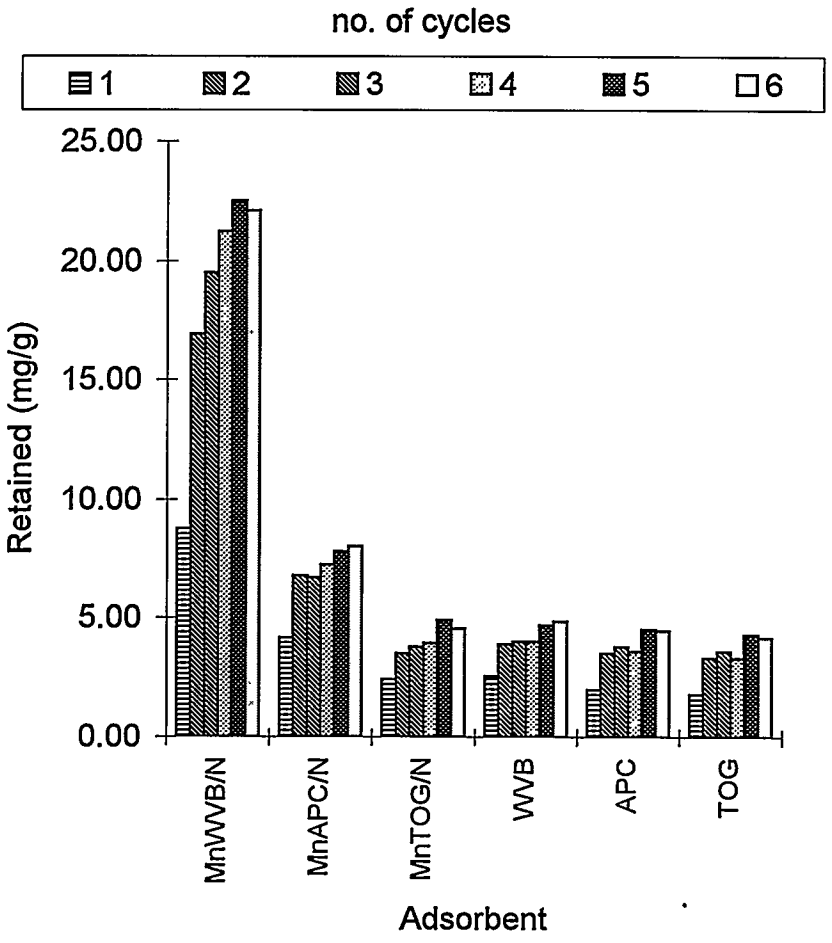

Figure 5.7. Cu(II) Retained in MnGAC and GAC in Multiple Adsorption Cycles

Cu(II) (about 22 mg Cu(II)/g), which was about four times higher than the amount retained by WVB itself. MnWVB/N may have stronger binding sites than WVB and these sites may be contributed by the coated Mn oxides. Coated GAC with higher Cu(II) removal had a higher amount of retained Cu(II), but this was not true for GAC. Mn oxide appears to dominate adsorption processes of coated GAC. Overall, these results suggest that the MnGAC can be used through several adsorption cycles but a fraction of the Cu(II) will be retained in the MnGAC after regeneration.

Nine composite adsorbents were prepared by using three GACs (WVB, APC, and TOG) and three manganese salts (manganese nitrate (N), manganese sulfate (S), and manganese chloride (C)). Both the type of salt and the type of GAC influenced the amount of Mn oxide coatings. In general, the sequences of the amount of coatings were manganese chloride > manganese nitrate > manganese sulfate and APC > WVB > TOG. Cu(II) adsorption capacities of these coated carbons were improved by applied Mn oxide coatings and the % removal of Cu(II) was a function of pH. In general, MnWVB had better Cu(II) adsorption capacities than did MnAPC or MnTOG. However, these results are not in agreement with the amount of Mn coatings on these GACs, probably because the GAC or type of Mn oxide differed.

5.4. Summary

Three GACs (APC, TOG, and WVB) and three coated GACs (MnAPC/N, MnTOG/N and MnWVB/N) were chosen for six cycles of multiple

adsorption/regeneration cycle tests. Cu(II) removal decreased to a certain value and then was maintained at that level at the end of the third cycle. MnWVB/N appeared to have the best Cu(II) removal. However, WVB also had the highest Cu(II) removal. Results suggest that the MnGAC can be used through several adsorption/regeneration cycles but a fraction of the Cu(II) will be retained in the MnGAC after regeneration.

CHAPTER VI

MnGAC PREPARED BY DRY OXIDATION METHOD

One composite adsorbent (MnTOG) was prepared by a dry oxidation method. MnTOG was prepared by mixing TOG, $Mn(NO_3)_2$, and 70 % HNO_3. This mixture was dried in an oven for 3 days at 105 °C to remove excess solution then dried at 160°C for 3 more days. The resulting composite adsorbent was washed with DDW adjusted to pH 3 with HNO_3, then dried again at 105 °C before further tests. TOG was sized (20*40 mesh size), washed, and dried (200 °C) before coating. MnTOG had a Mn content of about 27 mg Mn/g TOG. Adsorption properties of MnTOG such as Cu(II) or Cd(II) adsorption edge curves and adsorption isotherms, and pH_{zpc} of MnTOG are discussed in this chapter. Multiple cycles adsorption tests and column process will be shown in Chapter VII, and adsorption kinetics modeling will be evaluated in chapter VIII.

6.1. Adsorption Edge Tests of MnTOG and TOG

The relationship between Cu(II) adsorption capacity and pH was obtained from an adsorption edge test. A series of 250 mL bottles was filled with 0.1 g adsorbent, 4 mg Cu(II)/L, and 0.01 N $NaNO_3$ solution, then adjusted to a range of pH values (from 3 to 7). These bottles were rotated in a shaker for 3 days. Relative to TOG by itself, the Cu(II) adsorption capacity of TOG was greatly improved by applying Mn oxide (Figure 6.1). These results were typical of adsorption edge curves for oxides (Stumm and Morgan, 1981; Batchelor and Dennis, 1987). For both MnTOG and TOG, the extent of adsorption

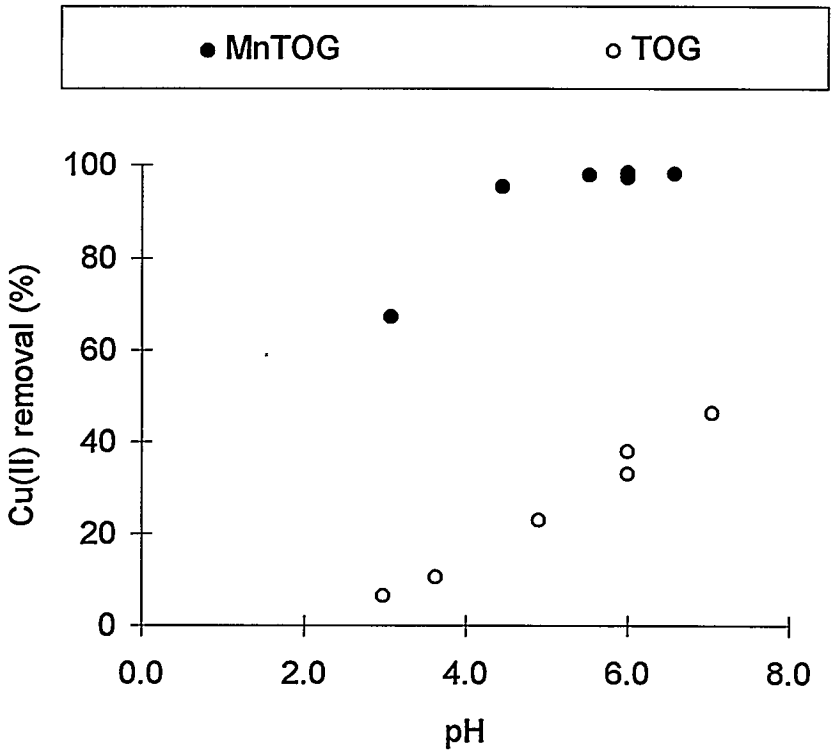

Figure 6.1. Adsorption of Cu(II) as a Function of pH by MnTOG and TOG. C_o = 4 mg Cu(II)/L, solid concentration 0.1g/250 mL, and 0.01 N $NaNO_3$.

of Cu(II) was strongly pH-dependent and higher pH values had better Cu(II) removal. However, in the pH range tested, MnTOG had a better Cu(II) removal than did TOG. For MnTOG, Cu(II) removal was about 65 % at pH = 3, and reached almost 100 % at pH = 6. For TOG, percent Cu(II) removal was in the range of 10 to 45 %. This curve also suggests that it is possible to recover the adsorbed metal by changing pH values. Multiple adsorption/regeneration tests were designed to test this hypothesis.

Cu(II) adsorption edge curves for three typical adsorbents prepared by dry oxidation (MnTOG), precipitation (MnTOG/N), and adsorption methods (MnWVB/ads) are shown in Figure 6.2. The adsorbent (MnTOG) prepared by dry oxidation had the highest Cu(II) adsorption capacity among these adsorbents, Therefore, MnTOG was chosen for further investigation such as adsorption isotherm, pH_{zpc}, batch and column tests, and adsorption kinetics modeling that will be discussed in this and the following chapters.

Cd(II) adsorption edge curves were also obtained in this studied by using the same procedures except that the initial concentration of Cd(II) was 2 mg/L (Figure 6.3). Cd(II) removal by MnTOG was also strongly pH-dependent. For example, Cd(II) removal increased from 15 % to 45, 82, and 98 % at pH 3, 4, 5.3, and 6, respectively. In contrast with MnTOG, TOG only removed 7, 7, 11, and 18 % of Cd(II) at pH 3, 3.7, 5, and 6, respectively. Not only did MnTOG have a higher Cd(II) adsorption capacity, but the adsorption capacity of MnTOG was more pH-dependent compared with TOG. Similar results were obtained from the Cu(II) adsorption edge test.

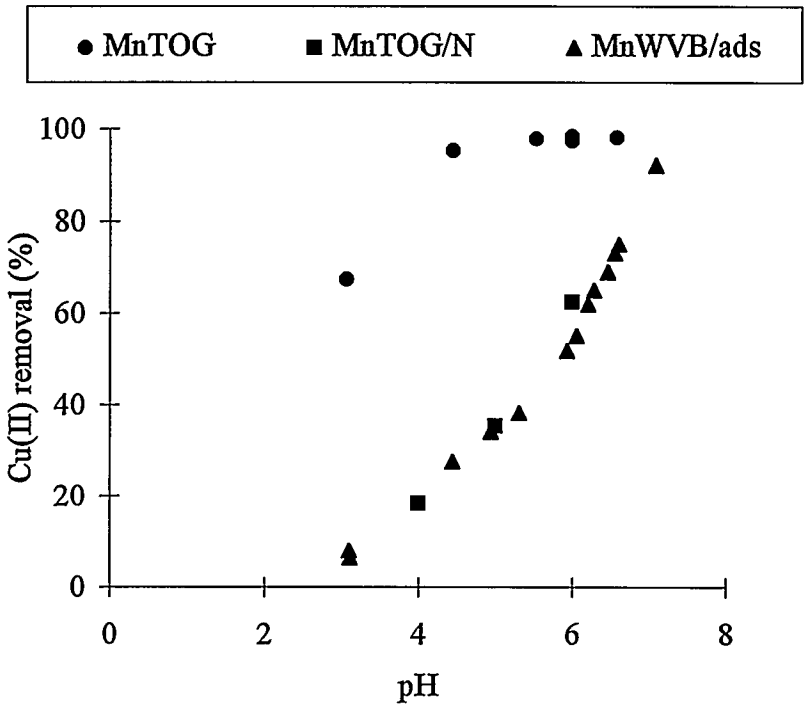

Figure 6.2. Adsorption of Cu(II) as a Function of pH by Adsorbents (MnTOG, MnTOG/N, and MnWVB/ads) Prepared by Three Coating Methods and Uncoated TOG. C_o = 4 mg Cu(II)/L, solid concentration 0.1g/250 mL, and 0.01 N $NaNO_3$.

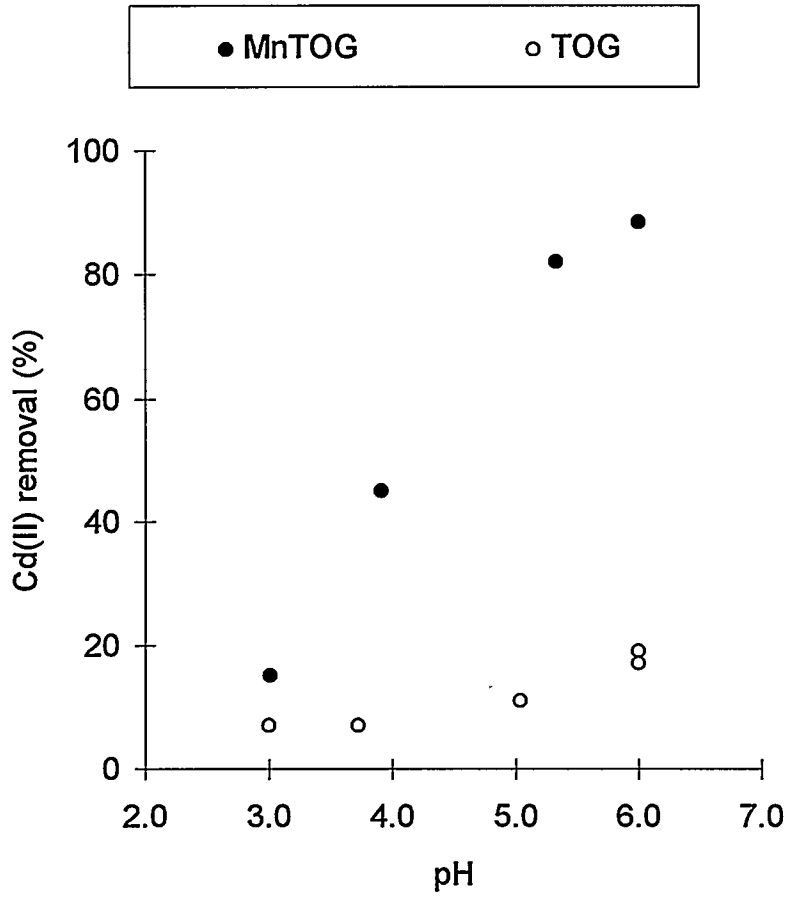

Figure 6.3. The Adsorption of Cd(II) as a Function of pH by MnTOG and TOG. C_o = 2 mg Cd(II)/L, solid concentration 0.1g/250 mL, and 0.01 $NaNO_3$.

6.2. Adsorption Isotherms

Cu(II) adsorption isotherms obtained at various times are shown in Figure 6.4. A longer adsorption time results in a higher adsorption capacity. These adsorption isotherms of MnTOG can be described by Freundlich isotherms, $q = K * C^n$, where q = mg Cu(II)/g MnTOG, K = Freundlich isotherm constant, n = Freundlich isotherm exponent, and C = mg Cu(II)/L. K and n of Freundlich isotherms at various adsorption times are listed in Table 6.1; both K and n increased with time. Freundlich isotherms will be used in the kinetics modeling in the Chapter VIII..

Cd(II) adsorption capacity of MnTOG can also be described by a Freundlich isotherm. Cd(II) adsorption isotherms measured at several times were also tested in this study (Figure 6.5). A longer adsorption time also resulted in a higher Cd(II) adsorption, however, the difference between isotherms measured at different times was much smaller compared to Cu(II). It appears that relative to Cu(II), Cd(II) reached equilibrium in a shorter time. K and n of Freundlich isotherms at various adsorption times can be found in Table 6.2. Adsorption kinetics of Cu(II) or Cd(II) onto MnTOG will be further investigated in Chapter VIII.

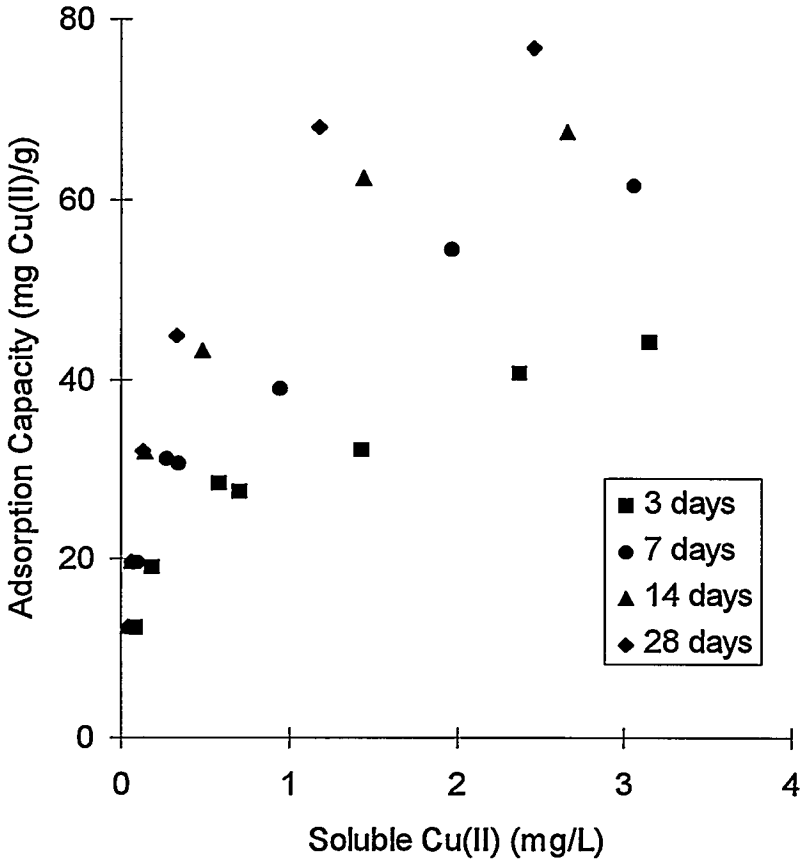

Figure 6.4. Adsorption Capacities of Cu(II) Adsorbed onto MnTOG at Various Adsorption Times. pH 6, C_o = 4 mg Cu(II)/L, 0.01 N $NaNO_3$, and $4*10^{-4}$ N $NaHCO_3$.

Table 6.1. Freundlich Isotherms of Cu(II) Adsorbed onto MnTOG at Various Adsorption Times. pH 6, C_o = 4 mg Cu(II)/L, 0.01 N $NaNO_3$, and $4*10^{-4}$ N $NaHCO_3$.

	Time(days)			
Isotherm constants	3	7	14	28
K	30.99	42.91	54.45	62.75
n	0.32	0.36	0.37	0.42

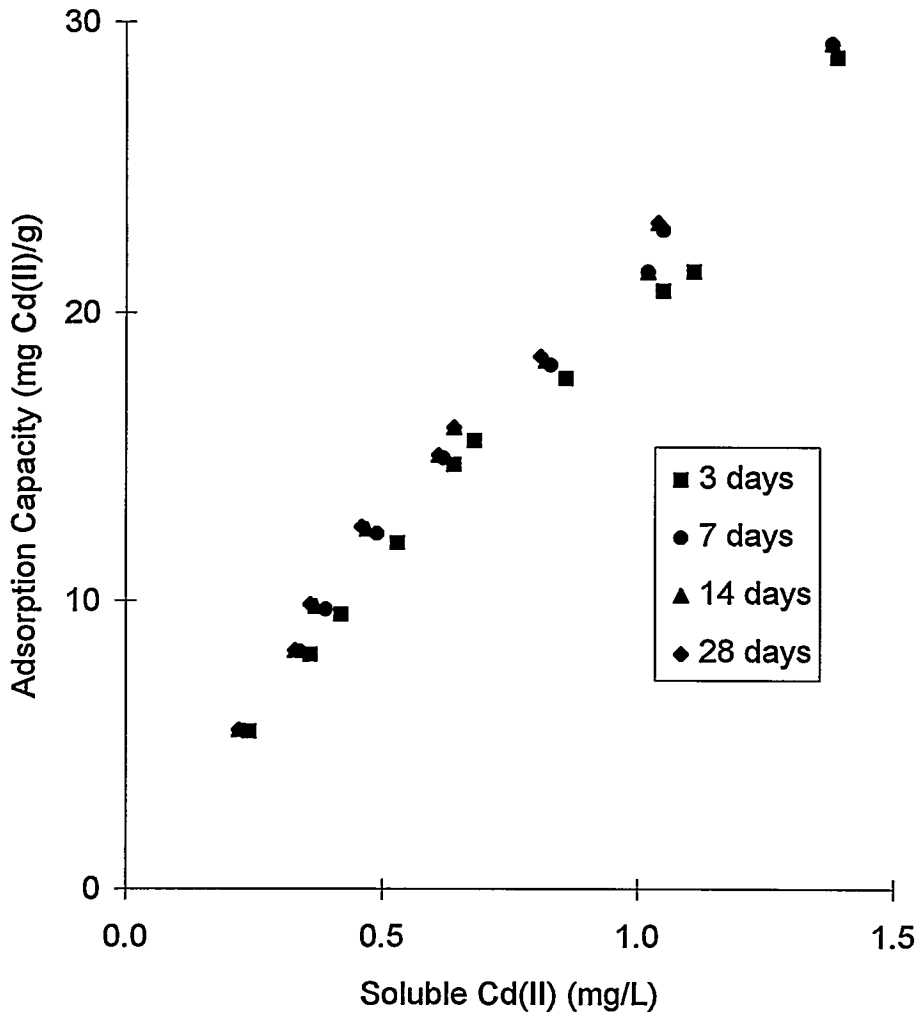

Figure 6.5. Adsorption Capacities of Cd(II) Adsorbed onto MnTOG at Various Adsorption Times. pH 6, C_o= 2 mg Cd(II)/L, 0.01 N $NaNO_3$, and $4*10^{-4}$ N $NaHCO_3$.

Table 6.2. Freundlich Isotherms of Cd(II) Adsorbed onto MnTOG at Various Adsorption Times. pH 6, C_o = 2 mg Cd(II)/L, 0.01 N $NaNO_3$, and $4*10^{-4}$ N $NaHCO_3$.

	Time(days)			
Isotherm constants	3	7	14	28
K	20.77	21.98	22.40	22.50
n	0.91	0.90	0.88	0.87

6.3. pH_{zpc} of Mn oxide, MnTOG, and TOG

The pH where surface charge equals zero is called the zero point of charge (pH_{zpc}). When the pH of the solution is less than the pH_{zpc}, the surface charge will be positive and the surface is more likely to adsorb anions. If the pH is higher than the pH_{zpc}, the surface has a negative charge and favors adsorption of cations.

pH_{zpc} of MnTOG was tested to further understand the surface properties of the adsorbent. pH_{zpc} can be obtained from experimental titration curves. The mean surface charge (Q) can be calculated form the following equation (Stumm and Morgan, 1981).

$$Q = (\{\equiv SOH_2^+\} - \{\equiv SO^-\} = (C_a - C_b - [OH^-] - [H^+])/m \qquad (6.1)$$

Where, Q = Mean surface charge on the adsorbent (mol/g)

$\{\equiv SOH_2^+\}$ = Concentration of protonated surface hydroxide species (mol/g)

$\{\equiv SO^-\}$ = Concentration of deprotonated surface hydroxide species (mol/g)

C_a = Concentration of acid added (mol/L)

C_b = Concentration of base added (mol/L)

$[OH^-]$ = Concentration of OH^-

$[H^+]$ = Concentration of H^+

m = weight of the adsorbent (g)

Results indicate that the MnTOG had a pH_{zpc} about 5.8 (Figure 6.6) and Mn oxide prepared by the same method as the MnTOG except without TOG present had a

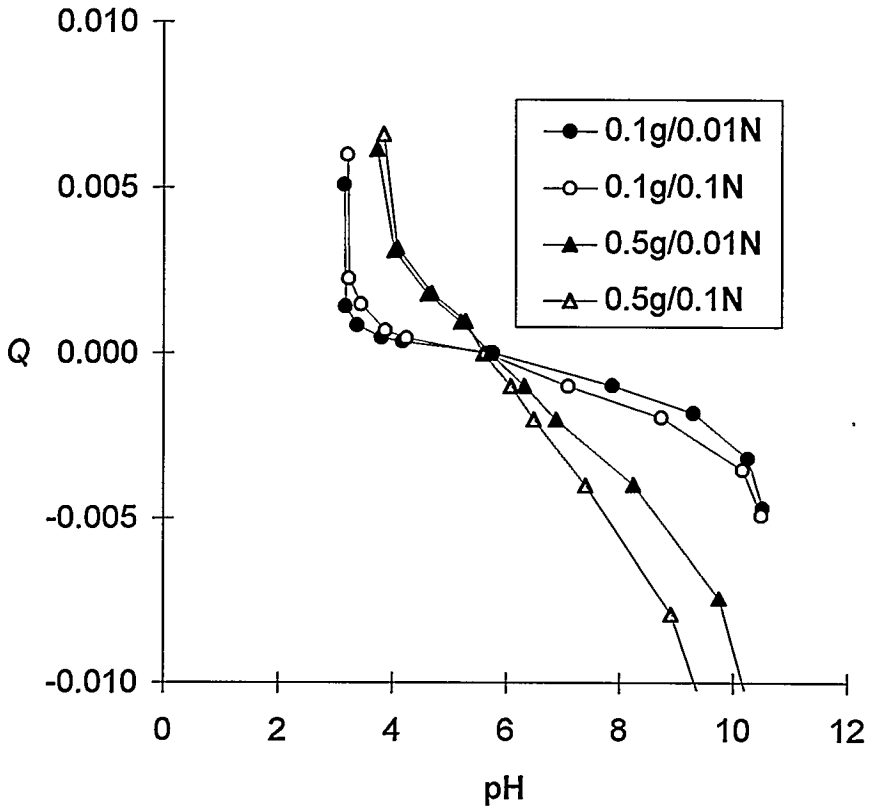

Figure 6.6. Surface Charge of the MnTOG Surface

pH_{zpc} about 6 (Figure 6.7). Wang (1995) reported that TOG had a pH_{zpc} about 8.5. The surface charge of MnTOG was closer to Mn oxide than to TOG; most of the surface charges of MnTOG were contributed by Mn oxide. Kinniburgh and Jackson (1981) reported that different Mn oxides have different pH_{zpc} values: δMnO_2, αMnO_2, βMnO_2, and γMnO_2 had pH_{zpc} values about 1.5-2.8, 4.5-4.6, 7.3, and 5.5-5.6, respectively. X-ray diffraction analysis of Mn oxide prepared by dry oxidation indicates that the Mn oxide is pyrolusite (βMnO_2) (Figure 6.8). The pH_{zpc} reported by Kinniburgh and Jackson (1981) for βMnO_2 was about 7.3, which is higher than the pH_{zpc} measured in this research. Mn oxide prepared in this research might contain some other Mn oxides or impurities that shift the value of pH_{zpc}. However, pH_{zpc} of pyrolusite was also reported as low as 6.4 which is close to the result obtained in this research (Huang, 1991).

6.4. Adsorption Competition Between Cu(II) and Cd(II)

When more than one metal is present in wastewaters, the adsorption of one metal may be hindered by the presence of other metals. Cu(II) and Cd(II) were chosen as model metals to study competition between metals. Experimental procedures were similar to the previous adsorption capacity tests. Although Cd(II) removal was significantly hindered by the presence of Cu(II), Cu(II) removal was only slightly influenced by the presence of Cd(II) (Figure 6.9).

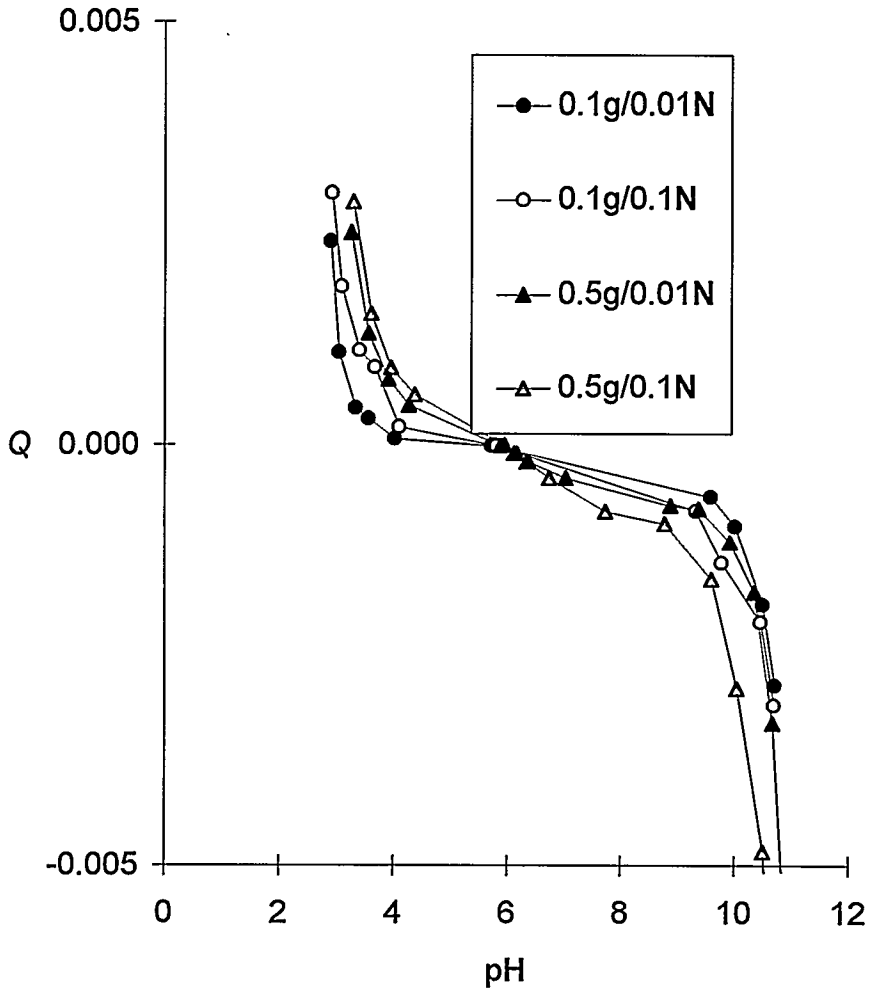

Figure 6.7. Surface Charge of the Mn Oxide Surface

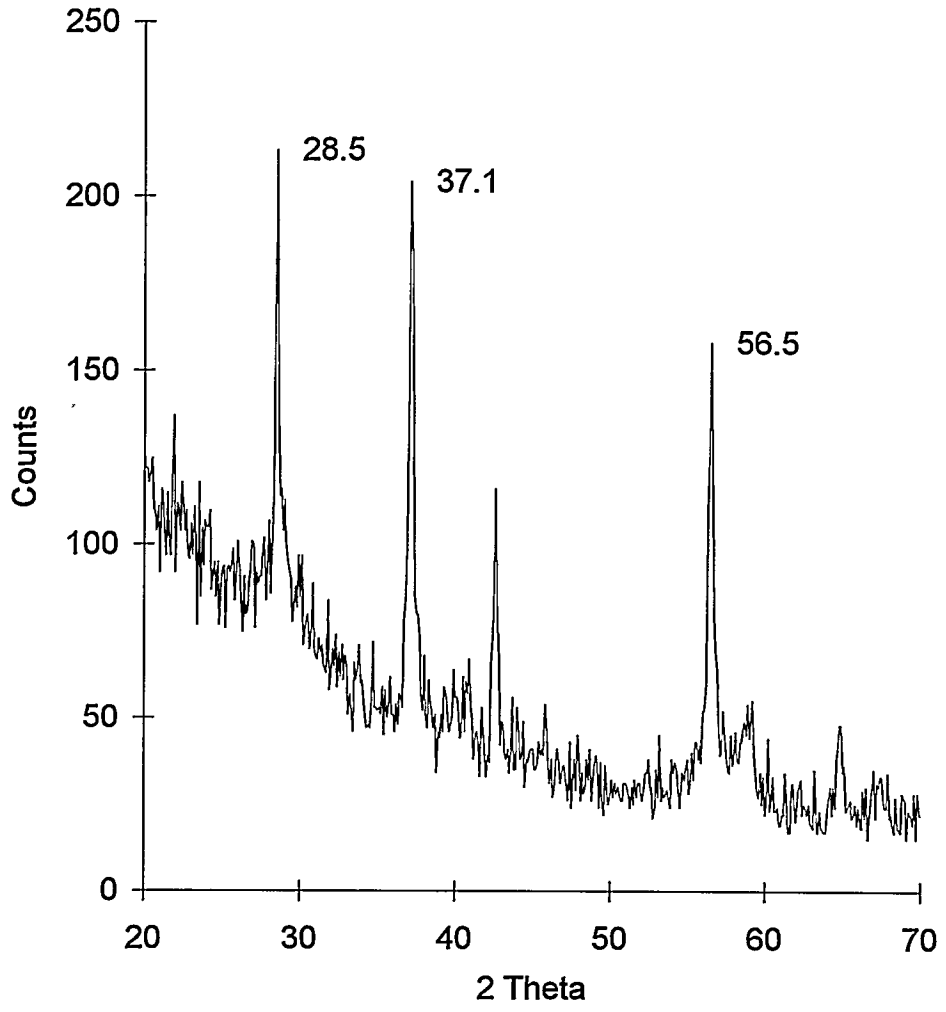

Figure 6.8. X-Ray Diffraction Test for Mn Oxide. Diffraction Peaks Matched with Pyrolusite (βMnO_2).

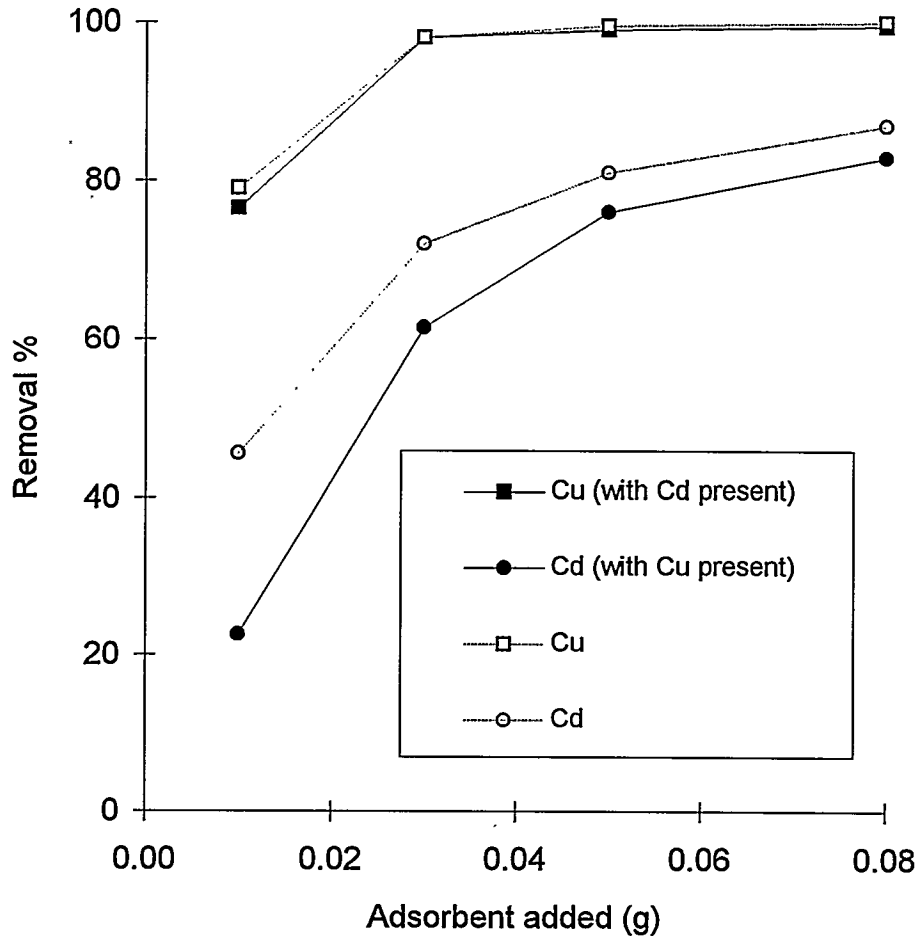

Figure 6.9. Competition Between Cu(II) and Cd(II) adsorbing on to MnTOG. Contact time = 7 days, pH 6, C_o = 2 mg/L, 0.01 N $NaNO_3$, and $4*10^{-4}$ N $NaHCO_3$.

6.5. Summary

One composite adsorbent (MnTOG) was prepared by the dry oxidation method in this research. MnTOG had a Mn content of about 27 mg Mn/g TOG. Relative to TOG by itself, the Cu(II) adsorption capacity of TOG was greatly improved by applying Mn oxide. Both Cu(II) and Cd(II) adsorption isotherms could be described by Freundlich isotherms and a longer adsorption time resulted in a higher adsorption capacity. pH_{zpc} of Mn oxide, MnTOG, and TOG were 6, 5.8, and 8.5, respectively. Because pH_{zpc} of the MnTOG was closer to Mn oxide than to TOG, most of the surface charges of MnTOG were contributed by Mn oxide. X-ray diffraction analysis showed that the Mn oxide was pyrolusite. However, x-ray diffraction analysis was unable to determine what type of Mn oxide was on the GAC surfaces. There was adsorption competition between Cu(II) and Cd(II). Although Cd(II) removal was significantly hindered by the presence of Cu(II), Cu(II) removal was only slightly influenced by the presence of Cd(II). The adsorbent (MnTOG) prepared by the dry oxidation had a higher Cu(II) adsorption capacity than did those adsorbents prepared by the adsorption and precipitation methods. Therefore, MnTOG was chosen for further investigation such as multiple adsorption/regeneration cycle, column tests (Chapter VII) and adsorption kinetics tests (Chapter VIII).

CHAPTER VII

MULTIPLE ADSORPTION/REGENERATION CYCLES AND COLUMN PROCESSES

The adsorbent (MnTOG with 27 mg Mn/g coating) prepared by dry oxidation had the highest Cu(II) adsorption capacity among the three adsorbents prepared by dry oxidation (MnTOG), precipitation (MnTOG/N), and adsorption methods (MnWVB/ads) (Figure 6.2). Therefore, MnTOG was chosen for further investigation. Multiple adsorption/regeneration cycles and column process tests will be presented in this chapter and adsorption kinetics modeling will be discussed in the following Chapter.

7.1. Multiple Cycle Processes

This test was designed to simulate multiple adsorption/regeneration column tests in a shorter time; equivalent column tests would require months to generate the same information. This test had two main objectives: To test the reusability of the adsorbent after regeneration, and to evaluate the feasibility of metal recovery after adsorption. Results of this test are shown in Figure 7.1. For MnTOG, Cu(II) removal was almost 100 % in each cycle. However, for TOG, Cu(II) removal fell from about 40 % in the first cycles to about 25 % in cycles four to six. Cu(II) recovery increased from 30 to 100

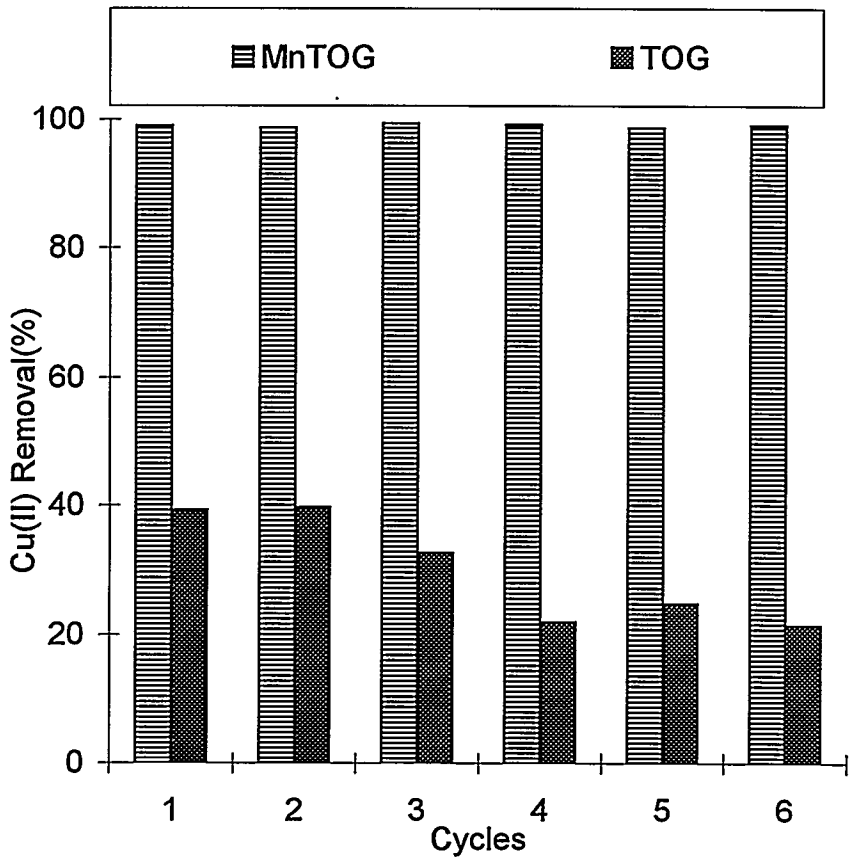

Figure 7.1. Cu(II) Removal from MnTOG and TOG in Multiple Adsorption Cycles. Adsorbent concentration 0.1 g/ 250 mL, contact time for each cycle = 3 days, pH 6, C_o = 4 mg Cu(II)/L, 0.01 N $NaNO_3$, and $4*10^{-4}$ N $NaHCO_3$.

% form the first to fifth cycle (Figure 7.2). About 70 % of the total cumulative adsorbed Cu(II) was recovered at the end of the sixth cycle. These results suggest that the adsorbent can be regenerated and reused through several cycles and most of the adsorbed Cu(II) can be recovered. The amount of retained Cu(II) estimated from a mass balance calculation (Figure 7.3), reached a maximum of about 13 mg Cu(II)/g after the fourth cycle. This amount of retained Cu(II) is larger than the amount of Cu(II) retained by TOG (5 mg Cu(II)/g), itself. Both nonexchangeable and exchangeable adsorption capacities or recoverable adsorption sites of MnTOG were apparently contributed by the coated Mn oxide. Compared to the adsorbents (MnWVB/ads, and MnTOG/N) prepared by the previous coating methods (adsorption, and precipitation method), MnTOG was more efficient for removal of Cu(II) in multiple adsorption/regeneration cycles (Figure 7.4).

7.2. Column Process

In the column tests, a 2.54 cm diameter polymethylmethacrylate column was filled with MnTOG (about 10 g) and 2 ppm Cu(II) or 1 ppm Cd(II) solution was fed from the bottom of the column. Effluent was collected periodically and analyzed for Cu(II) or Cd(II). A complete breakthrough curve for Cu(II) removal by MnTOG is shown in Figure 7.5. Complete breakthrough was reached at about 35000 bed volumes (about 100 days). The total Cu(II) adsorption capacity of MnTOG was about 86 mg Cu(II)/g , based on a simple mass balance calculation. Adsorption capacity can also be

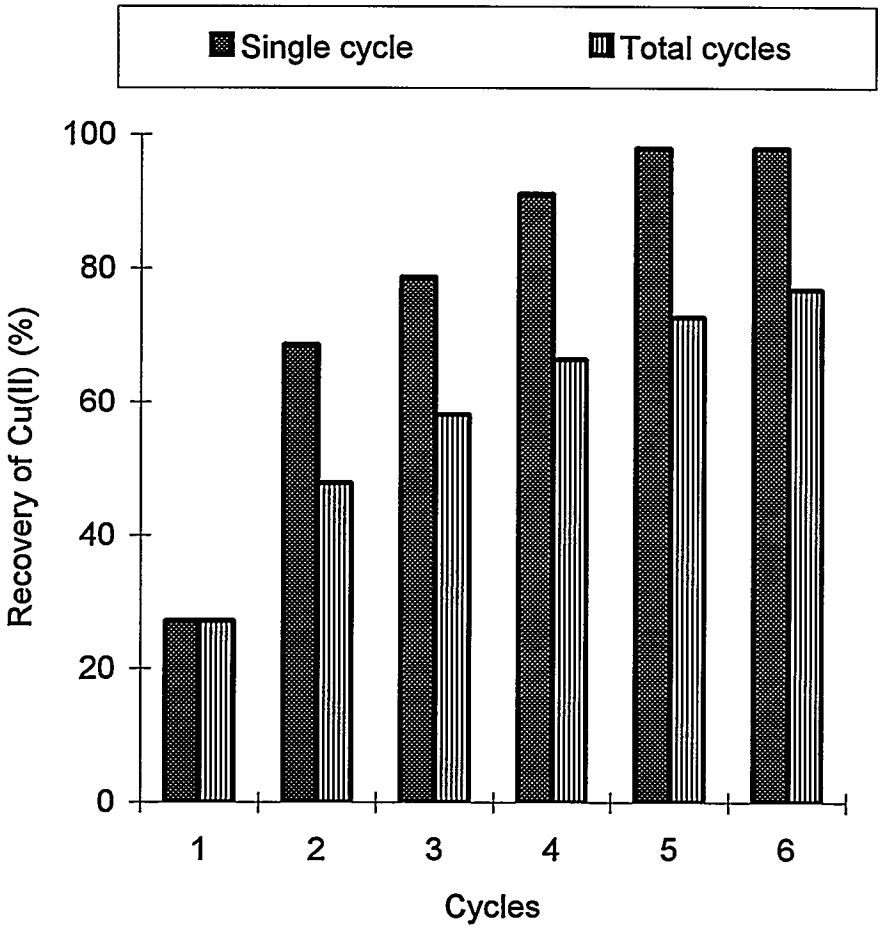

Figure 7.2. Cu(II) Recovery from MnTOG in Multiple Adsorption Cycles. pH 3, and contact time 1 day.

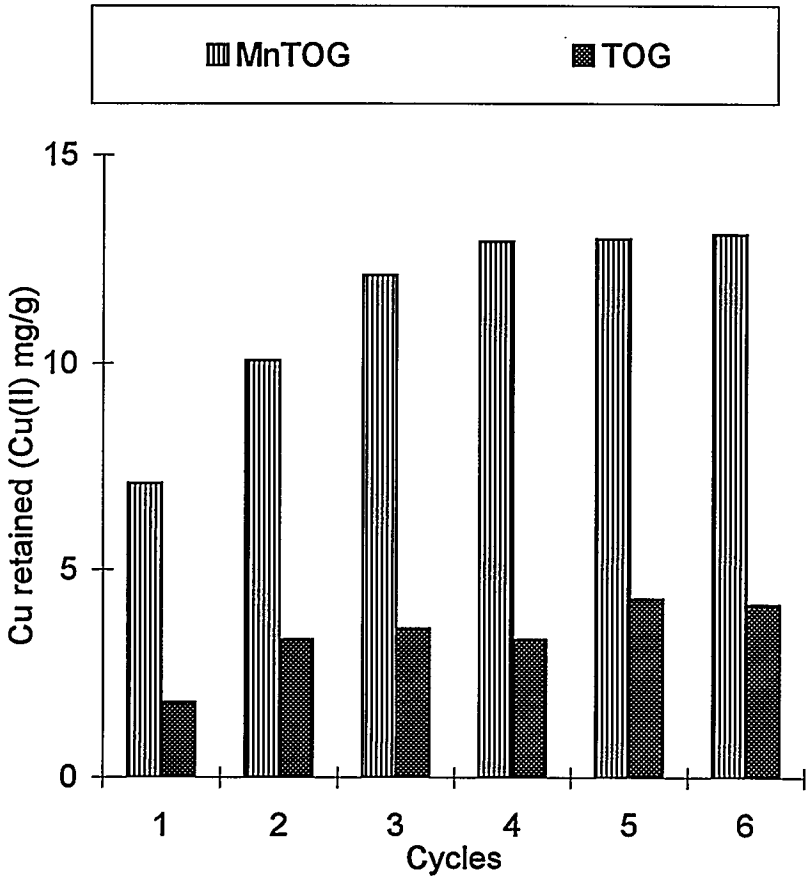

Figure 7.3. Cu(II) Retained in MnGACs and GACs in Multiple Adsorption Cycles

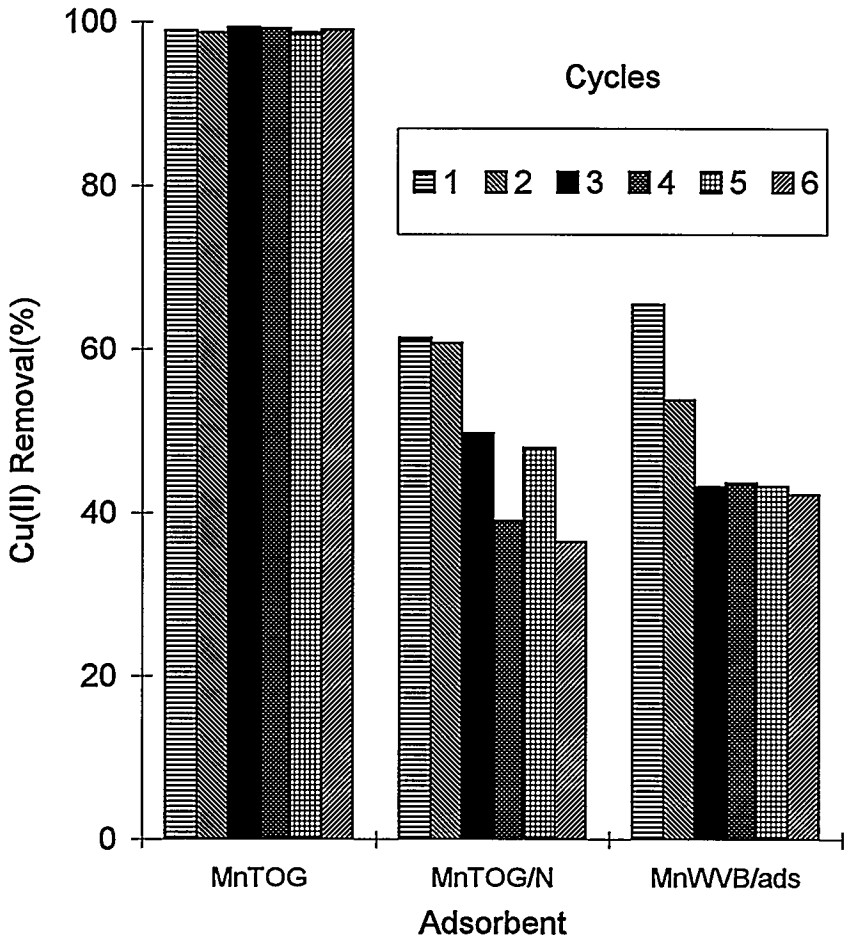

Figure 7.4. Cu(II) Removal from MnTOG, MnTOG/N, and MnWVB/ads in Multiple Adsorption Cycles. Adsorbent concentration 0.1 g/ 250 mL, contact time for each cycle = 3 days, pH 6, C_o = 4 mg Cu(II)/L, 0.01 N $NaNO_3$, and $4*10^{-4}$ N $NaHCO_3$.

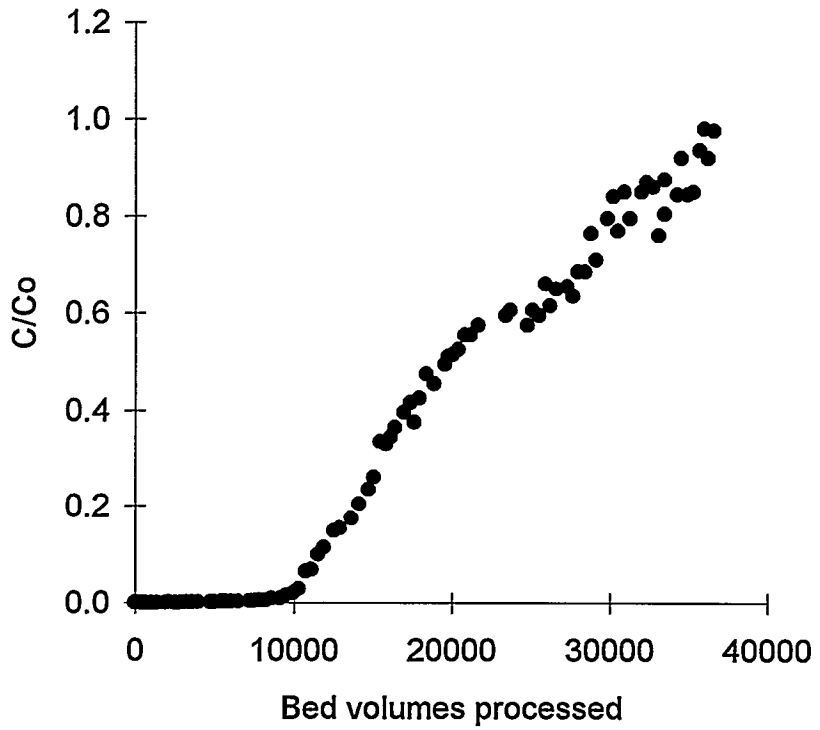

Figure 7.5. Complete Breakthrough Curve for Cu(II) Removal by MnTOG (27 mg Mn/g) in Column Processes. Loading 5 mL/min, influent Cu(II) = 2 mg/L, 0.01 N $NaNO_3$, $4*10^{-4}$ N $NaHCO_3$, and pH = 6.

obtained form adsorption isotherms (Figure 6.4) or Freundlich isotherms (Table 6.1). When solution concentration of Cu(II) was 2 mg Cu(II)/L, adsorption capacity was about 39, 55, 70, and 84 mg Cu(II)/g at 3, 7, 14, and 28 days isotherms, respectively. Freundlich isotherms obtained at a longer contact time are closer to the value obtained in the column process. Because the value predicted by the 28 days isotherm is closer to the value obtained from the column process, this isotherm will be used in the kinetics modeling in the next chapter.

The MnTOG was able to remove the influent Cu(II) (2 mg/L) to less than 4 ug/L at least for 3000 bed volumes, which was much better than MnWVB/ads which was prepared by the adsorption method. Effluent concentrations for MnTOG and MnWVB/ads are shown in Figure 7.6.

A complete breakthrough curve for Cd(II) removal by MnTOG was also obtained in this study (Figure 7.7). Complete breakthrough was reached at about 20000 bed volumes (about 60 days). Total Cd(II) adsorption capacity of MnTOG was about 28.7 mg Cd(II)/g which is slightly higher than the value (22.5 mg Cd(II)/g) predicted by the Freundlich isotherms (Table 6.2). This result suggests that Cd(II) adsorption in the column process might not be the same as in the batch system. One possible reason is the length of adsorption contact time. The adsorption isotherm used in this model was obtained in 28 days batch tests, however, the column process lasted more than 60 days. A longer contact time might result in a higher amount of Cd(II) adsorption due to a longer diffusion time. The ability of MnTOG to remove Cd(II) to trace level was also

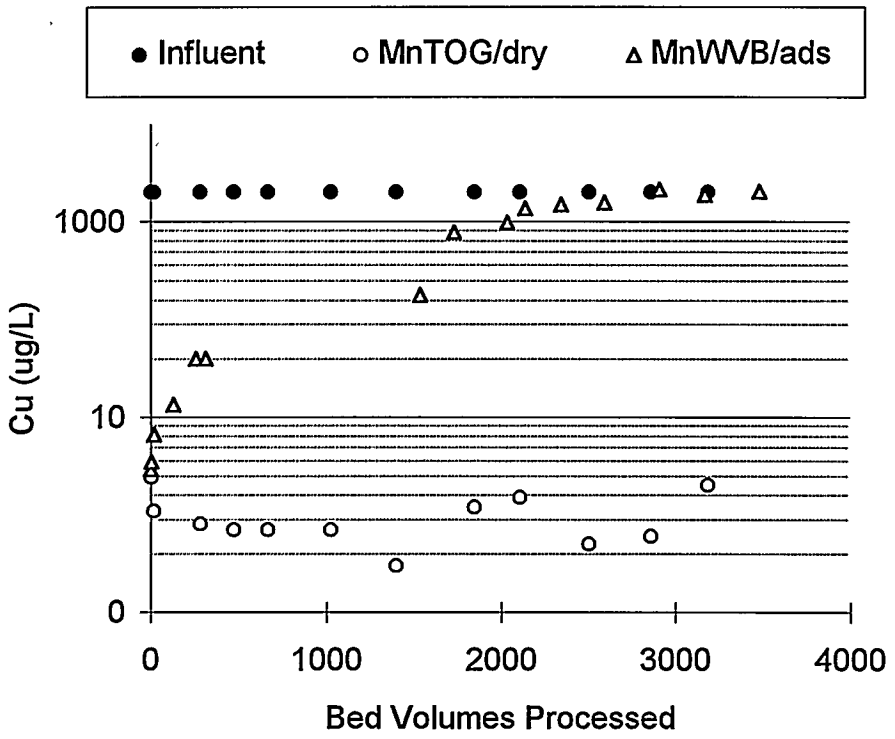

Figure 7.6. Cu(II) Removal by MnTOG/dry (27 mg Mn/g) and MnWVB/ads (20 mg Mn/g) in Column Processes. Loading 5 mL/min, influent Cu(II) = 2 mg/L, and pH = 6.

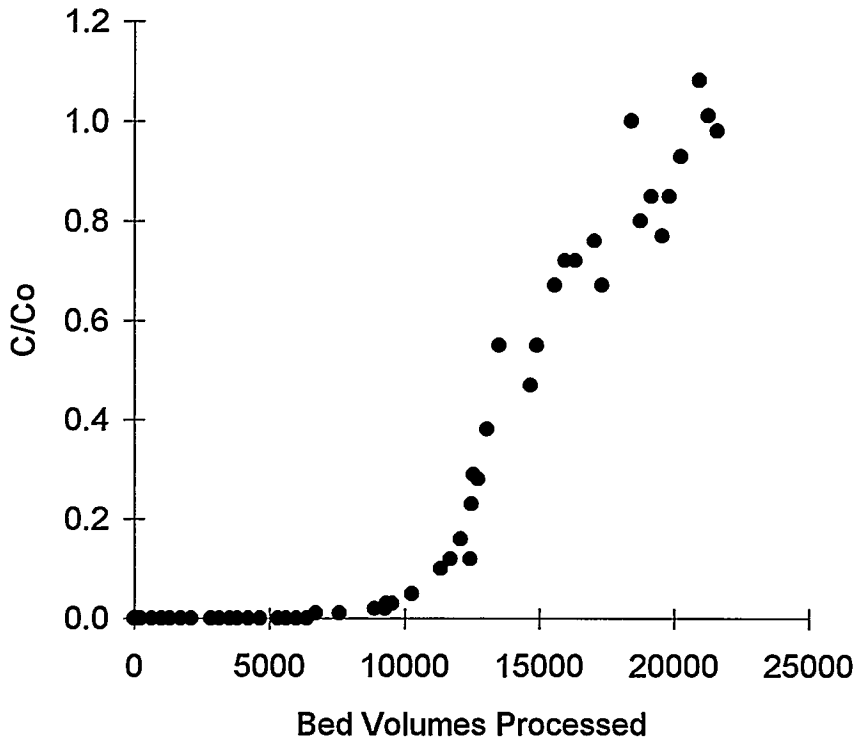

Figure 7.7. Complete Breakthrough Curve for Cd(II) Removal by MnTOG (27 mg Mn/g) in Column Processes. Loading 5 mL/min, influent Cd(II) = 1 mg/L, 0.01 N $NaNO_3$, $4*10^{-4}$ N $NaHCO_3$, and pH = 6.

demonstrated in a column test. MnTOG was able to remove Cd(II) from 1 mg/L to less than 2 μg/L at least through 1400 bed volumes (Figure 7.8).

7.3. Summary

MnTOG prepared by the dry oxidation method not only had a higher Cu(II) adsorption capacity, MnTOG can also be regenerated and reused through at least six adsorption/desorption cycles and more than 70 % of the adsorbed Cu(II) can be recovered. Both Cu(II) and Cd(II) complete breakthrough curves were obtained in this study. MnTOG was able to remove Cu(II) or Cd(II) to trace levels. To further understand the adsorption behaviors, adsorption kinetics will be discussed in the next chapter.

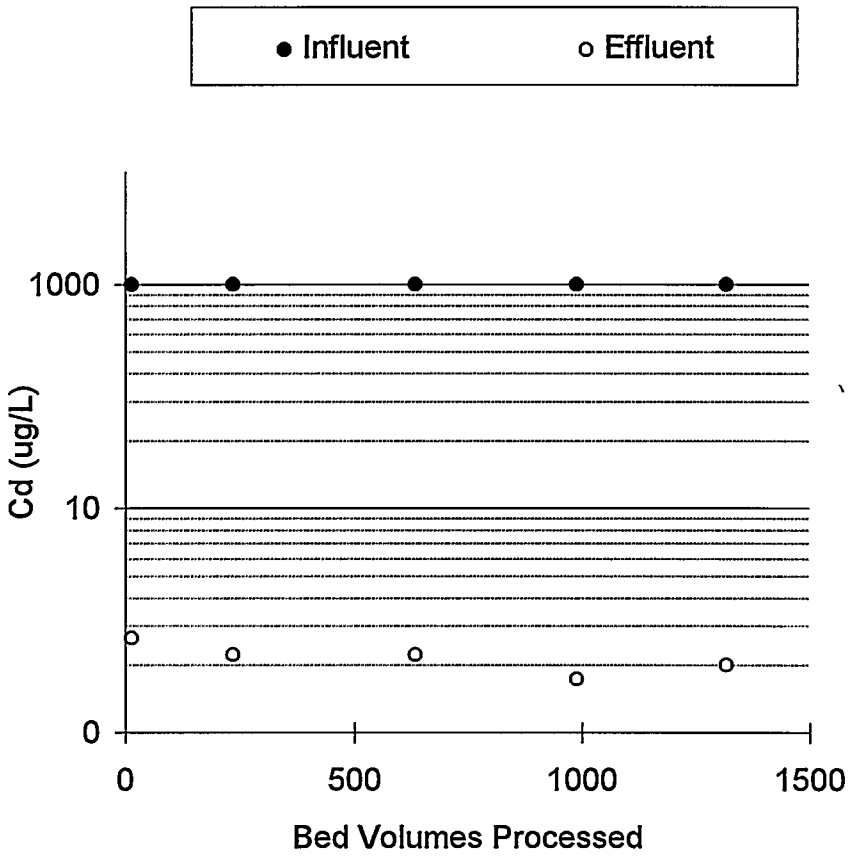

Figure 7.8. Cd(II) Removal by MnTOG in a Column Process. Loading = 5 mL/min, bed volume = 20 mL, influent Cd(II) = 1 mg/L, pH = 6, adsorbent 10 g, 0.01 N $NaNO_3$, and $4*10^{-4}$ N $NaHCO_3$.

CHAPTER VIII

KINETICS MODELING

A homogeneous surface diffusion model (HSDM) was used to model both batch and fixed-bed tests. Both Cu(II) and Cd(II) were chosen as model cations in this research.

8.1. Batch Reactor

A batch test was conducted in a 2 L beaker that contained 2 mg Cu(II)/L or 1 mg Cd(II)/L, 0.01 N $NaNO_3$, and $4*10^{-4}$ N $NaHCO_3$ adjusted to pH 6. MnTOG (1 g) was pre-equilibrated with a buffer solution (0.01 N $NaNO_3$ and $4*10^{-4}$ N $NaHCO_3$ adjusted to pH 6) before the test. This solution was completely mixed by a fixed propeller during the experiment. Samples were collected periodically and analyzed for Cu(II) or Cd(II).

Results of this batch test for Cu(II) and Cd(II) are shown in Figures 8.1 and 8.2, respectively. Both systems were modeled by a homogeneous surface diffusion model (HSDM) which is one of the most widely used models for activated carbons (Roy *et al.*, 1993; Wang and Roy, 1993; Traegner and Suidan 1989; Thacker *et al.*, 1981). The model used here is based on the following assumptions: The adsorbent (MnTOG) is a homogenous spherical particle, intraparticle transport can be described by surface or solid diffusion, liquid-diffusion resistance (liquid film) exists at the external surface of the

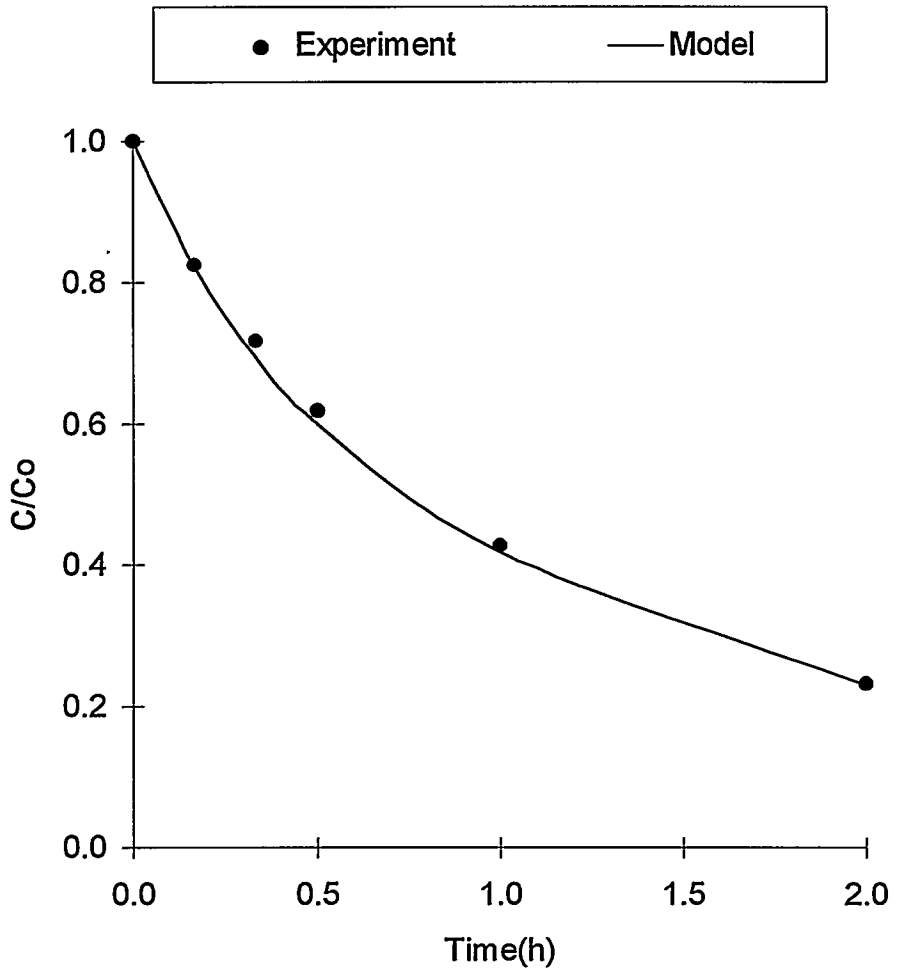

Figure 8.1. Uptake of Cu(II) by MnTOG as a Function of Time. Comparison of experimental data with homogeneous solid surface diffusion model (K_f = 0.005 cm/s and D_s = 9*10^{-11} cm^2/s). Adsorbent concentration 0.5 g/L, pH 6, C_o = 2 mg Cu(II)/L, 0.01 N $NaNO_3$, and 4*10^{-4} N $NaHCO_3$.

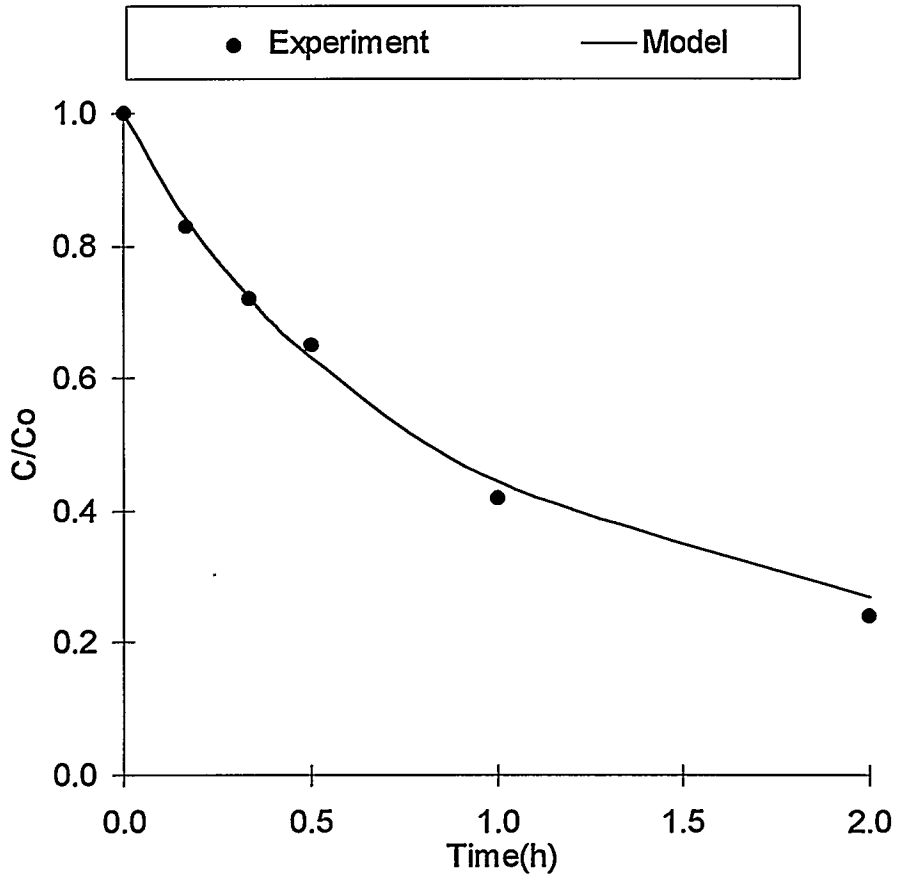

Figure 8.2. Uptake of Cd(II) by MnTOG as a Function of Time. Comparison of experimental data with homogeneous solid surface diffusion model (K_f = 0.005 cm/s and $D_s = 1*10^{-9}$ cm^2/s). Adsorbent concentration 0.5 g/L, pH 6, C_o = 1 mg Cd(II)/L, 0.01 N $NaNO_3$, and $4*10^{-4}$ N $NaHCO_3$.

adsorbent, and local equilibrium occurs at the external surface of an adsorbent particle and can be described by a Freundlich isotherm. Equations describing this model are (Thacker *et al.*, 1981):

$$\frac{\partial q}{\partial t} = \frac{D_s}{r^2}\frac{\partial}{\partial r}\left(r^2 \frac{\partial q}{\partial r}\right) \tag{8.1}$$

$$@\ t = 0,\ q = 0 \tag{8.2}$$

$$@\ t \geq = 0,\ r = 0,\ \frac{\partial q}{\partial r} = 0 \tag{8.3}$$

$$@\ t \geq = 0,\ R = 0,\ \frac{R^2 K_f (C - C_s)}{\rho} = \frac{\partial}{\partial t}\int_0^R q r^2 dr \tag{8.4}$$

$$\text{or } \rho D_s \left.\frac{\partial q}{\partial r}\right|_{r=R} = K_f (C - C_s) \tag{8.5}$$

$$@\ r = R,\ q = K * C^n \tag{8.6}$$

$$\frac{dC}{dt} = -\frac{3XK_f}{V\varepsilon R\rho}(C - C_s) \tag{8.7}$$

$$@\ t = 0,\ C = C_o \tag{8.8}$$

Where, C = Solution concentration (mg Cu(II)/L)

C_o = Initial concentration (mg Cu(II)/L)

C_s = Solution concentration at external surface of particle (mg Cu(II)/L)

D_s = Surface diffusivity (cm^2/s)

K = Freundlich isotherm constant

K_f = Film transfer coefficient (cm/s)

n = Freundlich isotherm exponent

q = Surface concentration (mg Cu(II)/g adsorbent)

r = Radial distance (cm)

R = Particle radius (cm)

t = Time (s)

V = Solution volume (L)

X = Mass of adsorbent (g)

ρ = Apparent density of particle (g/L)

ε = Porosity of batch reactor

Equation (8.1) is the homogeneous solid diffusion equation and equation (8.7) is a mass balance for the batch reactor. Parameters used in this model are listed in Table 8.1 and 8.2 for Cu(II) and Cd(II) systems, respectively. Two physical parameters (K_f and D_s) can be determined by minimizing the difference between the experimental values and the model calculated values. HSDM equations were solved by using orthogonal collocation (Finlayson, 1980; Thacker et al., 1981; Dipak *et al.*, 1993). For the Cu(II) system, the best fit D_s and K_f model values were $9*10^{-11}$ cm^2/s and 0.005 cm/s, respectively. For the Cd(II) the system, the best fit D_s and K_f model values were $1*10^{-9}$ cm^2/s and 0.005 cm/s, respectively. Results of both models gave very good agreement between the experiment

Table 8.1. Parameters Used for Cu(II)-MnTOG in Batch Modeling

Parameters	Values
Initial concentration (mg Cu(II)/L), C_o	2.0
Freundlich isotherm constant, K	62.75
Freundlich isotherm exponent, n	0.43
Particle radius (cm), R	0.03
Solution volume (L), V	2.0
Mass of adsorbent (g), X	1.0
Apparent density of particle (g/L), ρ	780

Table 8.2. Parameters Used for Cd(II)-MnTOG in Batch Modeling

Parameters	Values
Initial concentration (mg Cu(II)/L), C_o	1.0
Freundlich isotherm constant, K	22.5
Freundlich isotherm exponent, n	0.87
Particle radius (cm), R	0.03
Solution volume (L), V	2.0
Mass of adsorbent (g), X	1.0
Apparent density of particle (g/L), ρ	780

and model values. Surface diffusivity (D_s) of Cd(II) is more than ten times larger than that of Cu(II). Cu(II) with a smaller surface diffusivity will probably need a longer time to reach equilibrium, which is in agreement with the results obtained in the previous adsorption isotherm tests (Figure 6.4 and 6.5). Both D_s values were used to model the fixed-bed column tests.

8.2. Column Process

In the fixed-bed test, polymethylmethacrylate columns (2.54 cm diameter) were filled with MnTOG (about 10 g) and 2 ppm Cu(II) or 1 ppm Cd(II) solution was fed from the bottom of the column.

Cu(II) or Cd(II) adsorbed onto MnTOG in a fixed-bed could be described using HSDM equations (8.1-8.6) and a mass balance equation around the column (equation 8.9) (Weber *et al.*, 1991; Thacker *et al.*, 1981).

$$\frac{dC}{dt} = -D_h \frac{\partial^2 C}{\partial z^2} - v\frac{\partial C}{\partial z} - \frac{3(1-\varepsilon_B)}{\varepsilon_B R} K_f (C - C_s) \qquad (8.9)$$

Where, D_h = Dispersion coefficient (cm^2/s)

L_b = Bed length (cm)

v = Average linear velocity (cm/s)

z = Axial distance (cm)

ε_B = Porosity of fixed-bed

The D_s value obtained in the batch test was used for column modeling. Therefore, only one physical parameter (K_f) was needed as a fitting parameter. The best fit (K_f) was obtained by minimizing the difference between the experimental values and model values

Using the same D_s value ($9*10^{-11}$ cm^2/s) obtained from the Cu(II) batch tests, the best fit K_f for this model was about 0.00033 cm/s. K_f in the column process was smaller than the batch process (0.005 cm/s) because mixing was better in the batch than in the column. Other parameters values are listed in Table 8.3, and the model result is shown in Figure 8.3. There is a fairly good agreement between the experimental data and the model at least through 20000 bed volumes. However, the model predicted values were slightly higher than the experiment data after 20000 bed volumes. One possible reason for this difference is the length of adsorption contact time. The adsorption isotherm used in this model was obtained from a 28 day batch tests, however, the column process lasted more than 100 days. A longer contact time might result in a higher amount of Cu(II) adsorption due to a longer diffusion time, so the total Cu(II) adsorption capacity in the column process was underestimated by the batch isotherm tests. Adsorption isotherms obtained at various contact times (3, 7, 14, and 28 d) were used in the HSDM model (Figure 8.4). Model values are closer to the experimental data when an isotherm obtained from a longer contact time was used.

Another fixed bed test was conducted under the same conditions except that the influent was 1 ppm Cd(II). Parameters used in this model are listed in Table 8.4. The

Table 8.3. Parameters Used for Cu(II)-MnTOG in Fixed-Bed Modeling

Parameters	Values
Influent concentration (mg Cu(II)/L), *Co*	2.0
Freundlich isotherm constant, *K*	62.75
Freundlich isotherm exponent, *n*	0.43
Particle radius (cm), *R*	0.03
Mass of adsorbent (g), *X*	10.0
Apparent density of particle (g/L), ρ	780
Porosity of fixed-bed, ε_B	0.353
Dispersion coefficient (cm^2/min), D_h	0.03
Bed length (cm), L_b	4.2
Average Linear velocity(cm/min), *v*	3.0

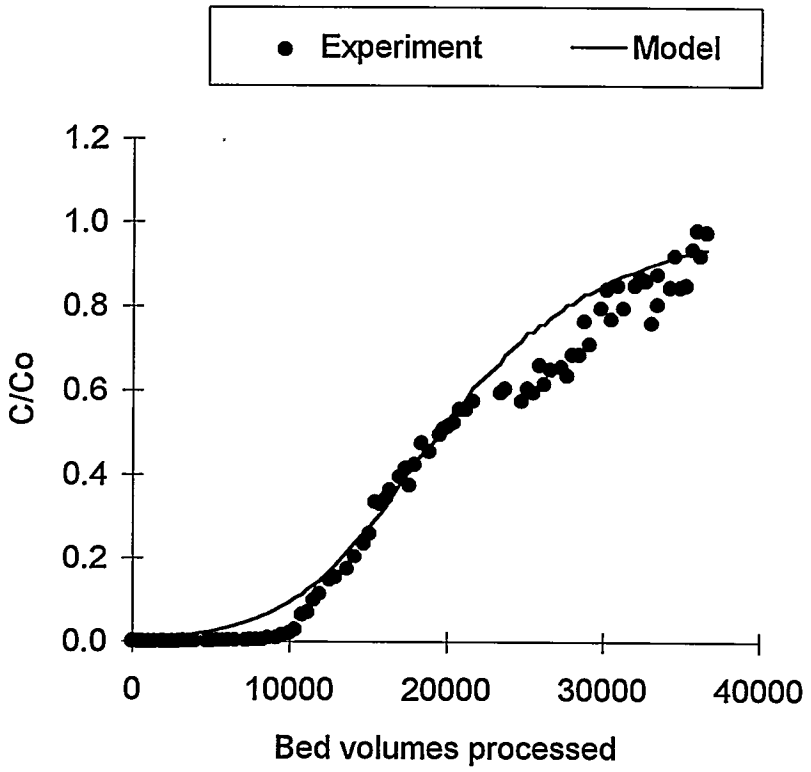

Figure 8.3. Breakthrough Curve for Cu(II) Removal by MnTOG. Comparison of experimental data with HSDM model (K_f = 0.00033 cm/s and $D_s = 9*10^{-11}$ cm^2/s). Adsorbent 10 g, loading 5 mL/min, bed volume = 20 mL, influent Cu(II) = 2 mg/L, pH = 6, 0.01 N $NaNO_3$, and $4*10^{-4}$ N $NaHCO_3$.

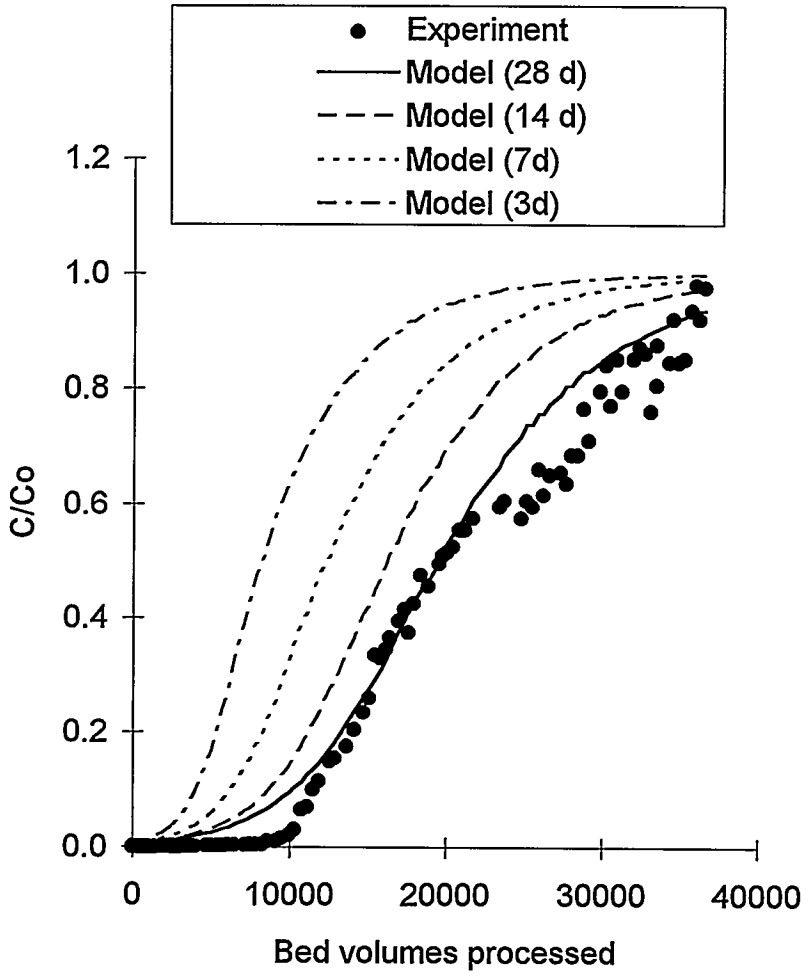

Figure 8.4. Breakthrough Curve for Cu(II) Removal by MnTOG. Comparison of experimental data with HSDM model using Freundlich isotherms obtained from various contact times. (K_f = 0.00033 cm/s and D_s = 9*10^{-11} cm^2/s). Adsorbent 10 g, loading 5 mL/min, bed volume = 20 mL, influent Cu(II) = 2 mg/L, pH = 6, 0.01 N $NaNO_3$, and 4*10^{-4} N $NaHCO_3$.

Table 8.4. Parameters Used for Cd(II)-MnTOG in Fixed-Bed Modeling

Parameters	Values
Influent concentration (mg Cu(II)/L), *Co*	2.0
Freundlich isotherm constant, *K*	22.5
Freundlich isotherm exponent, *n*	0.87
Particle radius (cm), *R*	0.03
Mass of adsorbent (g), *X*	10.0
Apparent density of particle (g/L), ρ	780
Porosity of fixed-bed, ε_B	0.353
Dispersion coefficient (cm^2/min), D_h	0.03
Bed length (cm), L_b	4.2
Average Linear velocity(cm/min), *v*	3.0

D_s value obtained in the Cd(II) batch test was used for column modeling. The best fit (K_f) by minimizing the difference between the experimental values and model values was about 0.00067 cm/s (Figure 8.5). However, the model was unable to predict the breakthrough completely. It is possible that the Cd(II) precipitated on the MnTOG surfaces which would result in increased Cd(II) removal.

8.3. Conclusions

Adsorption of Cu(II) or Cd(II) onto MnTOG in a batch reactor or fixed-bed reactor was modeled with a homogeneous surface diffusion model (HSDM) in this study. Model parameters (K_f and D_s) were determined by minimizing the difference between the experimental values and the model calculated values (Table 8.5). Cu(II) and Cd(II) adsorption isotherms obtained at various contact times (3, 7, 14, and 28 d) were obtained and used in the HSDM model. The HSDM model successfully described adsorption of Cu(II) or Cd(II) onto MnGAC in batch systems. In Cu(II) fixed bed tests, model values are closer to the experimental data when an isotherm obtained form a longer contact time was used. However, the model was unable to predict the breakthrough completely in the Cd(II) fixed-bed study. It is possible that Cd(II) surface precipitation occurred on the MnGAC surface in the column process, which may result in a higher amount of Cd (II) removal. Similar phenomena were reported by Loganathan *et al.* (1977). The authors reported that additional heavy metal (Co or Zn) removal was due to Co or Zn precipitation on Mn oxide surfaces. Wang (1995) also conducted a similar study by using

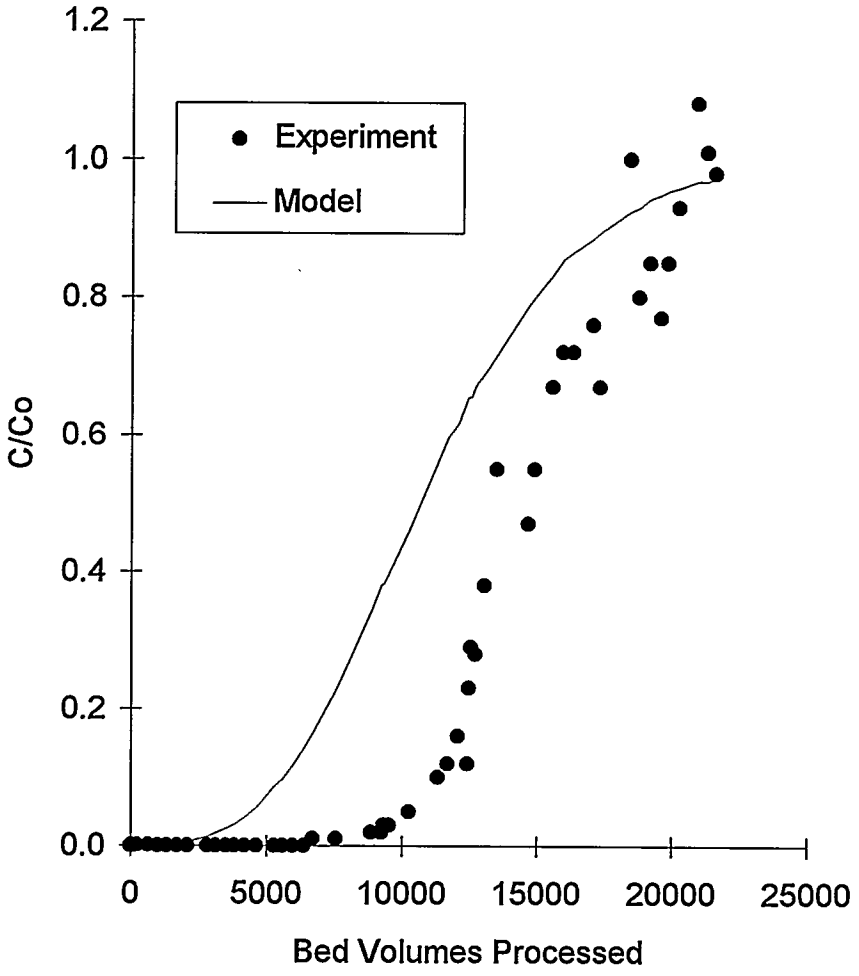

Figure 8.5. Breakthrough Curve for Cd(II) Removal by MnTOG. Comparison of experimental data with HSDM model (K_f = 0.00067 cm/s and $D_s = 1*10^{-9}$ cm^2/s). Adsorbent 10 g, loading 5 mL/min, bed volume = 20 mL, influent Cd(II) = 1 mg/L, pH = 6, 0.01 N $NaNO_3$, and $4*10^{-4}$ N $NaHCO_3$.

Table 8.5. K_f and D_s Obtained in Batch and Fixed-Bed Modeling

	MnGAC		FeGAC (Wang, 1995)	
Systems	K_f (cm/s)	D_s (cm^2/s)	K_f (cm/s)	D_s (cm^2/s)
Batch reactor				
Cu(II)	0.005	$9*10^{-11}$	0.001	$2*10^{-10}$
Cd(II)	0.005	$1*10^{-9}$	0.004	$4*10^{-10}$
Fixed-bed reactor				
Cu(II)	0.00033	$9*10^{-11}$	0.0004	$2*10^{-10}$
Cd(II)	0.00067	$1*10^{-9}$	0.0003	$4*10^{-10}$

Fe oxide-coated GAC as adsorbent and results of his research are also listed in the Table 8.5. Both results indicated that the D_s values of Cu(II) were smaller than the D_s values of Cd(II). This results are in agreement with the results obtained from Figures 6.4 and 6.5. Cu(II) with a smaller surface diffusivity (D_s) needed a longer diffusion time to reach equilibrium.

K_f values in the column process also can also be estimated by empirical equations (Crittenden *et al.* 1987, Weber and Smith, 1987). For example,

$$K_f = 2.4\ V_s / (Sc^{0.58}\ Re^{0.66}) \tag{8.10}$$

$$Re = 2\ R\ \rho_1\ V_s/(\varepsilon_B\ \mu) \tag{8.11}$$

$$Sc = \mu/(\rho_l D_l) \tag{8.12}$$

(Valid for $0.08 < Re < 150$ and $150 < Sc < 1300$)

Where, V_s = superficial loading velocity (L/t)

Sc = Schmidt number (dimensionless)

Re = Reynolds number (dimensionless)

ρ_1 = fluid density (M/L^3)

ε_B = porosity of fixed bed (dimensionless)

μ = viscosity of the fluid (centipose)

D_l = liquid phase diffusivity (L^2/t)

By assuming $D_l = 10^{-5}$ cm^2/s, K_f is about 0.0024 cm/s which is about one order of magnitude larger than the values (0.00033 or 0.00067 cm/s) calculated form the

column systems. However, the value obtained from the empirical equation is closer to the K_f obtained from the batch systems (0.005 cm/s).

Parameter sensitivity (K_f or D_s) of HSDM modeling results for Cu(II) adsorption onto MnTOG in a batch system are shown in Figure 8.6. With ± 50 % variations in K_f (from 0.0075 to 0.0025 cm^2/s) or D_s (from $1.4*10^{-10}$ to $4.5*10^{-11}$ cm/s), K_f had a larger impact on simulation values than did D_s. Furthermore, variation in K_f values changed the whole range of simulation results, while D_s had a greater influence on the later simulation results or time. Overall, K_f was more sensitive than D_s.

Another sensitivity analysis was also studied for the column process with ± 25 % variation away from the best fit K_f (0.00033 cm/s) (Figure 8.7). A larger K_f would enhance the removal of Cu(II) in the early adsorption time. For example, by setting the maximum relative effluent concentration to 0.1, the total volumes processed increased form 10000 to 13000 BV by increasing 25 % of K_f value. However, the changing of K_f values would not change the total adsorption capacity.

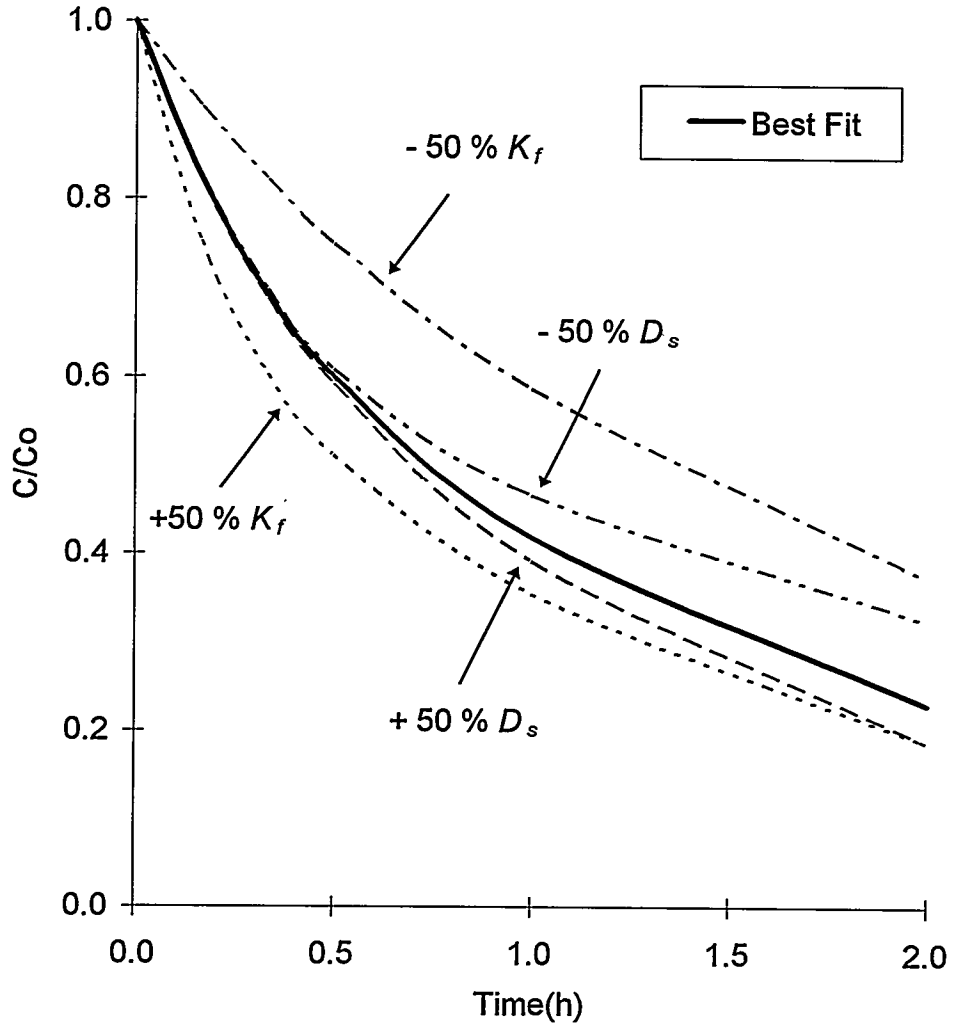

Figure 8.6. Parameter Sensitivity of HSDM Modeling Results for Cu(II) Adsorption onto MnTOG in a Batch System

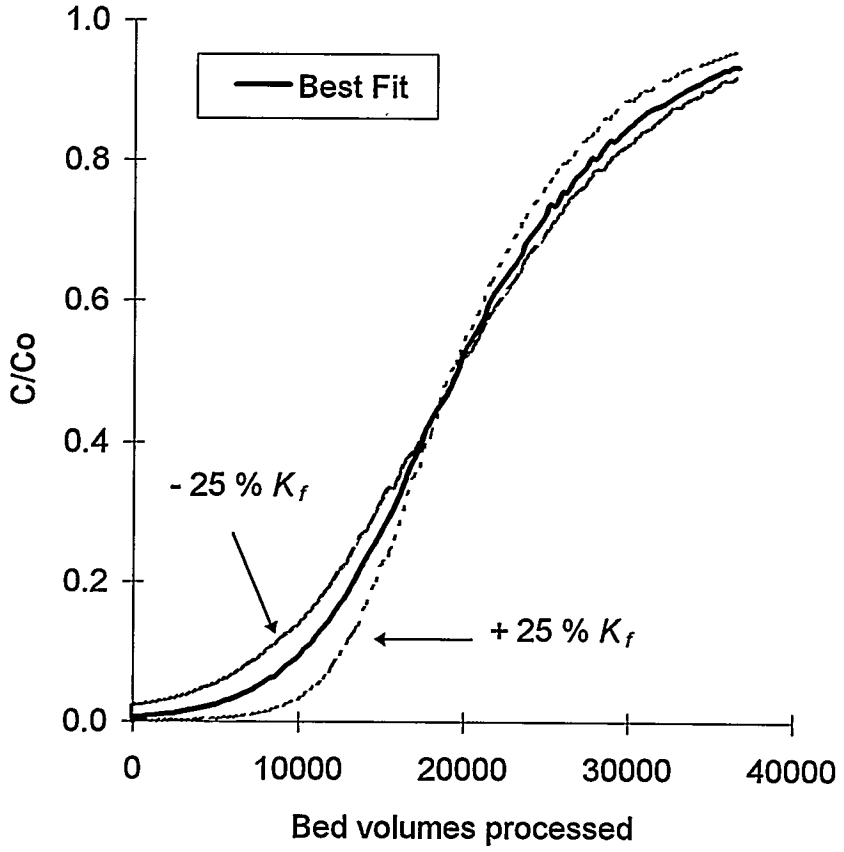

Figure 8.7. Parameter Sensitivity of HSDM Modeling Results for Cu(II) Adsorption onto MnTOG in a Column System

CHAPTER IX

CONCLUSIONS AND FUTURE STUDY

Mn oxide can be deposited on GAC to create a composite adsorbent with increased Cu(II) or Cd(II) adsorption capacity. Three coating methods (adsorption, precipitation, and dry oxidation) were developed and studied in this research.

In the adsorption method, factors affecting the amount of coating on GAC were type of GAC, GAC pore volume, GAC particle size, coating time, Mn dosage, and the duration of prewash time. WVB had the highest Mn coating efficiency and the highest Cu(II) adsorption capacity among the carbons tested. In general, a longer coating or prewash time, a larger pore volume of GAC, a higher amount of applied Mn dosage, or a smaller GAC particle size would result in a higher amount of Mn coating. In batch tests with Cu(II), relative to GAC by itself, adsorption capacities were increased more than three times after coating and Mn oxides dominated the adsorption process. Complete breakthrough for a column occurred after 3000 bed volumes (BV) were processed. In multiple adsorption/regeneration cycles although total Cu(II) removal decreased from the first to the third cycle, Cu(II) removal stayed about the same in the third and subsequent cycles.

In the precipitation method, the Mn oxide was precipitated on the GAC surfaces by evaporation. Nine composite adsorbents were prepared by using three GACs (WVB, APC, and TOG) and three manganese salts (manganese nitrate (N), manganese sulfate (S), and manganese chloride (C)). In general, the sequences of the amount of coatings were

manganese chloride > manganese nitrate > manganese sulfate and APC > WVB > TOG. However, in adsorption edge tests, MnWVB had the highest amount of Cu(II) adsorption capacity. This result is not in agreement with the amount of Mn coatings on these GACs, perhaps because of differences in GAC or Mn oxide crystal structure. Results also suggest that the MnGAC can be used through several adsorption/regeneration cycles but a fraction of the Cu(II) will be retained in the MnGAC after regeneration.

Finally, MnTOG (with 27 mg Mn/g coating) prepared by a dry oxidation method had a higher Cu(II) adsorption capacity than did other adsorbents prepared by adsorption and precipitation methods. MnTOG can be regenerated and reused through at least six adsorption/desorption cycles and more than 70 % of the adsorbed Cu(II) can be recovered. MnTOG had the ability to remove Cu(II) and Cd(II) to trace level (< 4 *ug*/L) in a column process at least through 3000 and 1400 BV, respectively. Cd(II) removal was hindered by the presence of Cu(II). However, Cu(II) removal was only slightly reduced by the be presence of Cd(II). Cu(II) adsorption in batch and fixed-bed processes onto MnTOG was successfully modeled with a homogeneous surface diffusion model (HSDM). However, the HSDM could only describe the adsorption of Cd(II) onto MnTOG in batch process, but not fixed-bed process. The difference is probably due to the Freundlich isotherm used in the HSDM model. The Freundlich isotherm obtained in 28 days batch tests underestimated the values obtained in the column process (60 days) based on a mass balance calculation. Perhaps a longer contact time would decrease the adsorption capacity difference between batch and column process. Further study should continue to explore the relationship between batch and fixed-batch systems.

A summary of some of the MnGACs and Mn oxide-coated sand (BHS, and PS) prepared by Stahl and James (1991) for Zn(II) removal is listed in the Table 9.1. In general, Mn oxide-coated GACs had higher metal adsorption capacities than did Mn oxide-coated sands. For example, Mn oxide-coated GACs (MnWVB, MnTOG/N, or MnTOG) had Cu(II) adsorption capacities from 5 to 23 μmole Cu(II)/mg Mn and Mn oxide-coated sands (BHS or PS) had Zn(II) adsorption capacity from 0.05 to 0.63 μmole Zn(II)/mg Mn. The surface areas of GACs were about 200 times larger than the surface areas of sands. The large surface area of GAC might spread out the coated Mn oxides and make more efficient use of Mn oxides. As a result, MnGAC had a higher amount of metal adsorption capacity. According to the coating procedures, adsorbents prepared by the adsorption, precipitation, and dry oxidation methods are probably amorphous Mn oxides, birnessite, and pyrolusite, respectively. The x-ray diffraction analysis was not able to determine the crystal structure of Mn oxides on MnTOG. It is probably that the Mn oxides randomly distributed on the surface of GAC and these Mn oxide clusters were too small to form clear x-ray diffraction patterns. However, x-ray diffraction analysis did identify Mn oxides as pyrolusite which was prepared by a similar procedure as MnTOG except without TOG present. Furthermore, The pH_{zpc} value of MnTOG is the same as the pH_{zpc} value of pyrolusite prepared in this research. Results also indicated that the pyrolusite-coated GAC (MnTOG) had a higher amount of Cu(II) adsorption capacity than the birnessite-coated GAC (MnTOG/N). Cu(II) adsorption capacity of pyrolusite-coated GAC (23 μmole/mg Mn) was more than four times higher than the birnessite-coated GAC (5 μmole/mg Mn). However, this result is in contrast with the results reported by Stahl

Table 9.1. Characteristics of Mn Coated Adsorbents

Adsorbent	MnWVB	MnTOG/N	MnTOG	BHS[1]	PS[1]
Coating method	Adsorption	Precipitation	Dry oxidation	Precipitation	Dry oxidation
Supported medium	WVB	TOG	TOG	Quartz sand	Quartz sand
Particle Size (mm)	1.0	0.5	0.5	NA	NA
Surface area (m^2/g)	1400-1600	800-900	800-900	4.5	4.5
Applied Mn (mg Mn/g)	97	55	55	4.29[2]	27.72[2]
Coating (mg Mn/g)	20	22	27	1.91[2]	26.93[2]
Possible crystal structure	Amorphous (MnO_2)	Birnessite (δ-MnO_2)	Pyrolusite (β-MnO_2)	Birnessite (δ-MnO_2)	Pyrolusite (β-Mn O_2)
Adsorbate	Cu(II)	Cu(II)	Cu(II)	Zn(II)	Zn(II)
Removal (%)[3]					
pH = 6	55	62	98	48[2] (pH 6.3)	56[2] (pH 6.6)
pH = 4	20	18	80	28[2] (pH 4.8)	4[2] (pH 4.2)
Adsorption capacity					
(mg/g)	9	7	40		
(μmole/g)	141 (pH 6)	110 (pH 6)	630 (pH 6)	1.2 (pH 6.3)	1.4 (pH 6.6)
(μmole/mg Mn)	7.05	5.00	23.33	0.63[2]	0.05[2]
C_e (mg/g)	2	1.5	2	2[2]	2[2]

(1) Stahl and James (1991)
(2) Values were estimated form Stahl and James's paper (1991)
(3) Mn GAC systems, solution C_o = 4 Cu(II) mg/L, V = 250 mL, 3 days contact time, C_e about 2 mg Cu(II)/L, and adsorbent 0.1 g
MnSand systems, solution C_o = 0.08 mM (5.2 mg/g), loading = 2500 μmol Zn(II)/kg sand, V = 85 mL, and contact time 1 days
NA = Not available, V = batch volume, and C_e = metal soluble concentration.

and James (1991) in a study of Mn oxide-coated sands. Stahl and James (1991) reported that birnessite-coated sand (BHS) had a higher Zn(II) adsorption capacity than pyrolusite-coated sand (PS). The higher metal adsorption capacity of birnessite was probably due to a higher surface area than that of pyrolusite. Birnessite had an almost complete lack of crystallinity or only had crystals about 2 or 3 atomic layers thick and had surface area about 300 m^2/g but, on the other hand, pyrolusite had a sharply crystalline (tetragonal) structure with a surface area only 8 m^2/g (Healy, 1966, Huang, 1991). In the case of Mn oxide-coated sand, sand provided a limited surface area (4.5 m^2/g), so the surface area of Mn oxide was important for metal adsorption. Because birnessite had a larger surface area than had pyrolusite, therefore, birnessite had a higher metal adsorption capacity when birnessite was coated on sand. However, in the case of Mn oxide-coated GAC, surface area was no longer a limiting factor because GAC provided a very large surface area for Mn oxides to spread on. The metal affinity of Mn oxides might became more important than surface area. Gary (1981) pointed out that pyrolusite had a higher electrostatic field strength than had birnessite. The higher electrostatic field strength of pyrolusite might contribute a higher metal adsorption capacity which was shown in this study.

Adsorption capacity and affinity of Cu(II) for MnTOG were larger than those of Cd(II) in this research. Similar findings were reported by Nordqvist *et al.* (1988) and Kinniburgh and Jackson (1981) for adsorption onto iron hydroxide, Fe or Al oxides. However, Kinniburgh and Jackson (1981) also pointed out that different structure forms of Mn oxides with different polarity and zpc (zero point of charge) may have different selectivity. For example, the selectivity sequence of δ-MnO_2 is $Cs^+ > Na^+$, but the

selectivity sequence of β-MnO_2 is $Na^+ > Cs^+$. Furthermore, Kinniburgh and Jackson (1981) also pointed out that pH might also affect the adsorption selectivity. For example, the adsorption sequence at pH 4 for MnO_2 is Cd(II) > Zn(II), but adsorption sequence is Zn(II) > Cd(II) at pH 6 and 8. Therefore, caution must be taken when dealing with adsorption competition between cations.

In adsorption capacity studies, Cu(II) takes a longer time to reach equilibrium. For example, Cu(II) adsorption capacities increased from 40 to 60 mg Cu(II)/g while the contact times increased from 3 to 28 days, but Cd(II) adsorption capacities remained relatively constant while the contact time increased. Further evidence of the slower diffusion of Cu(II) was also obtained in batch kinetics study. The surface diffusion coefficient (D_s) of Cu(II) was about 0.1 the value of D_s of Cd(II). With a smaller D_s value, Cu(II) would need a longer diffusion time to reach the adsorption sites. The smaller D_s value of Cu(II) might be partially due to its high affinity with MnTOG. In the process of surface diffusion, Cu(II) had to migrate from site to site along the MnTOG surfaces, a high affinity between Cu(II) and MnTOG might delay the migration process which might result a smaller D_s value.

There was a certain amount of Cu(II) retained in the MnGAC or GAC after regeneration at pH 3 in multiple adsorption/regeneration processes. Some of the retained Cu(II) can be further reduced by decreasing pH value which could be explained by the surface complex model (equations 2.14-17). However, a lower pH solution might dissolve some of coated Mn oxides which would reduce the total Cu(II) adsorption capacity for the next adsorption cycle. Some of the retained Cu(II) may be attributed to

stronger adsorption sites on MnGAC surfaces. Although the strength of adsorption sites was treated equal in the HSDM modeling process these adsorption sites had a range of affinities for metals. Weak adsorption sites could be regenerated and reused after adsorption, but strong adsorption sites could not. Because the retained Cu(II) increased about 3 times from TOG (4 mg Cu(II)/g) to MnTOG (13 mg Cu(II)/g), most of the retained Cu(II) was adsorbed by Mn oxides or Mn oxide-TOG complex on MnTOG.

To better understand the MnGAC, surface characteristics of MnGAC should be further investigated to identify mineral types and the distribution of coated Mn oxides. Different crystal structures have different metal adsorption capacity and adsorption behavior, and the distribution of Mn oxides on the surface may affect the metal diffusion process. In addition to the adsorption reactions studied in this research, other interactions such as redox reactions between metals and Mn oxides, surface precipitation, Mn oxide dissolution, and ion substitution in the oxide structure (Loganaathan, 1977, Gary, 1981, Huang, 1991) should be further investigated. Finally, because coal processing wastewaters are far more complicated than a single metal solution, interactions between metals, organic, and chelating agents should be studied, and an actual coal processing wastewater should be applied to a column process.

ACKNOWLEDGMENTS

The authors appreciate funding of this project by the Department of Energy under the University Coal Research Program, Grant DE-FG22-93PC93207.

BIBLIOGRAPHY

Bachelor, B. and Dennis, R. (1987) A surface complex model for adsorption of trace components from wastewater. *J. WPCF*, 59(12), 1059-1068.

Benjamin, M. M., Hayes, K. F., Leckie, J. O. (1982) Removal of toxic metals from power-generation waste streams by adsorption and coprecipitation. *J. Water Pollut. Control Fed.*, 54,1472-1481.

Benjamin, M. M. and Leckie, J. O. (1982) Effect of complexation by Cl, SO_4, and S_2O_3 on adsorption behavior of oxide species. *Environ. Sci. Technol.*, 16, 162.

Bhattacharyya, D. and Cheng, R. C. Y. (1987) Activated carbon adsorption of heavy metal chelates from single and muticomponent systems. *Environ. Progress*, 6(2),110-118.

Bowers, A. R. and Huang, C. P. (1980) Activated carbon processes for the treatment of chromium (VI)-containing industrial wastewaters. *Prog. Wat. Tech.*, 12, 629-650.

Bricker, O. (1965) Some stability relations in the system Mn-O_2-H_2O at 25° and one atmosphere total pressure. *Am. Mineral.*, 50, 1296-1354.

Chadwick, M. J. and Lindman, N. (1982) *Environmental Implications of Expanded Coal Utilization.* Pergamon Press, New York.

Chapman, B. N. and Anderson, J. C. (1974) *Science and Technology of Surface Coating.* Academic Press, New York.

Clark, R. M. and Lykins, B. W. Jr. (1989) *Granular activated carbon, design, operation and cost.* Lewis Publishers, New York.

Clesceri, L. S., Greenberg, A. R. and Trussell, R. R. (1989) *Standard Methods for the Examination of Water and Wastewater*, 17th edition. American Public Health Association, Washington, DC.

Corapcioglu, M. O. and Huang, C. P. (1987a) The surface acidity and characterization of some commercial activated carbons. *Carbon*, 25(4) ,569-578.

Corapcioglu, M. O. and Huang, C. P. (1987b) The adsorption of heavy metals onto hydrous activated carbon. *Wat. Res.*, 21(9) ,1031-1044.

Cowan, C. E., Zachara, J. M. and Resch, C. T. (1991) Cadmium adsorption on iron oxides in the presence of alkaline-earth elements. *Environ. Sci. Technol.*, 25(3), 437-446.

Crittenden, J. C., Hand, D. W., Arora, H., and Lykins, B. W. Jr. (1987) Design Considerations for GAC Treatment of Organic Chemicals. *J. AWWA*, Jan., 1987, 74-82.

Davis, J. A. and Leckie, J. O. (1978) Surface ionization and complexation at the oxide/water interface II. Surface properties of amorphous iron oxyhydroxide and adsorption of metal ions. *J. Colloid Interface Sci.*, 67(1), 90-107.

Dunbar, L. E. (1987) Implementation of a water quality-based strategy for protection of aquatic life. *J. Water Pollut. Control Fed.*, 59, 761-766.

Dzombak, D. A. and Morel, F. M. M. (1987) Adsorption of inorganic pollutants in aquatic systems. *J. Hydraulic Eng. ASCE*, 113, 430-475.

Dzombak, D. A. and Morel, F. M. M. (1990) *Surface complexation modeling-hydrous ferric oxide.* Jonn wiley & son, New York.

Edwards, M. and Benjamin, M. M. (1989a) Regeneration and reuse of iron hydroxide adsorbents in treatment of metal-bearing wastes. *J. Water Pollut. Control Fed.*, 61, 481-490.

Edwards, M. and Benjamin, M. M (1989b) Adsorptive filtration using coated sand: A new approach for treatment of metal-bearing wastes. *J. Water Pollut. Control Fed.*, 61, 1523-1533.

Faust, S. D. and Aly, O. M. (1983) "Removal of inorganic contaminants-Manganese" in *Chemistry of water treatment.* Butterworth Publishers, Woburn, MA. 483-492.

Finalyson, B. A. (1980) *Nonlinear analysis in chemical engineering.* McGraw-Hill Inc., New York.

Fogler, H. S. (1992) "Diffusion and reaction in porous catalysts" in *Elements of chemical reaction engineering.* Prentice Hall, Englewood Cliffs, NJ, 607-659.

Froment, G. F. and Bischoff, K. B. (1990) *Chemical reactor analysis and design.* John Wiley & Sons, NY.

Gajghate, D. G., Saxena, E. R. and Aggarwal, A. L. (1992) Removal of chromium(VI) as chromium diphenyl carbazide (CDC) complex form aqueous solution by activated carbon. *Water, Air, and Soil Pollution.*, 65, 329-337.

Gray, M. J. (1981) Manganese dioxide as an adsorbent for heavy metals. *Effluent and Water Treatment Journal.*, 21, 201-203.

Healy, T. W., Herring, A. P. and Fuerstenau, D. W. (1966) The effect of crystal structure on the surface properties of a series of manganese dioxides. *Journal of Colloid and Interface Science*, 21, 435-444.

Huang, C. P. (1978) "Chemical interactions between inorganics and activated carbon" *in Carbon Adsorption Handbook.* Edited by P. N. Cheremisinoff and F. Ellerbusch, 281-329. Ann Arbor Science Publishers, Ann Arbor, MI.

Huang, C. P. and Bowers, A. R. (1979) Activated carbon processes for the treatment of wastewaters containing hexavalent chromium. USEPA 1990-600/2-79-130.

Huang, C. P. and Smith, E. H. (1981) "Removal of Cd(II) from plating waste water by an activated carbon process" in *Chemistry in Water Reuse Volume 2.* Edited by W. J. Cooper, 355-402. Ann Arbor Science Publishers, Ann Arbor, MI.

Huang, C. P. and Van, L. M. (1989) Enhancing As^{5+} removal by a Fe^{2+}-treated activated carbon *J. WPCF*, 61(9), 1596-1603.

Huang, C. P. and Wu, M. H. (1977) The removal of chromium(VI) form dilute aqueous solution by activated carbon. *Water Research*, 11, 673-679.

Huang, P. M. (1991) "Kinetics of Redox Reactions of Manganese Oxides and Its Impact on Environmental Quality" in *Rate of Soil Chemical Processes.* Special Publication no 27., Soil Science Society of America, Madison, WI.

Jenne, E. A. (1968) "Controls on Mn, Fe, Co, Ni, Cu and Zn concentrations in soils and water: the significant role of hydrous Mn and Fe oxides" in *Trace Inorganics in Water.* Advances in Chemistry Series 73, American Chemical Society, Washington, D.C.

Kemmitt, R. D. W. (1973) "Manganese" in *The Chemistry of Manganese, Technetium and Rhenium.*, 771-876. Pergamon press, Oxford..

Kinniburgh, D. G. and Jackson, M. L. (1981) "Cation adsorption by hydrous metal oxides and clays" in *Adsorption of organics at solid-liquid interfaces.*, 91-160. Edited by Anderson, M. A. and Rubin, A. J., Ann Arbor Science, Ann Arbor, MI.

Kline, S. D. (1990) *Production and characterization of a low-cost, activated Illinois No. 6 mild gasification char.* Master's thesis, Illinois Institute of Technology, Chicago, IL.

Knocke, W. R., Hamon, J. R. and Thompson, C. P. (1988) Soluble manganese removal on oxide-coated filter media. *JAWWA*, December, 65-70.

Knocke, W. R., Occiano, S. C. and Hungate, R. (1991) Removal of soluble manganese by oxide-coated filter media: Sorption rate and removal mechanisms. *JAWWA*, 83, Aug., 64-69.

Ku, Y. and Peters, R. W. (1987) Innovative use for carbon adsorption of heavy metals from plating wastewater: I. Activated carbon polishing treatment. *Environmental Progress*, 6(2), 119-124.

Kuennen, R. W., Taylor, R. M., Dyke, K. V. and Groeneult, K. (1992) Removing lead from drinking water with a point-of-use GAC fixed-bed adsorbent. *J. AWWA.*, February, 1992, 91-101.

Leckie, J. O., Benjamin, M. M., Hayes, K., Kaufman, G. and Altmann, S. (1980) "Adsorption/coprecipitation of trace elements from water with iron oxyhydroxide" CS-1513, Research Project 910-1, Electric Power Research Institute, Palo Alto, CA.

Lion, L. W., Altmann, R. S. and Leckle J. O. (1982) Trace-metal adsorption characteristics of Estuarine particle mater: evaluation of contribution of Fe/Mn oxide and organic surface coatings. *Environ. Sci. Technol.*, 16(10), 660-666.

Loganathan, R. G., Burau, R. G. and Fuerstenau, D. W. (1977) Influence of pH on the sorption of Co^{2+}, Zn^{2+} and Ca^{2+} by a hydrous manganese oxide. *Soil Sci. Soc. Am.* J., 41, 57-62.

Mattson, J. S. and Mark, H. B. (1971) *Activated carbon.* Marcel Dekker. New York.

McGuire, M. J. and Suffet, I. H. (1983) *Treatment of water by Granular activated carbon.* ACS, Washington, D.C.

McKenzie, R. M. (1977) "Manganese oxides and hydroxides" in *Minerals in Soil Environments*, J. B. Dixon and S. B. Weed (editors), Soil Science Society of America, Madison, WI.

McLaren, R. G. and Crawford, D. V. (1973) Studies on soil copper. II. The specific adsorption of copper by soils. *J. Soil Sci.*, 24(4), 443-452.

Murray, J. W. (1974) The surface chemistry of hydrous manganese dioxide. *J. Col. Int. Sci.*, 46, 357-371.

Netzer, A. and Hughes, D. E. (1984) Adsorption of copper, lead and cobalt by activated carbon. *Water Res.*, 18(8), 927-933.

Noll, K. E., Gounaris, V. and Hou, W-S. (1992) *Adsorption technology for air and water pollution control.* Lewis Publishers, Inc., Chelsea, MI.

Nordqvist, K. R. Rune, Benjamin, M. M, and Ferguson, J. F. (1988) Effects of Cyanide and Polyphosphates on Adsorption of Metals from Simulated and Real Mixed-Metal Plating Wastes. *Water Res.*, 22(7), 837-846.

Oakley, S. M., Nelson, P. O. and Williamson, K. J. (1981) Model of trace-metal partitioning in marine sediments. *Environ. Sci. Technol.*, 15, 474-480.

Reed, B. E. and Arunachualam, S. (1994) Use of granular activated carbon columns for lead removal. *J. of Environmental Engineering*, 120(2), 416-436.

Reed, B. E., Arunachualam, S. and Thomas, B. (1994) Removal of lead and cadmium from aqueous waste streams using granular activated carbon (GAC) columns. *Environmental Progress*, 13(1), 60-64.

Reed, B. E. and Matsumoto, M. R. (1992) Modeling Cd adsorption in single and binary adsorbent (PAC) systems. *J. of Environmental Engineering*, 119 (2), March/April, 332-348.

Roth, K. E. (1991) *Development of a Magnetite-based adsorption process for the removal of heavy metal ions from metal plating wastewater.* Master's thesis, Illinois Institute of Technology, Chicago, IL.

Roy, D., Wang, G. and Adrian, D. D. (1993) Simplified calculation procedure for carbon adsorption model. *Water Environ. Res.*, 65, 781.

Schiele, R. (1991) "Manganese" in *Metals and their Compounds in the Environment.* Edited by Merian, E. VCH. 1035-1044.

Schultz, M. F., Benjamin, M. M. and Ferguson, J. F. (1987) Adsorption and desorption of metals on ferrihydrite: Reversibility of the reaction and sorption properties of the regenerated solid. *Environ. Sci. Technol.*, 21, 863-869.

Sigworth, E. A. and Smith, S. B. (1972) Adsorption of inorganic compounds by activated carbon. *J. AWWA*, June 1972, 386-391.

Stahl, R. S. and James, B. R. (1991a) Zinc sorption by Iron-Oxide-Coated sand as a function of pH. *Soil Sci. Soc. Am. J.*, 55, 1287-1290.

Stahl, R. S. and James, B. R. (1991b) Zinc sorption by Manganese-Oxide-Coated sand as a function of pH. *Soil Sci. Soc. Am. J.*, 55, 1291-1294.

Stumm, W. and Morgan, J. J. (1981) *Aquatic Chemistry.* 2nd ed. John wiley & sons, New York.

Thacker, W. E., Snoeyink, V. L. and Crittenden, J. C. (1981) *Modeling of activated carbon and coal gasification char adsorbents in single-solute and bisolute systems.* U. of IL. at Urbana-Champaign, Water resources center, UILU-WRC-81-0161, July 1981.

Theis, T. L., Westrick, J. D., Hsu, D. K. and Marley, J. J. (1978). Field investigations of trace metals in ground water from fly ash disposal. *J. Water Pollut. Control Fed.*, 50, 2457-2469.

Theis, T. L. and Richter, R.. O. (1979). Chemical speciation of heavy metals in power plants ash pond leachate. *Environ. Sci. Technol.*, 13, 219-224.

Theis, T. L., Lyer, R. and Ellis, S. K. (1992) Evaluating a new granular iron oxide for removing lead from drinking water. *J.* AWWA, July 1992, 101-105.

Traegner, U. K. and Suidan, M. T. (1989) Evaluation of surface and film diffusion coefficients for carbon adsorption. *Wat. Res.*, 23(3) 267-273.

Voice, T. C. (1988) "Activated carbon adsorption" in *Standard handbook of hazardous waste treatment and disposal*, Edited by H. M. Freeman, McGraw-Hill, New York.

Wang, G. and Roy, D. (1993) Approximate semianalytical solution for nonlinear surface diffusion in a batch reactor. *Environ. Sci. Technol.*, 27(5), 923-927.

Wang, T. C. (1995) Copper and cadmium removal and recovery by iron oxide-coating granular activated carbon. Ph.D. dissertation, Illinois Institute of Technology, Chicago, IL.

Wang, T. C., Reddy, K. P. and Anderson, P. R. (1994) Evaluation of Fe oxide-coated granular activated carbon for removal and recovery of Cu(II) and Cr(VI) from aqueous solution. Hazardous Waste Research and Information Center, Champaign, Illinois.

Weber, Jr., W. J., and Smith, E. H. (1987) Simulation and Design Models for Adsorption Processes. *Environ. Sci. Technol.*, 21(11), 1040-1050.

Weber, W. J., McGinely, P. M. and Kaze, L. E. (1991) Sorption phenomena in surface systems: concepts, models and effects on contaminant fate and transport. *Wat. Res.*, 25(5), 499-528.

Wilczak, A. and Keinath, T. M. (1993) Kinetics of sorption and desorption of copper (II) and lead (II) on activated carbon. *Water Environment Research*, 65(3), 238-244.